National Library of Canada
Acquisitions and Bibliographic Services Branch
395 Wellington Street
Ottawa, Ontario
K1A 0N4

Bibliothèque nationale du Canada
Direction des acquisitions et des services bibliographiques
395, rue Wellington
Ottawa (Ontario)
K1A 0N4

Your file Votre référence

Our file Notre référence

NOTICE

The quality of this microform is heavily dependent upon the quality of the original thesis submitted for microfilming. Every effort has been made to ensure the highest quality of reproduction possible.

If pages are missing, contact the university which granted the degree.

Some pages may have indistinct print especially if the original pages were typed with a poor typewriter ribbon or if the university sent us an inferior photocopy.

Reproduction in full or in part of this microform is governed by the Canadian Copyright Act, R.S.C. 1970, c. C-30, and subsequent amendments.

AVIS

La qualité de cette microforme dépend grandement de la qualité de la thèse soumise au microfilmage. Nous avons tout fait pour assurer une qualité supérieure de reproduction.

S'il manque des pages, veuillez communiquer avec l'université qui a conféré le grade.

La qualité d'impression de certaines pages peut laisser à désirer, surtout si les pages originales ont été dactylographiées à l'aide d'un ruban usé ou si l'université nous a fait parvenir une photocopie de qualité inférieure.

La reproduction, même partielle, de cette microforme est soumise à la Loi canadienne sur le droit d'auteur, SRC 1970, c. C-30, et ses amendements subséquents.

Canada

UNIVERSITY OF ALBERTA

NMR and Kinetic Studies of Cobaloximes and $(H_2O)_5CrCH_2CN^{2+}$

BY

KEFEI WANG

A thesis submitted to the Faculty of Graduate Studies and Research in partial fulfillment of the requirement for the degree of Doctor of Philosophy.

DEPARTMENT OF CHEMISTRY

EDMONTON, ALBERTA

FALL, 1994

National Library
of Canada

Acquisitions and
Bibliographic Services Branch

395 Wellington Street
Ottawa, Ontario
K1A 0N4

Bibliothèque nationale
du Canada

Direction des acquisitions et
des services bibliographiques

395, rue Wellington
Ottawa (Ontario)
K1A 0N4

Your file Votre référence

Our file Notre référence

The author has granted an irrevocable non-exclusive licence allowing the National Library of Canada to reproduce, loan, distribute or sell copies of his/her thesis by any means and in any form or format, making this thesis available to interested persons.

L'auteur a accordé une licence irrévocable et non exclusive permettant à la Bibliothèque nationale du Canada de reproduire, prêter, distribuer ou vendre des copies de sa thèse de quelque manière et sous quelque forme que ce soit pour mettre des exemplaires de cette thèse à la disposition des personnes intéressées.

The author retains ownership of the copyright in his/her thesis. Neither the thesis nor substantial extracts from it may be printed or otherwise reproduced without his/her permission.

L'auteur conserve la propriété du droit d'auteur qui protège sa thèse. Ni la thèse ni des extraits substantiels de celle-ci ne doivent être imprimés ou autrement reproduits sans son autorisation.

ISBN 0-315-95279-2

Canada

UNIVERSITY OF ALBERTA

RELEASE FORM

NAME OF AUTHOR: KEFEI WANG

TITLE OF THESIS: NMR AND KINETIC STUDIES OF COBALOXIMES AND $(H_2O)_5CrCH_2CN^{2+}$

DEGREE: DOCTOR OF PHILOSOPHY

YEAR THIS DEGREE GRANTED: 1994

Permission is hereby granted to the University of Alberta Library to reproduce single copies of this thesis and lend or sell such copies for private, scholarly or scientific research purposes only.

The author reserves all other publication and other rights in association with the copyright in the thesis, and except as hereinbefore provided neither the thesis nor any substantial portion prior thereof may be printed or otherwise reproduced in any material form whatever without the author's prior written permission.

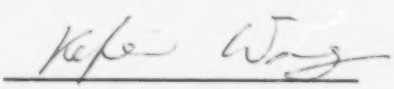

Apt# 107, 10635 - 83 Ave.

Edmonton, Alberta, T6E 2E3

July, 1994

UNIVERSITY OF ALBERTA

FACULTY OF GRADUATE STUDIES AND RESEARCH

The undersigned certify that they have read, and recommend to the Faculty of Graduate Studies and Research for acceptance, a thesis entitled **NMR and Kinetic Studies of Cobaloximes and $(H_2O)_5CrCH_2CN^{2+}$** submitted by Kefei Wang in partial fulfillment of the requirements for the degree of Doctor of Philosophy.

Professor Robert B. Jordan

Professor Josef Takats

Professor Ronald E. D. McClung

Professor Martin Cowie

Professor Gordon Swaters

Professor Thomas W. Swaddle
(External Examiner)

July 21, 1994

To Dong, Jason and my parents

Abstract

NMR solvent exchange kinetics of a series of cobaloximes(II) have been studied. The solvent exchange controlled region of the solvent proton transverse relaxation rate R_2 was observed for $Co(dmgH)_2$ ($dmgH^-$ = dimethylglyoximato(-1)) in acetonitrile and methanol, but this region was less defined for the $-BF_2$ derivative $Co(dmgBF_2)_2$ in acetonitrile, methanol and acetone, and for $Co(dpgH)_2$ ($dpgH^-$ = diphenylglyoximato(-1)) in methanol. For all these systems, the exchange rates are $10^{5\pm1}$ s^{-1} at 25 °C, and the negative $\Delta S^{\ddagger}$ values are consistent with an I_a exchange mechanism.

The solvent water proton relaxation rates have been studied for $(H_2O)_5CrCH_2CN^{2+}$ at various temperatures and $[H^+]$, and the results show three proton exchange pathways which are first-order, independent and inverse first-order in $[H^+]$. The kinetic parameters and general relaxation effects for this complex are similar to those for other aqua Cr(III) complexes.

Spectrophotometry has been used to measure the equilibrium constant for complexation of $Co(dmgBF_2)_2$ by 1-methylimidazole (MeIm) in acetonitrile. The proton NMR shifts and relaxation rate R_2 of free MeIm are consistent with fast exchange between free and coordinated MeIm, and relaxation parameters are consistent with a scalar relaxation mechanism. The R_2 values at high MeIm concentrations are higher than predicted from lower concentrations, and this has been explained by outer-sphere contribution to the R_2.

Reduction of $(H_2O)_2Co^{II}(dmgBF_2)_2$ by $XCo^{III}(NH_3)_5^{2+}$ ($X = Cl^-$, Br^- and N_3^-) proceeds by a bridged inner-sphere mechanism based on the pattern of the rate constants. Rates of reduction of $(H_2O)_2Co^{III}(dmgBF_2)_2^+$ and $(H_2O)_2Co^{III}(dmgH)_2^+$ by the outer-sphere reductant $Co(sep)^{2+}$ were used to estimated the self-exchange rates for

the two cobaloxime(III)/(II) couples from the Marcus theory. The calculated self-exchange rates are much smaller than predicted by the Franck-Condon factor, and should be multiplied by ~$10^{2.6}$ as a result of nonadiabaticity for the cross reactions.

Acknowledgments

I wish to express my sincere thanks to my advisor, Professor R. B. Jordan, for his guidance, encouragement, thoughtfulness, and especially patience during the course of this work. I was very fortunate to have an advisor from whom I could not have asked more in the way of experimental support: blowing glassware, fixing machines, booking NMR time, programming the computer, etc.

I am also indebted to Professor R. E. D. McClung, and the NMR staff members of the Chemistry Department for their assistance in NMR measurements; to Dr. Margaret Sisley and my fellow graduate student Zhongsheng Zhang, for their friendship and many helpful discussions.

I dedicated this thesis partially to my wife, Dong, for her love, patience, understanding and encouragement; and to my son, Jason, for giving up time that was rightfully his.

To my parents, to whom the thesis was also dedicated, goes my special thanks for their love and support during my many years of study, and for their persistent but understandably anxious query, "When will you be done with your degree and get a real job?"

Finally, I am grateful for financial assistance from the University of Alberta.

Table of Contents

Abstract

Acknowledgments

Table of Contents

List of Tables

List of Figures

Chapter 1. Introduction 1

Chapter 2. Solvent Exchange Kinetics of Cobaloximes(II) 13

Introduction 13

Basic Equations 14

Experimental Section 28

Results 33

Discussions 54

References 63

Chapter 3. NMR Shifts and Relaxation of 1-Methylimidazole (MeIm) in MeIm-Co($dmgBF_2$)$_2$ Complex in Acetonitrile 65

Introduction 65

Experimental Section 69

Results 71

Discussions 79

References 91

Chapter 4. Kinetics of Water Proton Exchange of $(H_2O)_2CrCH_2CN^{2+}$ in Aqueous Acid **92**

Introduction 92

Experimental Section 93

Results 94

Discussions 98

References 105

Chapter 5. Electron-Transfer Kinetics of Cobaloximes **106**

Introduction 106

Experimental Section 112

Results 116

Discussions 124

References 136

Chapter 6. Conclusions **139**

References 144

Appendix Tables of Experimental Data **145**

List of Tables

Table		Page
2.1	Least-Squares Best-Fit Parameters for the Temperature Dependence of the Solvent Proton Relaxation Rates in Acetonitrile Solution of $Co(dmgH)_2$	36
2.2	Solvent Proton Chemical Shifts (300 MHz) and the Scalar Coupling Constants of $Co(dmgH)_2$ Solutions in Acetonitrile and Methanol at 35 °C	37
2.3	Least-Squares Best-Fit Parameters for the Temperature Dependence of the Solvent Proton Relaxation Rates in Methanol Solution of $Co(dmgH)_2$	40
2.4	Least-Squares Best-Fit Parameters for the Temperature Dependence of the Solvent Proton Relaxation Rates in Acetonitrile Solution of $Co(dmgH)_2$ at $\Delta S^{\ddagger} = -6$ cal mol^{-1} K^{-1}	41
2.5	Least-Squares Best-Fit Parameters for the Temperature Dependence of the Solvent Proton Relaxation Rates in Acetonitrile Solution of $Co(dmgBF_2)_2$	45
2.6	Least-Squares Best-Fit Parameters for the Temperature Dependence of the Solvent Proton Relaxation Rates in Acetone Solution of $Co(dmgBF_2)_2$	48
2.7	Least-Squares Best-Fit Parameters for the Temperature Dependence of the Solvent Proton Relaxation Rates in Acetonitrile Solution of $Co(dpgH)_2$	51
2.8	Least-Squares Best-Fit Parameters for the Temperature Dependence of the Solvent Proton Relaxation Rates in Methanol Solution of $Co(dpgH)_2$	53
2.9	Kinetic Parameters for Solvent Exchange for Cobaloxime(II) Solutions	55
2.10	Summary of Electron Spin Relaxation Times and Temperature Dependence of Relaxation Rates	58
2.11	Summary of Proton Scalar Coupling Constants and Solvent Exchange Activation Enthalpies for Cobalt(II) Systems	60
3.1	Equilibrium Constants for Formation of Mono- and Bis- MeIm Adducts	

	of $Co(dmgBF_2)_2$ in Acetonitrile	75
3.2	Formation Constants of $(Base)_nCo(dmgBF_2)_2$ and Other Complexes	80
3.3	Estimation of C_2^i Values From Chemical Shifts $\Delta\nu_{obs}^i$	84
3.4	Results of Calculated Chemical Shifts and Relaxation Rates (Proton 1)	86
3.5	Temperature Independent Shift and Relaxation Parameters	89
4.1	Least-Squares Best-Fit Parameters for the Temperature Dependence of the Solvent Water Proton Relaxation Rates in Acidic Solution of $(H_2O)_5CrCH_2CN^{2+}$	99
4.2	Comparison of Exchange Rate Parameters for Coordinated Water Protons on Several Chromium(III) Complexes	102
5.1	Kinetic Data for Reactions Between $(H_3N)_5Co^{III}X^{2+}$ and Diaquacobaloximes(II)	117
5.2	Kinetic Results of Reactions of Cobaloximes(III) with $Co(sep)^{2+}$	121
5.3	Results of Self-Exchange Rates Calculated by Marcus Relationship	125
5.4	Observed First-order Decomposition Rates of $Co^{II}(dmgH)_2$ at 25 °C	126
5.5	Summary of Self-Exchange Rates (25 °C) of $(H_2O)_2CoL(III)/(II)$	132
5.6	Comparison of the Calculated and Observed Cross Reaction Rates for Reduction of Some Cobalt(III) Complexes by $Co(sep)^{2+}$ at 25 °C	134

List of Figures

Figure		Page
2.1	NMR spectra of solvent nuclei in the bound and bulk environments, in the absence and presence of chemical exchange	16
2.2	Illustrated plot of Log R_{2p} vs. $1/T$ as predicted by complete Swift -Connick equation and the delineated equations in limiting cases	21
2.3	Temperature dependence of solvent proton transverse and longitudinal relaxation rates for the acetonitrile solution of $Co(dmgH)_2$	34
2.4	Temperature dependence of solvent proton transverse and longitudinal relaxation rates for the methanol solution of $Co(dmgH)_2$	38
2.5	Refit of temperature dependence of solvent proton transverse and longitudinal relaxation rates for the methanol solution of $Co(dmgH)_2$ at $\Delta S^{\ddagger}$ = -6 cal mol^{-1} K^{-1}	42
2.6	Temperature dependence of solvent proton transverse and longitudinal relaxation rates for the acetonitrile solution of $Co(dmgBF_2)_2$	44
2.7	Temperature dependence of solvent proton transverse and longitudinal relaxation rates for the acetone solution of $Co(dmgBF_2)_2$	47
2.8	Temperature dependence of solvent proton transverse and longitudinal relaxation rates for the acetonitrile solution of $Co(dpgH)_2$	49
2.9	Temperature dependence of solvent proton transverse and longitudinal relaxation rates for the methanol solution of $Co(dpgH)_2$	52
3.1	Determination of equilibrium constant K_1 for $(MeIm)Co^{II}(dmgBF_2)_2$	73
3.2	Determination of equilibrium constant K_2 for $(MeIm)_2Co^{II}(dmgBF_2)_2$	74
3.3	Temperature dependence of equilibrium constants K_1 and K_2	76
3.4	Proton NMR spectrum of MeIm-$Co(dmgBF_2)_2$ in acetonitrile at -35 °C	78

4.1 Solvent water proton transverse and longitudinal relaxation rates for solution of $(H_2O)_5CrCH_2CN^{2+}$ in 0.051 M $HClO_4$ 95

4.2 Hydrogen ion dependence of 10^5R_{2p} for the water protons in solutions of $(H_2O)_5CrCH_2CN^{2+}$ at 50 ± 1 °C 97

4.3 Temperature and $[H^+]$ dependence of R_{2p} for solvent water protons in solutions of $(H_2O)_5CrCH_2CN^{2+}$ 100

5.1 pH dependence of the second-order rate constants for reduction of $Co^{III}(dmgH)_2^+$ by $Co(sep)^{2+}$ 118

5.2 pH dependence of the second-order rate constants for reduction of $Co^{III}(dmgBF_2)_2^+$ by $Co(sep)^{2+}$ 119

5.3 Correlation between the observed electron transfer rates and the driving forces for reduction of cobalt(III) complexes 129

5.4 Correlation between the observed and calculated cross reaction rates for reduction of some cobalt(III) complexes by $Co(sep)^{2+}$ 135

Chapter 1. Introduction

This study is concerned generally with the chemistry of cobalt(II) complexes formed with various glyoxime ligands, of which dimethylglyoxime is the most common. There has been a great deal of work on this family of complexes, but this has concentrated mainly on the cobalt(III) oxidation state. The interest in these compounds was stimulated by Schrauzer's work[1] in the 1960's which showed that they mimic many of the reactions of vitamin B_{12} coenzyme and its derivatives. In the present study a number of aspects of the cobalt(II) complexes have been investigated by various techniques. The details and background of the techniques are described in the introductions to the relevant chapters. The present section provides some overall chemical and structural background.

Cobaloximes. Cobaloxime (i.e. cobalt-oxime) is the trivial name for bis(dimethylglyoximato)cobalt complex, $Co(dmgH)_2$, in which $dmgH^-$ represents the monoanion of dimethylglyoxime (2,3-butanedione dioxime, $dmgH_2$, illustrated below). In forming cobaloxime complexes, two $dmgH^-$ ligands are joined by hydrogen bonds to make a chelate ring as shown below for $Co(dmgH)_2$. The two axial positions above and below the chelate ring may be occupied by various ligands.

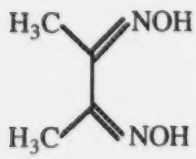

$dmgH_2$

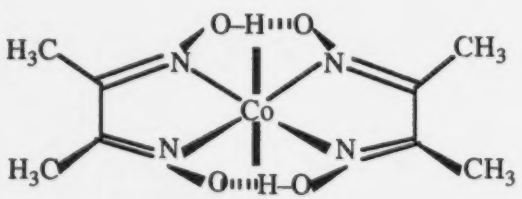

$Co(dmgH)_2$

There are a number of derivatives in which the methyl groups are replaced by other substituents, and in which the hydrogen bonds (H•••O—H) are replaced by a $-BF_2$ linkage. Two such derivatives, $Co(dpgH)_2$ and $Co(dmgBF_2)_2$, are illustrated below.

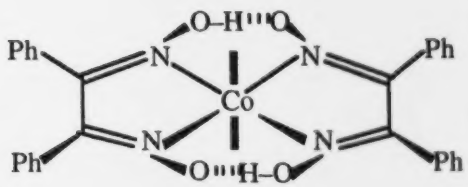

$Co(dpgH)_2$

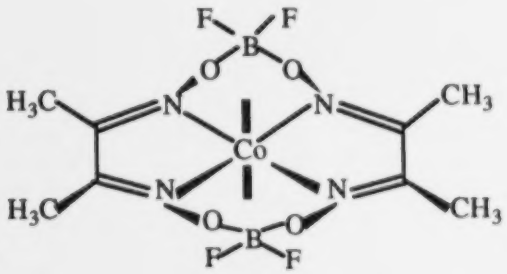

$Co(dmgBF_2)_2$

The cobalt in cobaloximes can have oxidation states (III), (II) and (I), and this provides a rich chemistry for this family of complexes.

Cobaloximes(III). These complexes are prepared by mixing a slight excess of the appropriate glyoxime with a cobalt(II) salt in the presence of oxidizing agents, such as O_2 and H_2O_2.[2] The Co(III) in these complexes has a low-spin d^6 electronic configuration and the complexes are diamagnetic. Cobaloximes(III) are generally kinetically stable, and rather inert toward substitution, in both acidic and basic aqueous solution. X-ray crystallographic studies of the solids[3] and NMR studies in solution[3] reveal that the cobalt atom is 6-coordinate with a square planar arrangement of the $(dmgH)_2$ and with two axial positions occupied by Lewis bases to form *trans*-$XLCo^{III}(dmgH)_2$ complexes, where X and L may be the same or different Lewis bases. It should be noted that one of the axial ligands can be an alkyl group so that there is a wide range of organometallic derivatives.

Cobaloximes(I). Upon addition of 2 equivalent amounts of a reducing agent, such as $NaBH_4$, cobaloximes(III) can be reduced to cobaloximes(I).[4] Cobaloxime(I)

can also be obtained by disproportionation of a cobaloxime(II) complex in alkaline solution,[1] as shown by Eq 1.1:

$$2Co^{II}(dmgH)_2 \xrightarrow{OH^-} Co^{I}(dmgH)_2^- + Co^{III}(dmgH)_2^+ \qquad (1.1)$$

The Co(I) has a low spin d^8 electronic configuration, and the cobalt has a coordination number of 5 with a square-pyramidal arrangement of the ligands.[5]

Solutions of cobaloximes(I) are extremely oxygen sensitive and are only stable in alkaline solution. In acidic media they decompose to form cobaloxime(II) and hydrogen. The chemistry of the cobaloximes(I) is characterized by the high nucleophilicity of the Co atom. Cobaloximes(I) react with alkyl halides according to Eq 1.2

$$Co^{I}(dmgH)_2^- + RX \longrightarrow RCo^{III}(dmgH)_2 + X^- \qquad (1.2)$$

The reaction proceeds by a classical S_N2 mechanism based on the observation of second-order kinetics and the effects of R and X on the rate constants.[6]

Cobaloximes(II). These are generally prepared by mixing an appropriate glyoxime with a cobalt(II) salt under anaerobic conditions.[7] Cobaloximes(II) are generally sensitive to oxidation by O_2, and the sensitivity depends on the nature of the glyoxime ligands. Electron-withdrawing groups in the equatorial ligand plane tend to stabilize the Co(II) oxidation state, thus making the complexes more resistant to oxidation. For example, a solution of $Co^{II}(dmgH)_2$ is oxidized in few seconds on exposure to air, while $Co^{II}(dmgBF_2)_2$, with the strong electron-withdrawing $-BF_2$ substituents, can be handled in air without undergoing any oxidation.

The cobalt(II) in cobaloximes has a d^7 low-spin configuration in a distorted octahedral ligand field, as shown below.

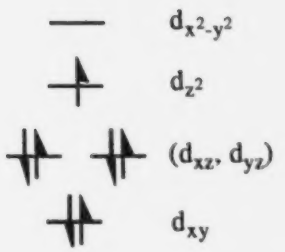

The electronic configuration with one unpaired electron is consistent with the observed magnetic moment μ_{eff} = 1.82 B.M. for $Co^{II}(dmgH)_2$ in the solid state.[8] The value is only slightly greater than the spin-only value of 1.73 B.M. for one unpaired electron, but distinctly different from that of 3.46 B.M. if Co(II) were high spin.

Studies of $Co^{II}(dmgH)_2$ in aqueous solution are somewhat limited by the low solubility of the complex and its decomposition in acidic solution to Co^{2+}(aq) and $dmgH_2$. The decomposition is nearly first-order in $[H^+]$ so that solutions are stable near pH 7, but decompose in a few seconds at pH 4.7.[9] The process is believed to involve protonation of the H•••O—H units, since the $Co^{II}(dmgBF_2)_2$ derivative without such units is much more stable in acidic solution.

X-ray structures of cobaloximes(II) are rare due to the air-sensitive nature of the complexes and the difficulty in obtaining single crystals. The bis(pyridine) adduct, $(py)_2Co^{II}(dmgH)_2$ [10] has the $(dmgH)_2$ chelate ring almost coplanar with the Co atom, and the axial Co–N bonds to py (2.25 Å) are 0.37 Å longer than the equatorial Co–N bonds to $dmgH^-$ (1.89 Å). The structure of $(CH_3OH)_2Co^{II}(dmgBF_2)_2$ [11] also shows axial elongation, with Co-N_{eq} and Co–O_{ax} (CH_3OH) bond lengths being 1.88 Å and 2.26 Å , respectively. The axial elongation can be attributed to the unpaired electron occupying the slightly antibonding d_{z^2} orbital in these low-spin d^7 complexes.

In the presence of a Lewis base in solution, cobaloxime(II) may form mono- and bis- Lewis base adducts. However, the structure of the cobaloxime(II) in solution

can be difficult to assess because the axial sites are labile. Depending upon such factors as solvent, nature and concentration of the Lewis base, and the temperature, the $Co^{II}(dmgH)_2$ moiety in solution may coordinate to one or two axial binding ligands. In fact, the complex may be 5-coordinate in solution even though it is 6-coordinate in the solid state, and vice versa. The structure may be further complicated if the solvent is a Lewis base and therefore a potential axial ligand.

The extent of coordination in solution has most often been deduced from EPR spectra of frozen solutions. EPR can provide the most direct indication of the extent of axial coordination in solution in cases where the donor atom of the axial ligand(s) has a nuclear spin. The pattern of superhyperfine (shf) coupling between the unpaired electron on the cobalt and the nuclear spin of the donor atom shows whether one or two donor atoms are attached to the cobalt center, and therefore gives the axial coordination number. For example, if the donor atom is N (nuclear spin quantum number $I = 1$), a triplet superhyperfine coupling pattern would indicate one axial ligand, while a quintet would indicate two axial ligands. Unfortunately, it is seldom possible to observe isotropic EPR spectra for fluid solutions containing cobaloxime(II) complexes, because the electron spin relaxation times are too short, so that the lines are broad. Therefore, EPR spectra are usually measured in frozen solutions at liquid nitrogen temperature (77 K). These spectra reflect the extent of axial coordination in the frozen state, but this is not necessarily the same as in solution.

Results of EPR measurements on cobaloximes(II) in frozen solutions[11-18] showed both 5- and 6-coordinate species. For N-donor Lewis bases, such as py (in methanol[13,14] and acetonitrile[17]) and 1-methylimidazole (in acetonitrile)[17], mono-adducts were generally found based on the triplet ^{14}N shf splitting multiplicity at low base concentrations (usually [B]/[cobalt] ≤ 1), while 6-coordinate bis- adducts were found based on the quintet splitting pattern of ^{14}N shf at higher base concentrations. In

frozen acetonitrile, bis- solvent adduct $(CH_3CN)_2Co^{II}(dmgBF)_2$ was observed. It is interesting to note that Lewis bases with a P-donor atom (^{31}P nuclear spin quantum number $I = 1/2$)[16] , such as PR_3 and $P(OR)_3$, form mono-adducts in toluene-ethanol solvent for all bases with identical R groups, based on the doublet ^{31}P shf splitting, whereas bis-adducts were observed, based on the triplet ^{31}P shf splitting with mixed substituents, $PR_1(R_2)_2$, $P(OR_1)(OR_2)_2$, $PR(OR)_2$, etc. These results were found to be independent of [Base]/[Cobalt] ratios from 1 to 4.

Electronic spectral measurements can be used to identify whether it is $BCo(dmgH)_2$ and/or $B_2Co(dmgH)_2$ (B = Lewis base) in solution if the two adducts have distinguishable spectra.[19] However, both this and the EPR method can be ambiguous if the solvent is a Lewis base, because the observation of 1:1 base adduct $BCo(dmgH)_2$ does not rule out coordination by a solvent in the second axial position to give 6-coordinate $(B)(Solvent)Co^{II}(dmgH)_2$.

Cobaloxime(II) complexes are mild reducing agents. The oxidation of cobaloxime(II) may be either *via* an inner-sphere or an outer-sphere mechanism, depending on the nature of the oxidant. Oxidation of cobaloxime(II) with $Co^{III}(NH_3)_5X^{2+}$ (X = halides and pseudohalides) in aqueous solution[9] was found to proceed *via* an inner-sphere mechanism because the product is $XCo^{III}(dmgH)_2^+$, and the rate order is $Br^- > Cl^- \gg F^-$. The latter order indicates a soft acid character for $Co^{II}(dmgH)_2$. The inner-sphere mechanism also was suggested for oxidation of $(H_2O)_2Co^{II}(dmgBF_2)_2$ by $Fe(OH_2)_6^{3+}$.[11] The mechanistic assignment is mainly based on the observed inverse-$[H^+]$ dependence of the reaction rate, which indicates a higher reactivity of the deprotonated form $(H_2O)_5FeOH^{2+}$ compared to $Fe(OH_2)_6^{3+}$.

Cobaloximes(II) have been found to react with organic halides,[20] dioxygen,[21] and molecular hydrogen.[19] Here the first two reactions will be discussed briefly.

Reactions with organohalides (RX) have been studied by many workers,[20] and

a general mechanism has emerged, as shown by Eqs 1.3 to 1.5 with the halogen abstraction step (Eq 1.3) being rate-determining.

$$Co^{II}(dmgH)_2B + RX \xrightarrow{slow} XCo^{III}(dmgH)_2B + R\bullet \quad (1.3)$$

$$Co^{II}(dmgH)_2B + R\bullet \xrightarrow{fast} RCo^{III}(dmgH)_2B \quad (1.4)$$

Overall Reaction:

$$2Co^{II}(dmgH)_2B + RX \longrightarrow XCo^{III}(dmgH)_2B + RCo^{III}(dmgH)_2B \quad (1.5)$$

The reactivity is inversely correlated with the R-X bond strength, with RI > RBr > RCl and with secondary halides being more reactive than primary halides. Furthermore, the increasing reactivity with stronger electron-donating axial bases B is consistent with a proposed transition state $[B–Co^{\delta+}\bullet\bullet\bullet X^{\delta-}\bullet\bullet\bullet R]^{\ddagger}$ characterized by some electron transfer from the Co to X, since the electron donating ligands will enhance the electron transfer.

Activation of dioxygen for homogeneous oxidations involves the formation of Co-O_2 adducts, which are better oxidants than O_2 itself. Schrauzer and Lee[21a] have suggested that the oxygen carrier process may involve the formation of μ-peroxo-dicobaloxime(III), Co-O_2-Co, (ligands omitted), followed by the slow disproportionation to O_2 and an EPR-active μ-superoxo-dicobaloxime(III), [Co-O_2-Co]$^+$. The latter slowly decomposed with Lewis base into derivatives of the deprotonated cobaloxime(III), Co(dmgH)(dmg), and the monomeric peroxoradical complex, B-Co-O_2•. The kinetics of individual stages have been studied by Simandi et al.[21b]

Cobaloximes and Coenzyme B_{12}. As noted above, Schrauzer[1] first found that cobaloximes mimic many reactions of coenzyme B_{12} and therefore serve as models for the coenzyme. Both cobaloximes and coenzyme B_{12} can have cobalt in oxidation

states (I), (II), and (III), and these are called B_{12s}, B_{12r}, and B_{12}, respectively in the coenzyme (r stands for reduced and s for super-reduced).

One remarkable feature of cobaloximes and coenzyme B_{12} is their ability to form rather stable organometallic alkyl derivatives with a σ bond between cobalt(III) and the carbon atom on the alkyl group. The Co-C bond in B_{12} was the first metal-carbon bond to be recognized in biology. The Co–C bond energies for $(py)(PhCH_2)Co^{III}(dmgH)_2$ and coenzyme B_{12} (Co–Adenosyl) were found to be 22 and ~ 30 kcal/mol, respectively.[22, 23]

It is now believed that the unique Co-C bonds in these systems may result from two features.[23] First, both the $(dmgH)_2$ in cobaloxime and the corrin ring in B_{12} have some π-conjugation to stabilize a σ-alkyl derivative. Too much π-conjugation does not appear to be favorable. Neither fully saturated ligands, such as 1,4,8,11-tetraazacyclotetradecane ([14]aneN_4), nor the more extensively delocalized porphyrin system, allow cobalt to form stable alkyl complexes. Second, alkyl derivatives with β-hydrogens cannot decompose readily *via* the common β-elimination pathway, shown by Eq 1.6, because the chelating equatorial ligand prevents the formation of a vacant site *cis* to the alkyl. Such a site is needed for β-elimination to take place by a concerted mechanism.

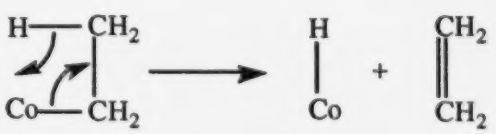

(1.6)

B_{12}-dependent enzymes and cobaloximes catalyze the so-called 'isomerase' reaction:

(1.7)

which involves the 1, 2-shift of a C, N, or O atom. The mechanism of such isomerase reactions have been studied extensively, and one possible mechanism[23] is illustrated in Scheme I. It starts with reversible homolysis of the Co(III)-R bond to generate Co(II), and a radical R•. The R• radical abstracts a H atom from the substrate to give RH and the substrate radical. This radical then undergoes a 1, 2-shift of an X group, to give the product radical. Then H-atom transfer from RH to the product radical gives the final product and the Co-R bond is re-established.

Scheme I

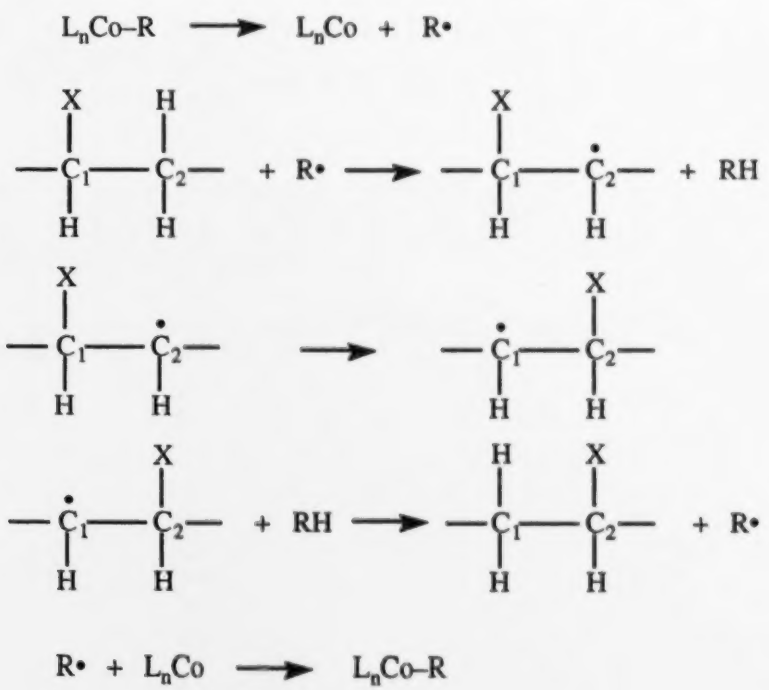

It should be noted that the details of step 3 of Scheme I involving the 1, 2 shift of X still are not clear, and several mechanisms have been suggested.[23,24]

The preceding outline provides a brief overview of cobaloxime chemistry. There is a great deal of information available on the stable cobaloxime(III) complexes. However, the cobaloximes(II) are much less well characterized, and the goal of the present study was to at least partially redress this deficiency. The rate of solvent exchange has been studied in order to give some quantitative measure of the substitution lability of these systems. The information is also important for an understanding of redox reactions because substitution might be rate limiting in inner-sphere oxidation of cobaloximes(II). Some outer-sphere redox reactions also have been studied in order to provide an estimate of the self-exchange rates for cobaloxime(III)/(II) through the application of Marcus theory. The complexation of 1-methylimidazole has been studied to explore axial ligation effects and paramagnetic shifts caused by cobaloxime(II). It is hoped that this information will be relevant to the properties of the corresponding coenzyme B_{12} species.

References

(1) Schrauzer, G. N. *Acc. Chem. Res.* **1968**, *1*,97.

(2) Ablov, A. V.; Samus, N. M. *Russ. J. Inorg. Chem.* **1960**, *5*, 410.

(3) Bresciani-Pahor, N.; Forcolin, M.; Marzilli, L. G.; Randaccio, L.; Summers, M. F.; Toscano, P. J. *Coord. Chem. Rev.* **1985**, *63*, 1. and references therein.

(4) Ramasami, T.; Espenson, J. H. *Inorg. Chem.* **1980**, *19*, 1523.

(5) Shi, S; Espenson, J. H. *Inorg. Chem.* **1991**, *19*, 1523.

(6) (a) Schrauzer, G. N.; Deutsch, E. *J. Am. Chem. Soc.* **1969**, *91*, 3341. (b) Schrauzer, G. N.; Deutsch, E.; Windgassen, R. J. *Ibid.* **1968**, *90*, 6681.

(7) Schrauzer, G. N. *Inorg. Synth.* **1968**, *11*, 61.

(8) Sharp, A. G.; Wakefield, D. B. *J. Chem. Soc.* **1957**, 281.

(9) Adin, A.; Espenson, J. H. *Inorg. Chem.* **1972**, *11*, 686.

(10) Fallon, G. D.; Gatehouse, B. M. *Cryst. Struct. Comm.* **1978**, *7*, 263.

(11) Bakac, A.; Brynildson, M. E.; Espenson, J. H. *Inorg. Chem.* **1986**, *25*, 4108.

(12) Schrauzer, G. N.; Lee, L. P. *J. Am. Chem. Soc.* **1968**, *90*, 6541.

(13) Rockenbauer, A; Zahonyi, E. B.; Simandi, L. I. *J. Chem. Soc. Dalton Trans.* **1975**, 1729.

(14) Rockenbauer, A; Zahonyi, E. B.; Simandi, L. I. *J. Coord. Chem.* **1972**, *2*, 53.

(15) Hoshino, M.; Konishi, S.; Terai, Y.; Imamura. M. *Inorg. Chem.* **1982**, *21*, 89.

(16) De Castro, B.; Rangel, M.; Raynor, J. B. *J. Chem. Soc. Dalton Trans.* **1990**, 3311.

(17) Lance, K. A.; Goldshy, K. A.; Busch, D. H. *Inorg. Chem.* **1990**, *29*, 4537.

(18) Acros, T.; De Castro, B.; Ferreira, M. J.; Rangel, M.; Raynor, J. B. *J. Chem. Soc. Dalton Trans.* **1994**, 369.

(19) Simandi, L. I.; Zahonyi, E. B.; Szverenyi, Z.; Nemeth, S. *J. Chem. Soc. Dalton*

Trans. **1980**, 276.

(20) (a) Schneider, P. W.; Phelan, P. F.; Halpern, J. *J. Am. Chem. Soc.* **1969**, *91*, 77. (b) Halpern, J.; Phelan, P. F. *Ibid.* **1972**, *94*, 1881. (c) Espenson, J. H.; McDowell, M. S. *Organometallics* **1982**, *1*, 1514

(21) (a) Schrauzer, G. N.; Lee, L. P. *J. Am. Chem. Soc.* **1970**, *92*, 1551. (b) Simandi, L. I.; Savage, C. R.; Schelly, Z. A.; Nemeth, S. *Inorg. Chem.* **1982**, *21*, 2765.

(22) Hay, B. P.; Finke, R. G. *J. Am. Chem. Soc.* **1986**, *108*, 4820.

(23) Halpern, J. *Science* **1985**, *227*, 869.

(24) (a) Wollowitz, S.; Halpern, J. *J. Am. Chem. Soc.* **1988**, *110*, 3112. (b) Murakami, Y.; Hisaeda, Y.; Ozaki, T.; Ohno, T.; Fan, S. D.; Matsuda, Y. *Chem. Lett.* **1988**, 839. (c) Choi, S. C.; Dowd, P. *J. Am. Chem. Soc.* **1989**, *111*, 2312. (d) Finke, R. G.; Schiraldi, D. A. *Ibid.* **1983**, *105*, 7605. (e) Finke, R. G.; Schiraldi, D. A.; Mayer, B. J. *Coord. Chem. Rev.* **1984**, *54*, 1.

Chapter 2. Solvent Exchange Kinetics of Cobaloximes(II)

Introduction

Nuclear relaxation rates of solvent nuclei in solutions containing paramagnetic ions have been studied extensively to determine the rate of solvent exchange between bulk (S) and metal-ion coordinated (S^*) solvent as shown in Eq 2.1.

$$[MS^*_n] + S \rightleftharpoons [MS^*_{n-1}S] + S^* \qquad (2.1)$$

Since the original work by Swift and Connick,[1] most of the studies have been on the first-row transition metal ions in aqueous and nonaqueous solutions. Under favorable conditions, these studies have yielded, in addition to the kinetic parameters for the solvent exchange reaction, other information such as the contribution of various relaxation mechanisms (dipolar and scalar interactions), the electron spin relaxation time of the unpaired electron(s), the scalar (hyperfine) coupling constant and the form of delocalization of spin density in the complex, the distance between the paramagnetic ion and the nuclei of the solvent and the solvation number of the paramagnetic ion.

In addition to being the model compounds for vitamin B_{12r},[2] low-spin d^7 cobaloxime(II) complexes, like many other cobalt(II) macrocyclic complexes, are mild reducing agents.[3] Oxidation of these complexes in solution can proceed by either an outer-sphere or inner-sphere mechanism, depending on the nature of the oxidants used. For the inner-sphere mechanism, the rate of electron-transfer may be limited by the rate of substitution of the bridging group onto the cobalt(II) macrocyclic complex to form the bridged-precursor complex. This substitution may be limited by the exchange lability of the coordinated solvent of the macrocyclic complex. Thus solvent exchange rate has fundamental importance for the assignment of the electron transfer mechanism

of the macrocyclic complexes and coenzyme B_{12r}. If the observed rate of electron-transfer is greater than that of solvent exchange, an outer-sphere mechanism is assumed, otherwise it could be either an inner-sphere or an outer-sphere mechanism. Furthermore, if the rate-limiting step in an inner-sphere electron-transfer mechanism is the substitution of a coordinated solvent by an oxidant, then the electron transfer rate will be comparable to the rate of solvent exchange. However, there is very limited information about the axial solvent lability of the Co(II) macrocyclic complexes,[4] and nothing is known about the solvent exchange lability of cobaloxime(II) complexes.

In this study, the temperature dependence of the solvent proton nuclear relaxation rates has been studied for three cobaloxime(II) derivatives, $Co(dmgH)_2$, $Co(dpgH)_2$ and $Co(dmgBF_2)_2$ in several nonaqueous solvents. The limited solubility of these complexes in water prevented a study in aqueous solution. Acetonitrile is used for all three complexes, while methanol is an additional solvent for $Co(dmgH)_2$ and $Co(dpgH)_2$, and acetone for $Co(dmgBF_2)_2$. These solvents were chosen because their long liquid ranges provide the best chance to attain temperatures at which solvent exchange controls the NMR relaxation. These studies yield activation parameters of solvent exchange and the inner-sphere (solvation shell) and outer-sphere (second or higher solvation shell) solvent relaxation, as well as the scalar coupling constants and electron spin relaxation times, all of which may be useful in future studies of low-spin cobalt(II) macrocyclic complexes in these solvents.

Basic Equations

Swift-Connick Equations. The expressions for the effect of solvent exchange on R_{2obs}, the NMR transverse relaxation time of the bulk solvent, and $\Delta\omega_{obs}$, the chemical shift of the bulk solvent nuclei in the presence of a paramagnetic metal ion,

were first given by Swift and Connick.[1] Their solution is based on the Bloch equations modified for chemical exchange, and is given by Eqs 2.2 and 2.3

$$R_{2obs} - R_{2s} = nP_m r_m \left[\frac{R_{2m}(R_{2m} + r_m) + \Delta\omega_m^2}{(R_{2m} + r_m)^2 + \Delta\omega_m^2} \right] \tag{2.2}$$

$$\Delta\omega_{obs} = \frac{nP_m \Delta\omega_m}{(R_{2m}/r_{2m} + 1)^2 + \Delta\omega_m^2 / r_m^2} \tag{2.3}$$

where R_{2obs} is the observed transverse relaxation rate for the bulk solvent nuclei, R_{2s} is the relaxation rate of the bulk solvent in the absence of chemical exchange, r_m is the first-order solvent exchange rate constant, n is the number of exchangeable coordinated solvent molecules in the solvation shell of the metal ion M, P_m =[MS^*_n]/[S] is defined as the ratio of molar concentration of metal ion to that of bulk solvent, R_{2m} is the transverse relaxation rate of the bound solvent nuclei in the absence of the exchange, $\Delta\omega_{obs}$ is the observed chemical shift of the bulk solvent nuclei in the presence of chemical exchange, and $\Delta\omega_m$ is the chemical shift of the bound solvent nuclei in the absence of chemical exchange. Both shifts are relative to that of bulk solvent in the absence of chemical exchange, which is essentially the resonance frequency of the pure solvent because the effect of paramagnetic ion on the shift of the bulk solvent in the absence of exchange is too small to be observed. The NMR spectrum of such a system, when the signals of the bulk and the bound solvent nuclei are well-resolved, is shown in Figure 2.1.

Swift and Connick assumed that R_{2s} was equal to that of pure solvent R_{2solv}, but subsequent work by Luz and Meiboom[5] showed the two are not necessarily equal. Luz and Meiboom ascribed this to the outer-sphere relaxation contribution R_{2o} which results from paramagnetic dipolar relaxation effects in the second and subsequent solvation

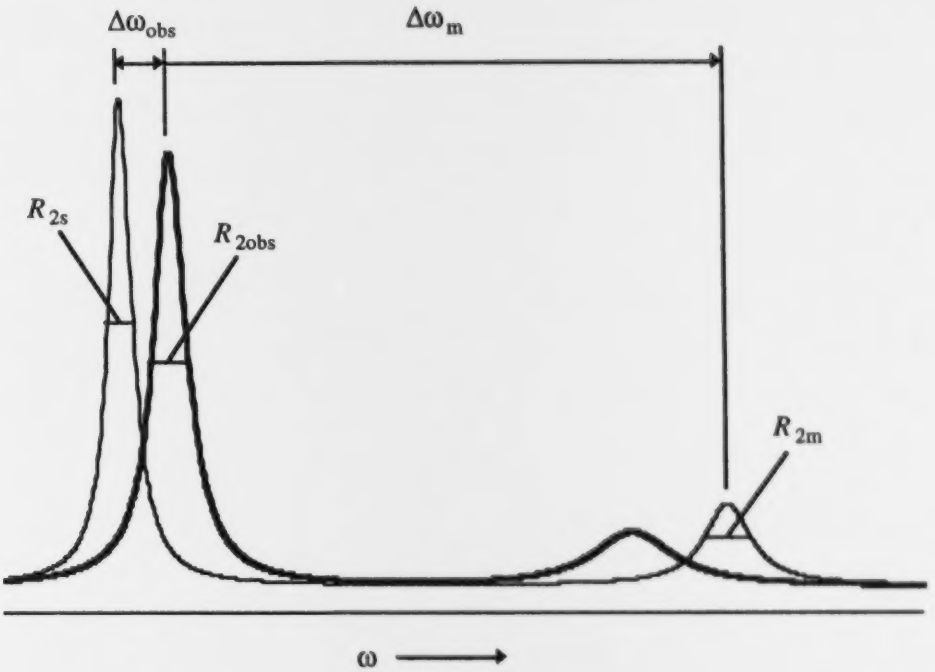

Figure 2.1. NMR spectra of solvent nuclei in the bound (right) and bulk (left) environments, in the absence (normal) and presence (bold) of chemical exchange.

shells. Since this effect is expected to be proportional to the mole fraction of metal ion in solution P_m, we may write

$$R_{2s} = R_{2solv} + P_m R_{2o} \tag{2.4}$$

Since the relaxation rates are measured at varied P_m values, it is convenient to normalize the observed data by defining

$$R_{2p} = \frac{1}{P_m}(R_{2obs} - R_{2solv}) \tag{2.5}$$

From Eq 2.4 and 2.5, we obtain

$$R_{2p} = \frac{1}{P_m}(R_{2obs} - R_{2solv}) = nr_m\left[\frac{R_{2m}(R_{2m} + r_m) + \Delta\omega_m{}^2}{(R_{2m} + r_m)^2 + \Delta\omega_m{}^2}\right] + R_{2o} \tag{2.6}$$

Eq 2.6 has been widely used and is called the modified Swift-Connick equation, or the Swift-Connick equation. The expression for the longitudinal NMR relaxation rate R_{1p}, which was given by Bloembergen and Morgan[6] and later derived by Luz and Meiboom,[5] is given by Eq 2.7

$$R_{1p} = \frac{1}{P_m}(R_{1obs} - R_{1solv}) = \frac{nr_m R_{1m}}{(R_{1m} + r_m)} + R_{1o} \tag{2.7}$$

where the R_1's are defined analogously to their corresponding R_2's. Eq 2.7 can be obtained from the Swift-Connick equation, by setting $\Delta\omega_m = 0$ and replacing the R_{2m} and R_{2o} with R_{1m} and R_{1o}.

Temperature Dependence of Solvent Relaxation Rate and Chemical Shift. The temperature dependence of the terms in the Swift-Connick equation are now discussed. The R_{im} and R_{io} (i = 1, 2) are proportional to the correlation time τ_c (see Dipolar and Scalar Relaxation Mechanisms in this section) of the paramagnetic species in the solvent, and τ_c generally follows the Debye-Stokes-Einstein relationship

$$\tau_c = \frac{4\pi a^3}{3k_B T}\eta \tag{2.8}$$

where a is the radius of the complex ion, k_B is the Boltzman constant, and η is the solvent viscosity whose temperature dependence may be given by

$$\eta = \eta_\infty \exp\left(\frac{E}{RT}\right) \tag{2.9}$$

or for water[7]

$$\eta = \eta_\infty \exp\left(\frac{E}{RT^3}\right) \tag{2.10}$$

where η_∞ and E are temperature independent constants for each solvent, and R is the ideal gas constant. Thus, the temperature dependence of inner-sphere and the outer-sphere solvent R_{im} and R_{io} (i = 1 or 2) can be described respectively by Eqs 2.11 and 2.12.

$$R_{im} = \frac{C_{im}}{T}\exp\left(\frac{E_{im}}{RT}\right) \tag{2.11}$$

$$R_{io} = \frac{C_{io}}{T}\exp\left(\frac{E_{io}}{RT}\right) \tag{2.12}$$

or for water[8]

$$R_{im} = \frac{C_{im}}{T}\exp\left(\frac{E_{im}}{RT^3}\right) \tag{2.13}$$

$$R_{io} = \frac{C_{io}}{T}\exp\left(\frac{E_{io}}{RT^3}\right) \tag{2.14}$$

where C's and E's are temperature independent parameters. The first-order solvent exchange rate constant r_m is given by the Eyring equation from transition state theory,

$$r_m = \frac{k_B T}{h}\exp\left(\frac{-\Delta H^{\ddagger} + T\Delta S^{\ddagger}}{RT}\right) \tag{2.15}$$

where $\Delta H^{\ddagger}$ and $\Delta S^{\ddagger}$ are the activation enthalpy and entropy for the solvent exchange, and h is Planck's constant . The expression for $\Delta\omega_m$ was first given by Bloembergen[9]

$$\Delta\omega_m = -\omega_0 \frac{\mu_{eff}\beta\sqrt{S(S+1)}}{3k_B T\gamma_I}\left(\frac{A}{\hbar}\right) \tag{2.16}$$

where ω_0 is the operating frequency of the NMR spectrometer, μ_{eff} is the effective magnetic moment of the paramagnetic species in solution, β is the Bohr magneton, S is the electron spin quantum number, γ_I is the proton magnetogyric ratio, and $A/\hbar$ is the scalar (hyperfine) coupling constant (in units of radians s^{-1}, or s^{-1}) of the interaction between the unpaired electron(s) on the paramagnetic site with the nuclei in the coordinated solvent. If μ_{eff} is temperature independent, then $\Delta\omega_m$ follows the Curie law

$$\Delta\omega_m = \frac{C_\omega}{T} \tag{2.17}$$

where C_ω is a temperature independent constant.

The overall temperature dependence of R_{2p} predicted by the Swift-Connick equation can now be considered.[10] A plot of log R_{2p} vs. $1/T$ is illustrated in Figure 2.2, and the curve can be analyzed in terms of various limiting conditions which depend on the relative magnitudes of R_{2m}, $\Delta\omega_m$ and r_m at different temperatures. These conditions assume that $\Delta H^{\ddagger} > E_{im} \approx E_{io}$ so that r_m has a greater temperature dependence than R_{2o} and R_{2m}, and $\Delta\omega_m$ has the smallest temperature dependence, as expected from Eq 2.17.

In Figure 2.2 at high temperature (region I), chemical exchange is faster than R_{2m} ($r_m^2 \gg R_{2m}^2, R_{2m}r_m$) and relaxation is controlled by R_{2m}.

$$R_{2p} = nR_{2m} \tag{2.18}$$

At lower temperature (region II), the chemical exchange is still fast ($r_m^2 \gg R_{2m}^2$, $R_{2m}r_m$, $\Delta\omega_m^2$; $\Delta\omega_m^2 \gg R_{2m}^2, R_{2m}r_m$), but relaxation is controlled by the dephasing due to the chemical shift difference between the bound and the bulk nuclei.

$$R_{2p} = n\frac{\Delta\omega_m^2}{r_m} \tag{2.19}$$

At still lower temperature (region III), relaxation is controlled by the rate of chemical exchange ($\Delta\omega_m^2 \gg r_m^2, R_{2m}^2$).

$$R_{2p} = nr_m \tag{2.20}$$

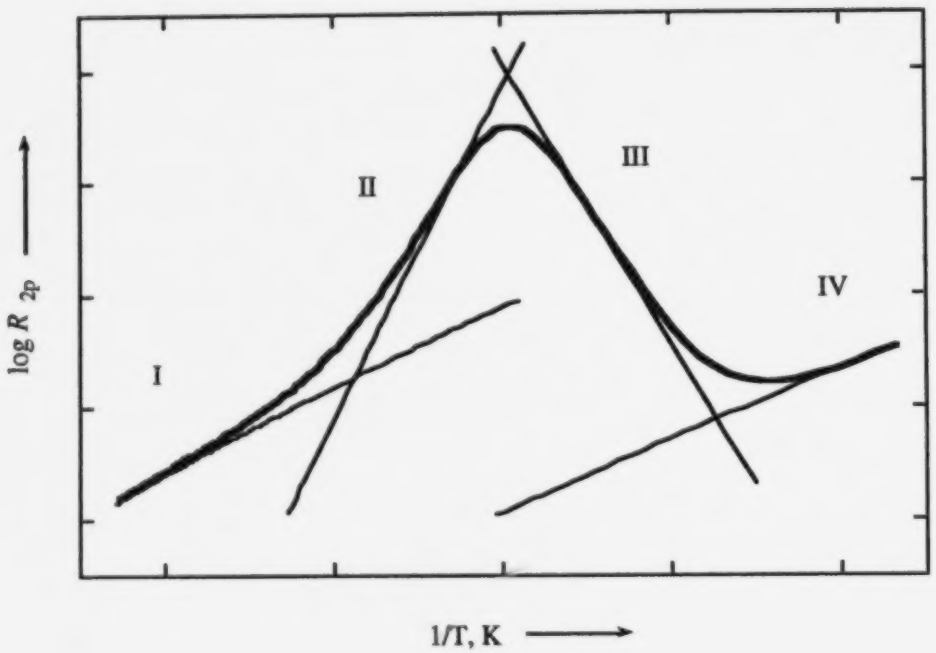

Figure 2.2. Variation of Log R_{2p} with $1/T$ as predicted by the complete Swift-Connick equation (bold). The lines (normal) represent the limiting cases as discussed in the text.

In the low temperature limit (region IV), the chemical exchange rate is so slow ($\Delta\omega_m^2 \gg r_m^2, R_{2m}^2$, and $r_m \ll R_{2o}$) that only outer-sphere relaxation contributes to the observed relaxation rate.

$$R_{2p} = R_{2o} \tag{2.21}$$

It is apparent from Figure 2.2 that analysis of the data with only one of the Swift-Connick limiting equations could result in systematically biased parameters compared to those obtained by the complete Swift-Connick equation. For example, in region III of Figure 2.2, a linear approximation to the bold curve would have a smaller slope than the correct line for r_m (Eq 2.20), and give too low an activation energy for the rate of chemical exchange. Similarly in region II, using Eq 2.19 alone and ignoring contributions from Eqs 2.18 and 2.20 would give a smaller $\Delta H^{\ddagger}$ than that given by the full Swift-Connick equation. Therefore, curve fitting of R_{2p} data in a wide temperature range to the complete Swift-Connick equation should be used to minimize the errors when obtaining the kinetic and relaxation activation parameters.

It should be noted that all four regions can rarely be observed for the accessible temperature range of one system, and some regions may not even be present in some cases. For example, if $\Delta\omega_m$ is very small, region II may not be observed at all.

Chemical Shift. Measurements of the bulk solvent chemical shift at various temperatures provide an independent method of determining the solvent exchange rate parameters according to Eq 2.3, especially when $\Delta\omega_m^2 / r_m^2$ is of the order of 1. In the fast exchange temperature region where $r_m^2 \gg R_{2m}^2, \Delta\omega_m^2$, Eq 2.3 is reduced to

$$\Delta\omega_{obs} = nP_m\Delta\omega_m \tag{2.22}$$

Thus $\Delta\omega_m$ can be obtained from the bulk solvent chemical shift measurements in the fast exchange region. However, the values are not useful in determining the C_{2m} and E_{2m} because of the difficulty of resolving R_{2m} from r_m.

Dipolar and Scalar Relaxation Mechanisms. The relaxation rates of the coordinated solvent nuclei, R_{1m} and R_{2m}, consist of two contributions representing nucleus-electron dipole-dipole and spin-spin interactions called the dipolar (R_{iDD}) and scalar (R_{iSC}) contributions, respectively. The expressions for R_{1m} and R_{2m} have been given by Solomon[11] and Bloembergen:[12]

$$R_{1m} = R_{1DD} + R_{1SC}$$

$$= \frac{2}{15}\frac{S(S+1)(\gamma_I \beta g)^2}{r^6} f_{D1}(\tau_D) + \frac{2}{3}S(S+1)\left(\frac{A}{\hbar}\right)^2 f_{e1}(\tau_e) \qquad (2.23)$$

$$R_{2m} = R_{2DD} + R_{2SC}$$

$$= \frac{1}{15}\frac{S(S+1)(\gamma_I \beta g)^2}{r^6} f_{D2}(\tau_D) + \frac{1}{3}S(S+1)\left(\frac{A}{\hbar}\right)^2 f_{e2}(\tau_e) \qquad (2.24)$$

where R_{1DD} and R_{2DD}, are the dipolar contributions to the longitudinal and transverse relaxations respectively, and R_{1SC} and R_{2SC}, are the analogous scalar contributions. In Eqs 2.23 and 2.24, g is the electron g-factor, r is the average distance between the paramagnetic metal center and the bound solvent nuclei, $f_{D1}(\tau_D)$ and $f_{D2}(\tau_D)$ are the spectral densities for dipolar interaction for longitudinal and transverse relaxations, and $f_{e1}(\tau_e)$ and $f_{e2}(\tau_e)$ are those for the longitudinal and transverse scalar relaxations, respectively. The expressions for these correlation functions are given by the following

equations:

$$f_{D1}(\tau_D) = \frac{3\tau_D}{1+\omega_n{}^2\tau_D{}^2} + \frac{7\tau_D}{1+\omega_e{}^2\tau_D{}^2} \tag{2.25}$$

$$f_{D2}(\tau_D) = 4\tau_D + \frac{3\tau_D}{1+\omega_n{}^2\tau_D{}^2} + \frac{13\tau_D}{1+\omega_e{}^2\tau_D{}^2} \tag{2.26}$$

$$f_{e1}(\tau_e) = \frac{\tau_e}{1+\omega_e{}^2\tau_e{}^2} \tag{2.27}$$

$$f_{e2}(\tau_e) = \tau_e + \frac{\tau_e}{1+\omega_e{}^2\tau_e{}^2} \tag{2.28}$$

where ω_n and ω_e are the Larmor precession frequencies of the nucleus and electron respectively, τ_D and τ_e are the dipolar and electronic correlation times, respectively, and are defined as

$$\tau_D{}^{-1} = \tau_r{}^{-1} + \tau_m{}^{-1} + T_e{}^{-1} \tag{2.29}$$

$$\tau_e{}^{-1} = \tau_m{}^{-1} + T_e{}^{-1} \tag{2.30}$$

where τ_r is the rotational correlation time characterizing the tumbling of the metal complex in the solvent, τ_m is the average lifetime of a solvent molecule bound to the metal complex, and T_e is the electron spin relaxation time[13] of the paramagnetic complex. For small metal complex species in nonviscous solvents, τ_r is ~ 10^{-11} s, and in general, $\tau_m \gg \tau_r$, thus Eqs 2.29 and 2.30 reduce to Eqs 2.31 and 2.32 respectively.

$$\tau_D^{-1} = \tau_r^{-1} + T_e^{-1} \tag{2.31}$$

$$\tau_e^{-1} = T_e^{-1} \tag{2.32}$$

The electron spin relaxation time T_e may be estimated from the linewidth of the EPR hyperfine signal of the metal complex. In practice, the EPR signals for many paramagnetic metal complexes are too broad to be reliably measured, or even observed. In general, if the solution EPR spectrum can be observed, T_e must be on the EPR time scale, i.e., $T_e > 3\times10^{-10}$ s, otherwise $T_e < 3\times10^{-10}$ s.

The relative contributions of R_{iDD} and R_{iSC} to the R_{im} (i = 1, 2) can now be discussed in terms of the magnitudes of the correlation times τ_D and τ_e, based on our experimental conditions. For proton NMR at 89.5 MHz, $\omega_n = 2\pi(89.5\times10^6) \approx 5.6\times 10^8$ s^{-1}, and $\omega_e = (\gamma_e / \gamma_H)\omega_n = 658\omega_n \approx 3.7\times10^{11}$ s^{-1} (γ_e and γ_H are the electron and proton magnetogyric ratios, respectively). If $\tau_D \approx 1\times10^{-11}$ s, then $\omega_n^2\tau_D^2 \ll 1$, and Eqs 2.25 and 2.26 simplify to

$$f_{D1}(\tau_D) = 3\tau_D + \frac{7\tau_D}{1+\omega_e^2\tau_D^2} \tag{2.33}$$

$$f_{D2}(\tau_D) = 7\tau_D + \frac{13\tau_D}{1+\omega_e^2\tau_D^2} \tag{2.34}$$

Furthermore, if τ_D is controlled by the rotational correlation time τ_r, (i.e., $T_e \gg \tau_r$) then from Eq 2.31, $\tau_D = \tau_r \approx 1\times10^{-11}$ s, and $\omega_e^2\tau_D^2 \approx 13.7$. Inserting this value into Eqs 2.33 and 2.34, gives $f_{D1}(\tau_D) \approx 3.5\tau_D$ and $f_{D2}(\tau_D) \approx 7.9\tau_D$. Substitution of these $f_{Di}(\tau_D)$ into Eqs 2.23 and 2.24 gives $R_{1DD}/R_{2DD} \approx 7/8$, i.e., the dipolar contributions for R_{1m} and R_{2m} are about the same.

For the scalar contribution, if $\tau_e = T_e > 10^{-11}$ s, then $\omega_e^2\tau_e^2 \gg 14$, and Eqs 2.27 and 2.28 give $f_{e2}(\tau_e) \approx \tau_e$ and $f_{e1}(\tau_e) < 0.07\tau_e$. Then the scalar relaxation terms in Eqs 2.23 and 2.24 show that $R_{2SC} \gg R_{1SC}$. Therefore, the difference between the R_{2m} and R_{1m} can be attributed to the transverse scalar relaxation rate , i.e.,

$$R_{2m} - R_{1m} \approx R_{2SC} = \frac{1}{3}S(S+1)\left(\frac{A}{\hbar}\right)^2 T_e \qquad (2.35)$$

On the other hand, if the electron spin relaxation time $T_e \ll \tau_r$, then both τ_D and τ_e are controlled by the T_e, i.e., $\tau_D = \tau_e = T_e$, and if $\omega_e^2\tau_e^2 \ll 1$, $f_{D1}(\tau_D) = 10T_e$; $f_{D2}(\tau_D) = 20T_e$; $f_{e1}(\tau_e) = T_e$; $f_{e2}(\tau_e) = 2T_e$. Thus, $R_{1DD} = R_{2DD}$, $R_{1SC} = R_{2SC}$, and $R_{1m} = R_{2m}$, and Eqs 2.23 and 2.24 reduce to the following form:

$$R_{2m} = R_{1m} = \left[\frac{4}{3}\frac{S(S+1)(\gamma_1\beta g)^2}{r^6} + \frac{2}{3}S(S+1)\left(\frac{A}{\hbar}\right)^2\right]T_e \qquad (2.36)$$

If $T_e \approx \tau_r$, then Eq 2.29 must be used to calculate τ_D, and the whole spectral densities of Eqs 2.33, 2.34, 2.27, and 2.28 must be calculated in order to evaluate the contributions of R_{iDD} and R_{iSC} to R_{im}.

The temperature dependence of R_{im} is due to the spectral densities, $f_{Di}(\tau_D)$ and $f_{ei}(\tau_e)$, which, in turn, are governed by the temperature dependencies of the correlation times τ_r and τ_e. Assuming τ_r and τ_e both to have an Arrhenius type temperature dependence, we will obtain the form of Eq 2.11 for R_{im}. As previously mentioned, τ_r is related to the solvent viscosity, thus its activation energy value should be similar to that of the viscosity of pure solvent. On the other hand, the temperature dependence of T_e is the property of the paramagnetic metal complex, and could be different from that of τ_r.

However, since T_e is also affected by the fluctuation of the micromagnetic field due to the tumbling of the metal complex in solution, T_e may have an activation energy similar to that of τ_r.

The outer-sphere relaxation R_{io} is due to the interaction of the unpaired electron on the metal complex and protons on solvent molecules in second or higher coordination spheres of the complex. In general, the scalar contribution to the outer-sphere relaxation is considered to be insignificant because the unpaired electron spin density on the metal center is not expected to extend beyond the ligand bound to the metal in the first coordination sphere. In this case, only the dipole-dipole interaction contributes R_{io}, and $R_{1o} \approx R_{2o}$. However, the scalar relaxation could contribute to the outer-sphere relaxation if the spin density of the unpaired electron on the metal complex center can be effectively delocalized onto the first coordination sphere ligands so that it can interact with the solvent nuclei in the second coordination sphere.

Luz and Meiboom[5] have estimated the outer-sphere dipolar relaxation by assuming a spherical shape for the metal complex and averaging the dipole-dipole interaction distance term $(1/r)^6$ by integration over the volume between the closest approach of the nuclei in the second coordination sphere, of radius d, and infinity. Following their treatment of R_{2o}, the expression for R_{1o} is derived as follows:

$$R_{1o} = \frac{2}{15}(\rho N_A S_o \times 10^{-3}) S(S+1)(\gamma_I \beta g)^2 f_{DI}(\tau_D) \int_d^\infty \frac{4\pi r^2}{r^6} dr$$

$$= \frac{8\pi}{45}(\rho N_A S_o \times 10^{-3}) \frac{S(S+1)(\gamma_I \beta g)^2}{d^3} f_{DI}(\tau_D) \qquad (2.37a)$$

$$= \frac{8.28 \times 10^{13} S(S+1) \rho S_o}{d^3} f_{DI}(\tau_D) \qquad (2.37b)$$

where ρ is the solvent density, N_A is Avogadro's number, S_o is the solvent molality, and the units for d are Ångstroms in Eq 2.37b . Meanwhile, if $R_{1m} = R_{1DD}$, inserting g, β, γ_H values (in c.g.s. units) into Eq 2.23 gives

$$R_{1m} = \frac{3.29\times10^{16}\, S(S+1)}{r^6} f_{D1}(\tau_D) \tag{2.38}$$

where r is also in Ångstroms. Thus, if $R_{1m} = R_{1DD}$ and R_{1o} is experimentally known, then one should be able to find a consistent $f_{D1}(\tau_D)$ and reasonable values of r and d which are consistent with the observed R_{1m} and R_{1o}.

The ratio of R_{1m} to R_{1o} is obtained by dividing Eq 2.38 by Eq 2.37b as follows:

$$\frac{R_{1m}}{R_{1o}} = \frac{3.97\times10^{2}}{\rho S_o}\left(\frac{d}{r}\right)^3 \frac{1}{r^3} \tag{2.39}$$

This ratio is independent of τ_D, and Eq 2.39 is useful to estimate either R_{1m} or R_{1o} if one of them can be determined experimentally, and if values of d and r are known.

Experimental Section

Materials. The monosodium salt of dimethylglyoxime, Na(dmgH), was prepared by neutralizing one proton of dimethylglyoxime. Sodium hydroxide (0.38 g 9.5×10^{-3} mol, BDH) was dissolved in ca. 3 mL of distilled water and then ca. 10 mL of methanol was added. This solution was added to 60 mL of methanol containing 1.16 g (1.0×10^{-2} mol) of dimethylglyoxime (Kodak). The resulting solution was stirred for 1 hour and filtered to remove any unreacted dimethylglyoxime. The solvent was removed by vacuum evaporation. The yellowish-white solid was washed twice with methanol and dried in vacuum.

The monosodium salt of diphenylglyoxime, Na(dpgH), was prepared by dissolving 2.4 g (1.0×10^{-2} mol) of diphenylglyoxime (Aldrich) in ca. 130 mL of 1, 4-dioxane (Caledon), and 10 mL of water containing 0.38 g (9.5×10^{-3} mol) of NaOH was added slowly while stirring. The solution was brought to room temperature and then cooled in ice overnight. Some white crystals precipitated from this solution and more were obtained by slowly adding 300 mL of hexanes. The product was washed with water several times and dried in the air.

Cobalt(II) trifluoromethanesulfonate ($Co(CF_3SO_3)_2$, cobalt triflate) was prepared by adding trifluoromethanesulfonic acid (CF_3SO_3H, Aldrich) dropwise to an aqueous suspension containing 6.3 g of $CoCO_3$ (Allied Chemical) until all the $CoCO_3$ was dissolved. The solution was then filtered and heated to evaporate the water. The pinkish-white solid was recrystallized from methanol twice, dried in vacuum at room temperature, and 15 g of dark-pink solid was obtained. The percent cobalt in the product was determined spectrophotometrically as described below and found to be 12.57%, corresponding to a experimental formula of $Co(CF_3SO_3)_2\bullet3.5CH_3OH$. The cobalt content was checked frequently and was found stable for more than two years.

The percent cobalt was determined by the method of Kitson.[14] A sample containing 0.02 mmol of cobalt was dissolved in 10 mL of water. Then 1.25 g of solid NH_4SCN (Baker) was added, and 25.00 mL of acetone was added from a pipette. The solution was brought to 25 °C, diluted to 50.00 mL with water and the absorbance at 622 nm was recorded. The amount of cobalt present was calculated using the molar extinction coefficient of 1786 M^{-1} cm^{-1}.

The $Co(dmgBF_2)_2\bullet2H_2O$ was prepared according to the published procedure.[3c] About 150 mL of diethyl ether, deoxygenated by bubbling argon, was added to a 250-mL Erlenmeyer flask containing a mixture of 2.0 g (8.0×10^{-3} mol) of $Co(OAc)_2\bullet4H_2O$ (Fisher Scientific) and 1.9 g (1.6×10^{-2} mol) of $dmgH_2$. The resulting suspension was

stirred for several minutes, and 10 mL of boron trifluoride etherate (BF_3•OEt_2, Aldrich) was added from a syringe. The mixture was stirred at room temperature under a slow stream of argon for 6 h, during which time the desired product precipitated. The brown solid obtained by filtration was washed several times with ice-cold water and methanol, and was air-dried.

The purity of the $Co(dmgBF_2)_2$•$2H_2O$ was checked by chemical analysis and spectroscopy. For percent cobalt analysis, 0.018 mmol of $Co(dmgBF_2)_2$•$2H_2O$ was dissolved in 15 mL of 1 M NaOH solution, the solution was heated and stirred on a hotplate while 2 mL of H_2O_2 solution was added slowly with a dropper over 30 min. The solution was brought to 70 - 85 °C and stirred for 2 h, during which time small portions of water were added to keep the solution volume at about 15 mL. Then the solution was acidified (pH > 2) by slowly adding 2 mL of concentrated HCl (BDH). After being boiled for 15 min to destroy any excess H_2O_2, the solution was removed from the hotplate and cooled to room temperature. The cobalt percent analysis was by Kitson's method described above. Elemental analysis for C, H and N were performed by Microanalytical Laboratory at the University of Alberta Chemistry Department. Anal. Calculated for $CoC_8H_{10}O_4B_2F_4$: Co%: 14.0; C%, 22.8; H%, 3.80; N%, 13.3. Found: Co%, 14.0; C%, 23.5; H%, 3.76; N%, 13.1.

UV-Visible spectra of $Co(dmgBF_2)_2$ in various solvents were measured on a Cary 219 spectrophotometer at room temperature. Sample solutions were prepared by adding the solvent, deoxygenated by argon, to a 50-mL volumetric flask containing a weighed amount of $Co(dmgBF_2)_2$•$2H_2O$. The solution was stirred under argon until all the solid dissolved and then transferred with a syringe to an argon-filled 1-cm cuvette sealed with a serum cap. The $Co(dmgBF_2)_2$ solution is generally much less air sensitive than that of $Co(dmgH)_2$ and the air sensitivity somewhat depends on the solvent used, aqueous solution being the most stable one. Thus, for the purpose of UV-Vis

measurement, aqueous solutions of $Co(dmgBF_2)_2$ could be prepared as above but without deoxygenation. The electronic spectrum of $Co(dmgBF_2)_2$ in water was characterized by the absorption maxima at 454, 326, and 260 nm with molar extinction coefficients of 4.00×10^3, 2.08×10^3 and 6.57×10^3 M^{-1} cm^{-1}, respectively. These values are consistent with those reported by Espenson and co-workers[3b,15] 456, 328, 260 nm with 4.06×10^3,1.92×10^3, and 5.88×10^3 $M^{-1}cm^{-1}$, respectively. The spectra were also recorded for $Co(dmgBF_2)_2$ in other solvents, and the absorption maxima (in nm) along with their molar extinction coefficients (in brackets) are: 461(4.11×10^3) and 330 (1.92×10^3) in methanol; 425 (3.10×10^3) and 328 (2.45×10^3) in acetonitrile; and 447 (3.41×10^3) in acetone.

For solvents used in NMR experiments, methanol was a Mallinckrodt reagent containing 0.013% water; acetonitrile was an Anachemia reagent containing 0.3% water; acetone was a Fisher Scientific reagent containing less than 0.05% water. All solvents were dried over 4-A molecular sieves (BDH) for at least 24 h before use.

Sample Preparation. $Co(dmgH)_2$ is especially sensitive to oxygen and must be prepared anaerobically. The solvent was dried over 4-A molecular sieves under vacuum and degassed by at least two freeze-pump-thaw cycles on a vacuum line. Then 12-15 mL of the solvent was vacuum-distilled to a pre-weighed bottle containing weighed amounts of $Co(CF_3SO_3)_2\cdot3.5CH_3OH$ (12.57% Co) and a slight stoichiometric excess of Na(dmgH). The bottle was weighed again to determine the weight of the solvent transferred. The resulting yellow-orange solution was transferred under vacuum to a 10-mm flat-bottom NMR tube (Wilmad Glass Co) and sealed under vacuum. The molar concentration of the $Co(dmgH)_2$ complex in each sample solution was calculated from the weights of cobalt and solvent, and the density of the solvent.

$Co(dpgH)_2$ samples were prepared in the same way as above from $Co(CF_3SO_3)_2\cdot3.5CH_3OH$ and Na(dpgH). For $Co(dmgBF_2)_2$ samples, solvent was

distilled onto $Co(dmgBF_2)_2 \cdot 2H_2O$ instead of a mixture a cobalt and ligand salts as in the preparation of the other two complexes.

NMR Measurements. A Bruker SXP pulse spectrometer operating at 89.5 MHz was used.[16] Pulses were generated and data collected with a Nicolet Instrument Corp. Model 1180 computer and 293A programmable pulser. Relaxation rate data were collected and analyzed by using programs developed in these laboratories. The sample volume (0.8-1.2 cm^3) was less than that of the H_1 coil to avoid problems associated with inhomogeneity in the H_1 field. Temperature was controlled by the Bruker B-ST 100/700 temperature control unit for above room temperature measurements. For low temperature measurement, a stream of nitrogen gas, cooled by either methanol-dry ice or liquid nitrogen, passed through the NMR probe. Temperature was measured before and after each set of experiments with a copper-constantan thermocouple inserted into the corresponding solvent contained in an NMR sample tube. The stability of the temperature was ± 0.5 °C over the typical recording time of 0.5 - 2 h.

Longitudinal Relaxation Rates (R_1). These were measured by the standard 180°- τ - 90° pulse sequence by using fifteen to eighteen τ values in the range of 0.8-3.5T_1 (T_1 is the longitudinal relaxation time, $T_1 = 1/R_1$). The delay time between each measurement was at least 5T_1. Data analysis was by a standard least-squares method for one exponential decay and the reported values were the average of five replicate measurements, with a typical standard deviation of less than 2%.

Transverse Relaxation Rates (R_2). These were measured by the Carr-Purcell-Meiboom-Gill (CPMG) pulse sequence.[17] At least 200 echoes were collected under computer control and the data were analyzed by a least-squares method. The typical t_{cp}, which is the time interval between the pulses in the CPMG experiment, is 0.2 to 0.6 ms. The reported R_2 values were the average of at least five replicate determinations, with a standard deviation of less than 5%.

Shift Measurements. Samples of more concentrated $Co(dmgH)_2$ solutions for shift measurements was prepared as described above. In each case, the $Co(dmgH)_2$ solution was transferred under vacuum to a standard 5-mm NMR tube (Wilmad Glass) containing an internal standard, *p*-dimethoxybenzene (Kodak) and cyclohexane (Fisher Scientific) were used as internal standards for acetonitrile and methanol samples, respectively. The chemical shift of the solvent proton relative to internal standards was recorded on a Bruker AM 300 MHz NMR at 35 °C.

Results

The temperature dependence of solvent proton relaxation rates R_{1obs} and R_{2obs} were measured for three cobaloxime(II) complexes, $Co(dmgH)_2$, $Co(dmgBF_2)_2$ and $Co(dpgH)_2$ in various solvents. The R_{iobs} data were corrected for pure solvent relaxation[18] and normalized by P_m according to Eq 2.5, then analyzed by least-squares fittings to Eqs 2.7 and 2.8 to determine as many as possible of the parameters $\Delta H^{\ddagger}$, $\Delta S^{\ddagger}$ for solvent exchange, and C_{im}, C_{io}, E_{im}, E_{io}, and $|C_{\omega}|$. The solvent NMR shifts could be measured in some cases to provide an independent value of C_{ω}. There is still an uncertainty about the solvation number of the Co(II) macrocyclic complexes in solutions.[19] For the present analysis a solvation number $n = 1$ is assumed. If $n = 2$, then the values of C_{im}, C_{ω} and the solvent exchange rates would decrease by a factor of 2. This corresponds to a decrease of $R\ln 2 \approx 1.38$ cal mol^{-1} K^{-1} for the $\Delta S^{\ddagger}$ values given. The parameter C_{io} does not depend on the value of n according to Eq 2.9.

$Co(dmgH)_2$ in Acetonitrile. The temperature dependence of solvent proton relaxation rates for this system were measured from - 43 to 35 °C, and the Log R_{ip} vs. $1/T$ plots are shown in Figure 2.3. From the previous discussion, the Log R_{2p} curve in Figure 2.3 shows regions corresponding to those of I, II, and III in Figure

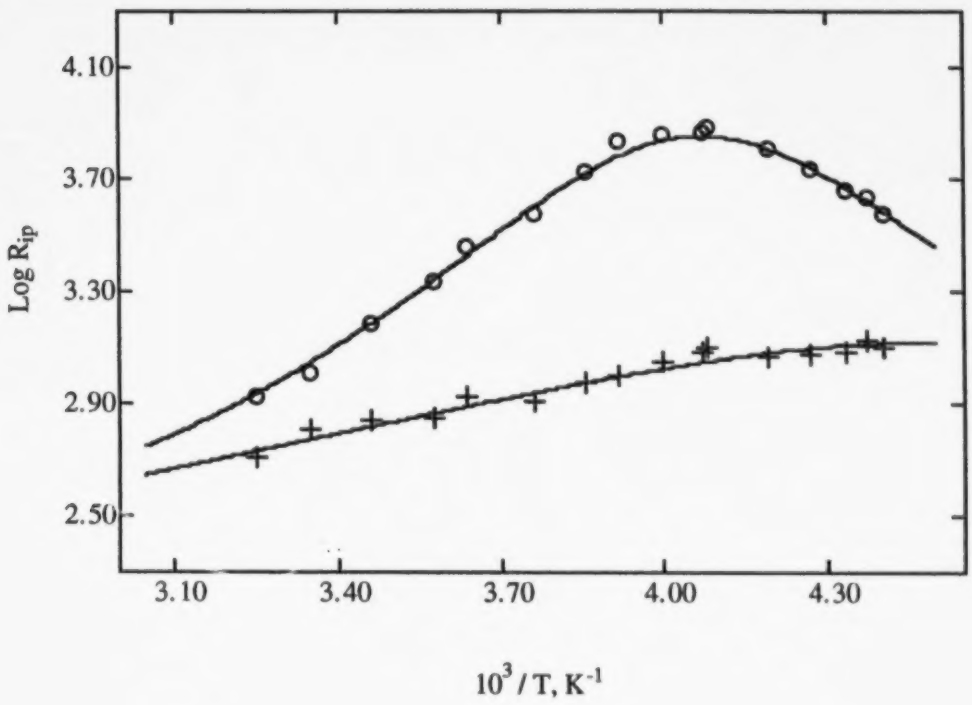

Figure 2.3. Temperature dependence of solvent proton transverse (R_{2p}, o) and longitudinal (R_{1p}, +) relaxation rates for the acetonitrile solution of $Co(dmgH)_2$. (P_m = 2.73×10^{-4}, the fitting curves are calculated values based on parameters in Table 2.1)

2.2. The outer-sphere region IV cannot be observed above the freezing point of the solvent. The Log R_{1p} vs. $1/T$ is close to a straight line and not sensitive to the solvent exchange, as expected from Eq 2.7 when $r_m \gg R_{1m}$, since then $R_{1p} \approx R_{1m} + R_{1o}$.

The analysis of the temperature dependence of the R_{ip} data is based on the following considerations. First, since R_{1m} and R_{1o} are likely to have the same temperature dependence, it is assumed that $E_{1m} = E_{1o}$. The value of E_{1m} or E_{1o} can be estimated from the slope of the Log R_{1p} plot in Figure 2.3. Then, the value of C_{1o} is calculated from the estimated E_{1o} value and Eq 2.37b by using $d = 5.3$ Å and $\tau_r = 6.2\times10^{-11}$ s ($= \tau_D$) as determined in a previous study on low-spin Co(*trans*-[14]diene)$^{2+}$ in acetonitrile.[4] Then least-squares fitting of R_{1p} and R_{2p} data together was performed by fixing C_{1o} at the calculated value and assuming that $E_{2m} = E_{2o} = E_{1m} = E_{1o}$, $C_{2o} = C_{1o}$ and $C_{2m} = C_{1m}$ to yield $\Delta H^{\ddagger}$, $\Delta S^{\ddagger}$, C_{im}, E_{1m}, and $|C_\omega|$. It should be noted that the last assumption was required in this case to avoid obtaining $C_{2m} < C_{1m}$ since in any event, $R_{2m} \geq R_{1m}$. The fitting was repeated by adjusting the C_{1o} value until the most self-consistent parameters were obtained. The best-fit parameters and the calculated $|A/\hbar|$ and T_e values are listed in Table 2.1 and these give the calculated curves in Figure 2.3. The observed and calculated relaxation rates are given in Table A-1 in the Appendix.

The solvent proton paramagnetic shift relative to that of pure solvent for the $Co(dmgH)_2$ in acetonitrile was measured at 300 MHz and 35 °C, and the shift in ppm was converted to Hz at the operating frequency of 89.5 MHz for the relaxation rate measurement. The shift value was used to calculate C_ω and then the scalar coupling constant $A/\hbar$ according to Eqs 2.16 and 2.17 respectively. The result (Table 2.2) shows that the C_ω value is in good agreement with that from the R_{2p} fit (Table 2.1).

$Co(dmgH)_2$ in Methanol. The relaxation rates were measured for this system from - 89 to 60 °C, and are plotted in Figure 2.4. The Log R_{2p} curve shows regions corresponding to those of II, III and IV in Figure 2.2. The extreme fast

Table 2.1. Least-Squares Best-Fit Parameters for the Temperature Dependence of the Solvent Proton Relaxation Rates in Acetonitrile Solution of $Co(dmgH)_2$

Parameters	Values[a]
$\Delta H^{\ddagger}$ (kcal mol^{-1})	7.24 ± 0.19
$\Delta S^{\ddagger}$ (cal mol^{-1} K^{-1})	$- 9.76 \pm 0.73$
k (s^{-1}), 25 °C[b]	2.3×10^{5}
$C_{1m} = C_{2m}$ (s^{-1} K)	$(1.42 \pm 0.28)\times10^{4}$
$E_{im} = E_{io}$ (kcal mol^{-1})	1.32 ± 0.07
$C_{1o} = C_{2o}$ (s^{-1} K)	5000[c]
$\lvert C_{\omega}\rvert$ (s^{-1} K)	$(3.38 \pm 0.08)\times10^{6}$
$\lvert A/\hbar\rvert$ (s^{-1})[d]	4.76×10^{6}
T_e (s), 25 °C[e]	$< 1.5\times10^{-11}$

[a] The errors given are one standard deviation. [b] k is the first-order solvent exchange rate constant at 25 °C calculated from the $\Delta H^{\ddagger}$ and $\Delta S^{\ddagger}$ values listed above. [c] This value is fixed in the least-squares fitting to obtain the other parameters in the Table. [d] $\lvert A/\hbar\rvert$ is calculated from Eq 2.16 by using the $\lvert C_{\omega}\rvert$ value listed above. [e] The upper limit of T_e value is estimated from Eq 2.35 by using the values of $\lvert A/\hbar\rvert$ and E_{im} listed above, and by assuming an upper limit of one standard deviation of C_{im} for $(C_{2m} - C_{1m})$.

Table 2.2. Solvent Proton Chemical Shifts (300 MHz) and the Scalar Coupling Constants of $Co(dmgH)_2$ Solutions in Acetonitrile and Methanol at 35 °C

Parameters	Acetonitrile[a]	Methanol[b]
δ (ppm)		
— CH_3	- 0.019 ± 0.0024[c]	+0.032 ± 0.0024[c]
— OH	—	+0.030 ± 0.0024[c]
C_ω (s^{-1} K)[d]	-3.5×10^6	$+1.0\times10^7$ (CH_3), $+9.6\times10^6$(OH)
$A/\hbar$ (s^{-1})[e]	-4.9×10^6	$+1.5\times10^7$ (CH_3), $+1.4\times10^7$(OH)

[a] $P_m = 9.55\times10^{-4}$. [b] $P_m = 5.90\times10^{-4}$. [c] The errors given are the resolution limit of the NMR spectrometer. [d] From Eq. 2.17 with the shifts converted to rad s^{-1} at 89.5 MHz, and the number of bound solvent was assumed to be 1, i.e., $n = 1$ in Eq 2.21. [e] From Eq 2.16.

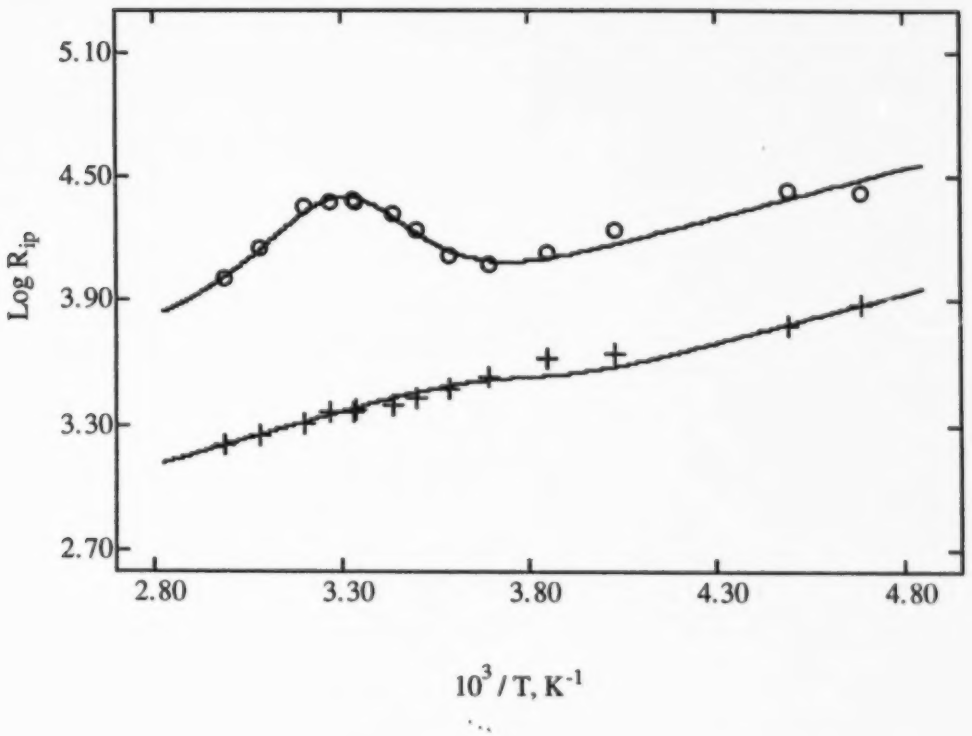

Figure 2.4. Temperature dependence of solvent proton transverse (R_{2p}, o) and longitudinal (R_{1p}, +) relaxation rates for the methanol solution of $Co(dmgH)_2$. (P_m = 1.21×10^{-4}, the fitting curves are calculated values based on parameters in Table 2.3)

exchange region I, where the relaxation is controlled by the R_{im}, is not well defined in this system. In the lowest temperature outer-sphere region (IV), the R_{2p} and R_{1p} plots are parallel, indicating that $E_{io} \approx E_{2o}$. The difference in magnitude of R_{2p} and R_{1p} in this region is attributed to an outer-sphere scalar relaxation contribution according to the discussion in the Basic Equations section.

The R_{ip} data were analyzed first by assuming that $E_{1o} \approx E_{1m}$ and that both R_{1m} and R_{1o} are due to dipolar relaxation. Taking r = 4.8 Å and d = 9.4 Å from the methanol methyl proton results for Co(*trans*-[14]diene)$^{2+}$ in CH_3OH,[4] one can use Eq 2.39 to calculate the ratio $C_{1m}/C_{1o} \approx 0.5$. Then, by assuming $E_{1m} = E_{2m} = E_{1o} = E_{1o}$ and $C_{1m} = 0.5C_{1o}$, the R_{1p} and R_{2p} were fitted to yield the $\Delta H^{\ddagger}$, $\Delta S^{\ddagger}$, C_{2m}, E_{im}, C_{1o}, C_{2o}, and $|C_{\omega}|$. The best-fit results are listed in Table 2.3 and are shown by the calculated curves in Figure 2.4. The observed and calculated relaxation rates are given in Table A-2 in the Appendix.

The positive $\Delta S^{\ddagger}$ value in Table 2.3 is in contrast to the negative $\Delta S^{\ddagger}$ values for the acetonitrile solution and other systems studied hereafter. This difference will be addressed in the Discussion section. For the purpose of discussion, the experimental R_{ip} data were also fitted by fixing the $\Delta S^{\ddagger}$ at various negative values from -10 to -4 cal mol^{-1} K^{-1}. Other conditions are kept the same as those described above except that C_{2m} is now required to equal C_{1m} to avoid obtaining a negative C_{2m} value. In all cases, the convergence can be achieved, and the standard error of the least-squares fit decreases upon change of $\Delta S^{\ddagger}$ to less negative values. The standard error of fitting could still be kept within 5% of that for the best-fit in Figure 2.4 by fixing the $\Delta S^{\ddagger}$ value at -6 cal mol^{-1} K^{-1}. More negative $\Delta S^{\ddagger}$ values increase the standard error of the fit rapidly, while more positive values do not improve the fitting significantly. Thus, $\Delta S^{\ddagger}$ = -6 cal mol^{-1} K^{-1} was chosen and the corresponding fitting results are listed in Table 2.4 and shown in Figure 2.5. The observed and calculated relaxation rates are listed in Table A-3 in the

Table 2.3. Least-Squares Best-Fit Parameters for the Temperature Dependence of the Solvent Proton Relaxation Rates in Methanol Solution of $Co(dmgH)_2$

Parameters	Values[a]
$\Delta H^{\ddagger}$ (kcal mol^{-1})	13.9 ± 0.24
$\Delta S^{\ddagger}$ (cal mol^{-1} K^{-1})	8.30 ± 0.64
k (s^{-1}), 25 °C[b]	2.8×10^{4}
C_{1m} (s^{-1} K)	1.28×10^{4} [c]
C_{2m} (s^{-1} K)	$(7.74 \pm 2.31)\times10^{4}$
$E_{im} = E_{io}$ (kcal mol^{-1})	1.76 ± 0.10
C_{1o} (s^{-1} K)	$(2.55 \pm 0.45)\times10^{4}$
C_{2o} (s^{-1} K)	$(1.03 \pm 0.22)\times10^{5}$
$\lvert C_{\omega}\rvert$ (s^{-1} K)	$(1.13 \pm 0.06)\times10^{7}$
$\lvert A/\hbar\rvert$ (s^{-1})[d]	1.60×10^{7}
T_e (s), 25 °C[e]	6.6×10^{-11}

[a] The errors given are one standard deviation. [b] k is the first-order solvent exchange rate constant at 25 °C calculated from the $\Delta H^{\ddagger}$ and $\Delta S^{\ddagger}$ values listed above. [c] This value is assumed to be half of that of C_{1o} in the least-squares fitting. [d] $\lvert A/\hbar\rvert$ is calculated from Eq 2.16 by using the C_{ω} value listed above. [e] T_e is calculated from Eq 2.35 by using the C_{1m}, C_{2m}, and $\lvert A/\hbar\rvert$ values listed above.

Table 2.4. Least-Squares Fit Parameters for the Temperature Dependence of the Solvent Proton Relaxation Rates in Methanol Solution of $Co(dmgH)_2$ at $\Delta S^{\ddagger}$ = -6 cal mol^{-1} K^{-1}

Parameters	Values[a]
$\Delta H^{\ddagger}$ (kcal mol^{-1})	9.7 ± 0.05
$\Delta S^{\ddagger}$ (cal mol^{-1} K^{-1})	-6[b]
k (s^{-1}), 25 °C[c]	2.4×10^{4}
$C_{1m} = C_{2m}$ (s^{-1} K)	1.12×10^{4} [d]
$E_{im} = E_{io}$ (kcal mol^{-1})	1.83 ± 0.10
C_{1o} (s^{-1} K)	$(2.24 \pm 0.40)\times10^{4}$
C_{2o} (s^{-1} K)	$(8.41 \pm 1.81)\times10^{4}$
$\lvert C_{\omega}\rvert$ (s^{-1} K)	$(1.07 \pm 0.05)\times10^{7}$
$\lvert A/\hbar\rvert$ (s^{-1})[d]	1.51×10^{7}

[a] The errors given are one standard deviation. [b] This value is fixed in getting the other parameters in the table. [c] k is the first-order solvent exchange rate constant at 25 °C calculated from the $\Delta H^{\ddagger}$ and $\Delta S^{\ddagger}$ values listed above. [d] This value is assumed to be half of that of C_{1o} in the least-squares fitting.

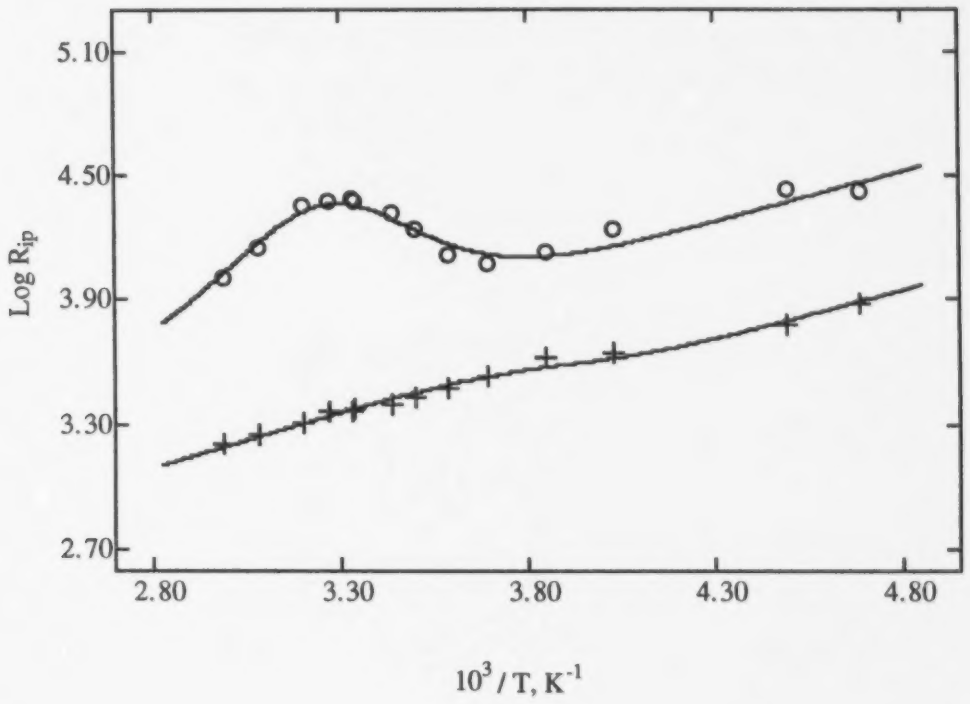

Figure 2.5. Refit of temperature dependence of solvent proton transverse (R_{2p}, o) and longitudinal (R_{1p}, +) relaxation rates for the methanol solution of $Co(dmgH)_2$ at $\Delta S^{\ddagger}$ = -6 cal mol^{-1} K^{-1}. ($P_m = 1.21 \times 10^{-4}$, the fitting curves are calculated values based on parameters in Table 2.4)

Appendix.

The solvent proton paramagnetic shifts of the methyl and hydroxyl group were measured and the results are shown in Table 2.2. The magnitude of the scalar coupling constant calculated from the paramagnetic shifts is in good agreement with those obtained from the R_{2p} fit in Table 2.3 and Table 2.4.

$Co(dmgBF_2)_2$ in Acetonitrile. The relaxation rates for this system were measured from 26 to -40 °C and are plotted in Figure 2.6. The solvent exchange region appears in the Log R_{2p} only as a slight leveling-off at low temperatures so that the whole exchange region is not defined. Other regions of the R_{2p} plot are similar to those described in $Co(dmgH)_2$–CH_3CN system.

The analysis of R_{ip} data was similar to that in $Co(dmgH)_2$–CH_3CN. The best-fit parameters are listed in Table 2.5 and shown by the calculated curves in Figure 2.6. The observed and calculated relaxation rates are given in Table A-4 in the Appendix.

The paramagnetic shift of the solvent for a concentrated sample solution of $P_m = 2.12\times10^{-4}$ for this system is only ~ 0.003 ppm and not reliable at all since this value is almost the same as the resolution limit of the NMR spectrometer as noted in Table 2.2. Nonetheless, the very small paramagnetic shift observed is consistent with the predicted shift of only ~ 0.0012 ppm at 300 MHz and 35 °C from Eqs 2.17 and 2.22 by using the $|C_\omega|$ value from Table 2.3 and the P_m value for this sample.

$Co(dmgBF_2)_2$ in Acetone. Acetone was chosen as a solvent because the complex is more soluble in acetone than in methanol. Since the relaxation rate of acetone is not available, as a preliminary experiment, the relaxation rate R_1 of pure acetone solvent was measured from -90 to 25 °C. The data (listed in Table A-5 in the Appendix) could be fitted well by the equation $R_1 = (C/T)exp(E/RT)$, with $C = 1.63 \pm 0.30$ s^{-1} K and $E = 1.375 \pm 0.082$ kcal mol^{-1}.

The relaxation rates for this system were measured at various temperatures from

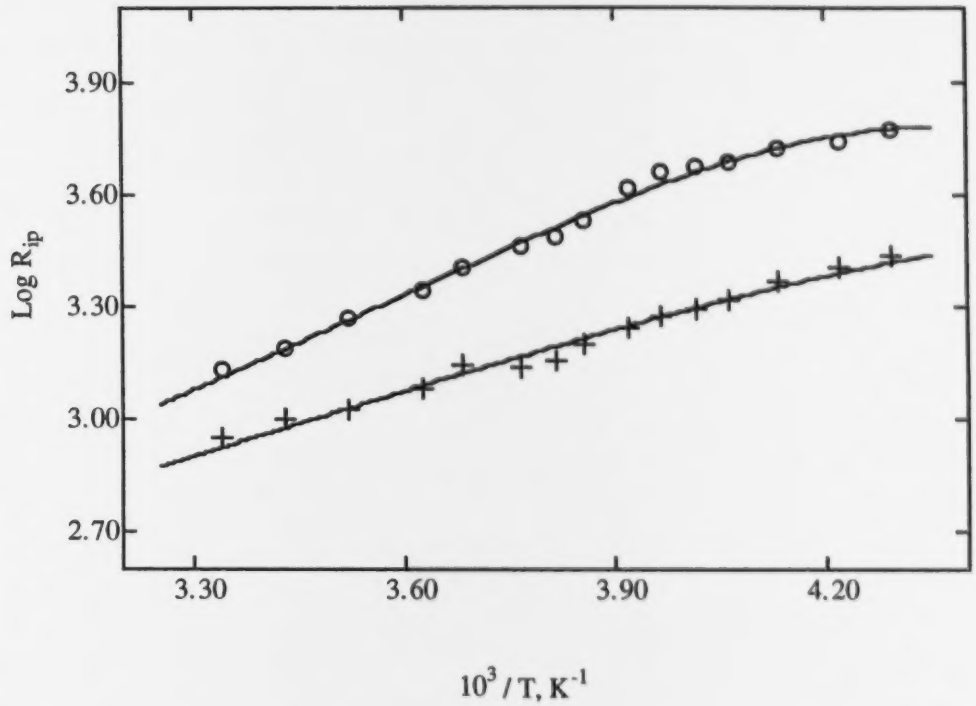

Figure 2.6. Temperature dependence of solvent proton transverse (R_{2p}, o) and longitudinal (R_{1p}, +) relaxation rates for the acetonitrile solution of $Co(dmgBF_2)_2$. ($P_m = 2.42\times10^{-4}$, the fitting curves are calculated values based on parameters in Table 2.5)

Table 2.5. Least-Squares Best-Fit Parameters for the Temperature Dependence of the Solvent Proton Relaxation Rates in Acetonitrile Solution of $Co(dmgBF_2)_2$

Parameters	Values[a]
$\Delta H^{\ddagger}$ (kcal mol^{-1})	4.33 ± 0.26
$\Delta S^{\ddagger}$ (cal mol^{-1} K^{-1})	-20.5 ± 0.95
k (s^{-1}), 25 °C[b]	1.4×10^{5}
$C_{1m} = C_{2m}$ (s^{-1} K)	$(5.88 \pm 1.14)\times10^{3}$
$E_{im} = E_{io}$ (kcal mol^{-1})	2.12 ± 0.08
$C_{1o} = C_{2o}$ (s^{-1} K)	1300[c]
$\lvert C_{\omega}\rvert$ (s^{-1} K)	$(2.40 \pm 0.10)\times10^{6}$
$\lvert A/\hbar\rvert$ (s^{-1})[d]	3.39×10^{6}
T_e (s), 25 °C[e]	$< 4.8\times10^{-11}$

[a] The errors given are one standard deviation. [b] k is the first-order solvent exchange rate constant at 25 °C calculated from the $\Delta H^{\ddagger}$ and $\Delta S^{\ddagger}$ values listed above. [c] This value is fixed during the least-squares fitting to obtain the other parameters in the table. [d] $\lvert A/\hbar\rvert$ is calculated from Eq 2.16 by using the C_{ω} value listed above. [e] The upper limit of T_e value is estimated from the Eq 2.35 by using the $\lvert A/\hbar\rvert$ and E_{im} listed above, and by assuming an upper limit of one standard deviation of C_{im} for $(C_{2m} - C_{1m})$.

-92 to 26 °C and corrected for pure solvent relaxation, and the R_{ip} plots are shown in Figure 2.7. The R_{2p} plot is similar to that of $Co(dmgBF_2)_2$–CH_3CN in Figure 2.6 in that the solvent exchange region is not well defined, and only appears as a bending of the curve at low temperature.

Quantitative data analysis was started with R_{1p} by estimating the E_{1m} and assuming $E_{1m} = E_{1o}$. Estimation of either C_{1m} or C_{1o} is complicated here because neither d nor r values for acetone are available. However, r can be approximated by using the bond lengths and angles of the acetone molecule (Co-O-C = 130°[20] and Co–O bond length of 2.3 Å are assumed[21]). An average r value of 4.7 Å is estimated for the methyl protons of the acetone by simple geometry. As expected, this r value is between that for CH_3CN (5.3 Å) and that of the methyl protons for CH_3OH (3.9 Å) for Co(*trans*-[14]diene)$^{2+}$ systems.[4] Since acetone and acetonitrile have similar viscosities at 25 °C,[22] it seems reasonable to assume that the $\tau_r (= \tau_D)$ in acetone will be the same as that for Co(*trans*-[14]diene)$^{2+}$ in CH_3CN.[4] Then the R_{1m} value at 25 °C can be estimated from Eq 2.38 and the difference between the observed R_{1p} and the R_{1m} at 25 °C is attributed to R_{1o}, which can be used to calculate C_{1o} with the estimated E_{1o} ($= E_{1m}$). The rest of the analysis is similar to that described for $Co(dmgH)_2$–CH_3CN except that it was not necessary to fix C_{2m} equal to C_{1m} during the fitting. The final results are given in Table 2.6 and the calculated curves are shown in Figure 2.7. The observed and calculated relaxation rates are given in Table A-6 in the Appendix.

The solvent paramagnetic shift for a sample with $P_m = 6.60\times10^{-4}$ at 35°C is only ~0.0025 ppm at 300 MHz. The shift, like that in $Co(dmgBF_2)_2$–CH_3CN, is too small to be reliable, but in agreement with a shift value of only 0.0016 ppm predicted by the $|C_\omega|$ in Table 2.6 for this sample.

$Co(dpgH)_2$ in Acetonitrile. The Log R_{2p} plot for this system in Figure 2.8 shows no sign of a solvent exchange region but is just a straight line. This could be

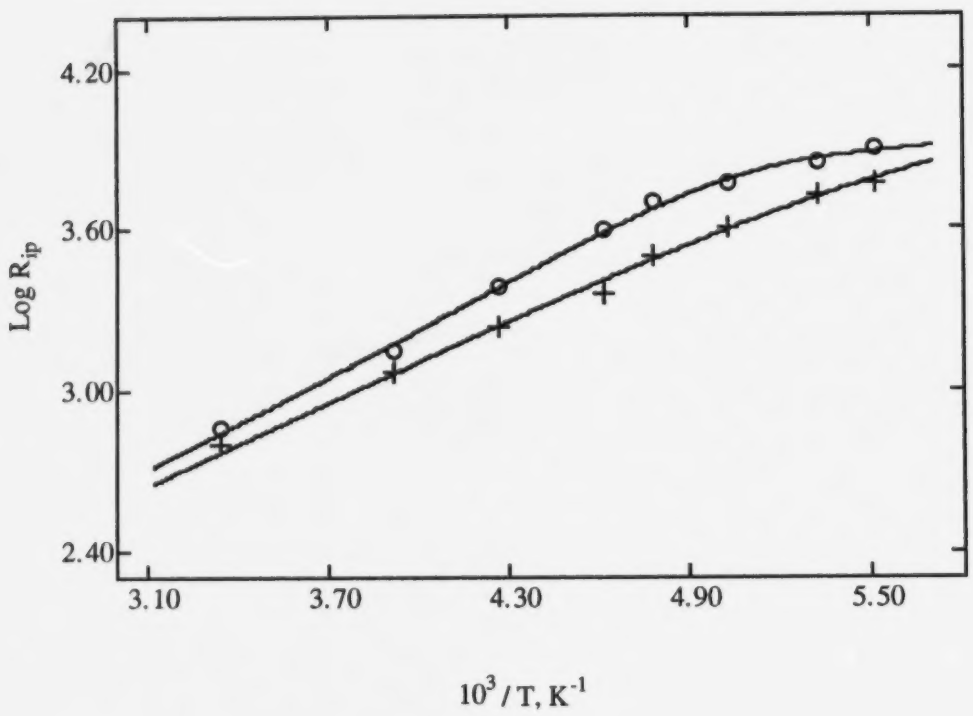

Figure 2.7. Temperature dependence of solvent proton transverse (R_{2p}, o) and longitudinal (R_{1p}, +) relaxation rates for the acetone solution of $Co(dmgBF_2)_2$. (P_m = 5.22×10^{-4}, the fitting curves are calculated values based on parameters in Table 2.6)

Table 2.6. Least-Squares Best-Fit Parameters for the Temperature Dependence of the Solvent Proton Relaxation Rates in Acetone Solution of $Co(dmgBF_2)_2$

Parameters	Values[a]
$\Delta H^{\ddagger}$ (kcal mol^{-1})	3.38 ± 0.90
$\Delta S^{\ddagger}$ (cal mol^{-1} K^{-1})	-21.8 ± 4.75
k (s^{-1}), 25 °C[b]	3.5×10^{5}
C_{1m} (s^{-1} K)	$(3.25 \pm 0.93)\times10^{3}$
C_{2m} (s^{-1} K)	$(4.02 \pm 1.41)\times10^{3}$
$E_{im} = E_{io}$ (kcal mol^{-1})	1.82 ± 0.05
$C_{1o} = C_{2o}$ (s^{-1} K)	5000[c]
C_{ω} (s^{-1} K)	$(1.32 \pm 0.20)\times10^{6}$
$\lvert A/\hbar \rvert$ (s^{-1})[d]	1.87×10^{6}
T_e (s), 25 °C[e]	6.4×10^{-11}

[a] The errors given are one standard deviation. [b] k is the first-order solvent exchange rate constant at 25 °C calculated from the $\Delta H^{\ddagger}$ and $\Delta S^{\ddagger}$ values listed above. [c] This value was not varied during the least-squares fitting. [d] $\lvert A/\hbar \rvert$ is calculated from Eq 2.16 by using the $\lvert C_{\omega} \rvert$ value listed above. [e] T_e is calculated from Eq 2.35 by using the C_{1m}, C_{2m}, E_{im}, and $\lvert A/\hbar \rvert$ values listed above.

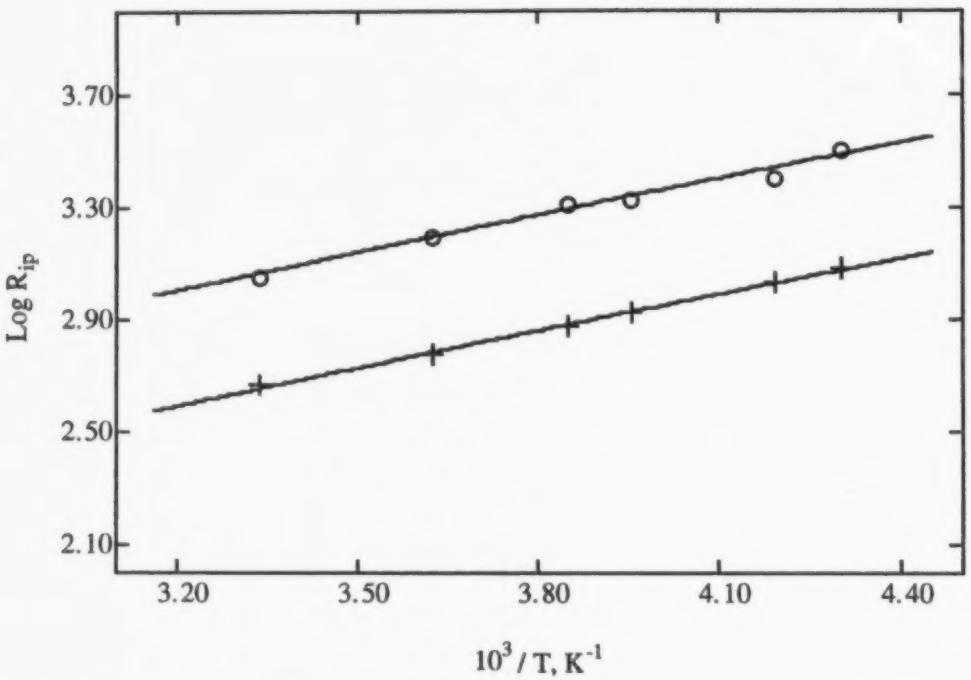

Figure 2.8. Temperature dependence of solvent proton transverse (R_{2p}, o) and longitudinal (R_{1p}, +) relaxation rates for the acetonitrile solution of $Co(dpgH)_2$. (P_m = 3.88×10^{-4}, the fitting lines are calculated values based on parameters in Table 2.7)

attributed to either region I for inner-sphere relaxation R_{2m} or region IV for outer-sphere relaxation R_{2o}.

The R_{1p} and R_{2p} data were fitted separately by the equation $R_{ip} = (C_i/T)\exp(E_i/RT)$ and the results are listed in Table 2.7. The observed and calculated relaxation rates are listed in Table A-6 in the Appendix. As expected, the E_1 and E_2 are essentially the same. In order to determine if the system is in region I or IV, values of R_{1m} and R_{1o} at 298 K were calculated using the d, r and τ_r ($=\tau_D$) values for Co(*trans*-[14]diene)$^{2+}$ in CH_3CN.[4] These estimates give $R_{1m} = 4.0\times10^2$ s^{-1} and $R_{1o} = 1.6\times10^2$ s^{-1}, compared to the experimental value of 4.6×10^2 s^{-1}. Therefore it appears that the system is in region I where the relaxation is equal to $R_{im} + R_{io}$, and dominated by R_{im}.

With the limiting condition that $r_m > R_{2m}$, a lower limit of 3×10^3 s^{-1} is calculated for the solvent exchange rate at -45 °C in this system.

Co(dpgH)$_2$ in Methanol. The experimental R_{ip} data are plotted in Figure 2.9 for this system, and the Log R_{ip} plots are similar to those of Co(dmgBF$_2$)$_2$ in acetonitrile and acetone in that the solvent exchange region is evident but is not well defined. The parallel dependence of R_{2p} and R_{1p} on temperature in region I indicates that $E_{1m} \approx E_{2m}$. The large difference between R_{2p} and R_{1p} can be attributed to the inner-sphere scalar relaxation contribution.

The R_{ip} data were first analyzed by assuming $C_{1m} = 0.5C_{1o}$, as for Co(dmgH)$_2$ in CH_3OH, $E_{1m} = E_{2m} = E_{1o} = E_{2o}$ and $C_{1o} = C_{2o}$. However, convergence of the least-squares fitting can only be obtained by fixing the C_{2m} value. For C_{2m} values in the range of 660-8000 s^{-1} K, the least-squares fits have essentially the same variance. The lower limit of C_{2m} is set by the C_{1m} value which is half of that of C_{1o}, while for $C_{2m} > 8000$, convergence could not be attained. The best-fit parameters corresponding to C_{2m} values of 660 and 8000, respectively are both listed in Table 2.8 and the curves in Figure 2.9 were calculated by a set of parameters obtained from the fitting by assuming a middle

Table 2.7. Least-Squares Best-Fit Parameters for the Temperature Dependence of the Solvent Proton Relaxation Rates in Acetonitrile Solutions of $Co(dpgH)_2$

Parameters	Values[a]
C_1 (s^{-1} K)	$(1.11 \pm 0.12) \times 10^4$
C_2 (s^{-1} K)	$(2.95 \pm 0.72) \times 10^4$
E_1(kcal mol^{-1})	1.49 ± 0.05
E_2 (kcal mol^{-1})	1.46 ± 0.12

[a] The errors given are one standard deviation.

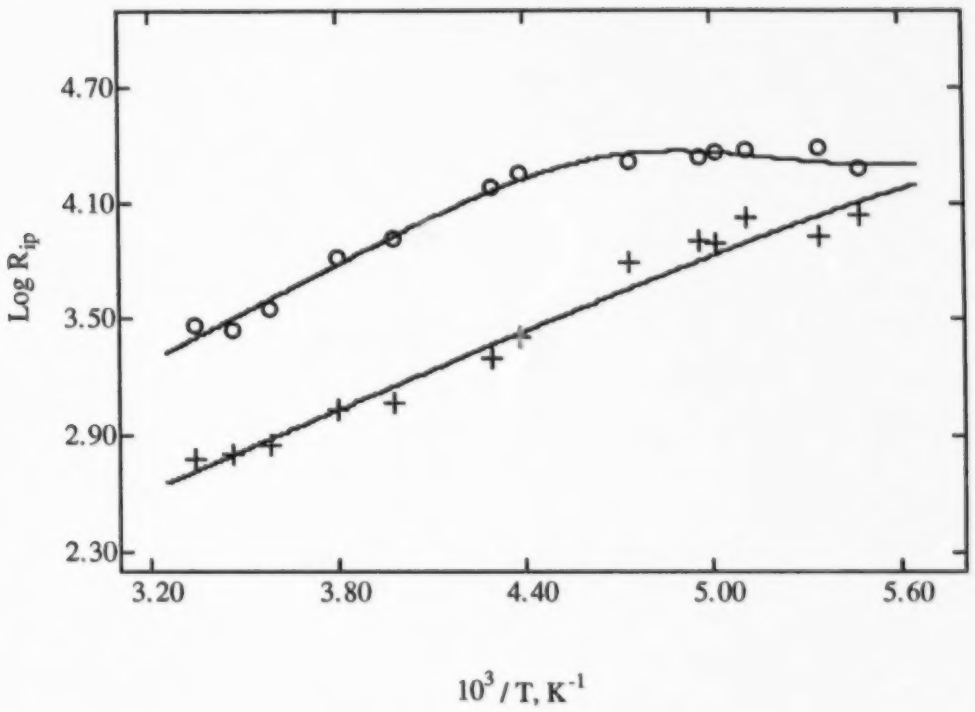

Figure 2.9. Temperature dependence of solvent proton transverse (R_{2p}, o) and longitudinal (R_{1p}, +) relaxation rates for the methanol solution of $Co(dpgH)_2$. (P_m = 1.82×10^{-4}, the fitting curves are calculated values based on a set of parameters in Table 2.8 with C_{2m} fixed at 5000 s^{-1} K)

Table 2.8. Least-Squares Best-Fit Parameters for the Temperature Dependence of the Solvent Proton Relaxation Rates in Methanol Solutions of $Co(dpgH)_2$

Parameters	Values[a]		
$\Delta H^{\ddagger}$ (kcal mol^{-1})	2.78 ± 1.86	3.35 ± 0.42	3.81 ± 0.84
$\Delta S^{\ddagger}$ (cal mol^{-1} K^{-1})	-23.7 ± 0.9	-20.5 ± 2.0	-18.0 ± 4.2
k (s^{-1}), 25 °C[b]	3.9×10^{5}	7.2×10^{5}	1.2×10^{6}
C_{1m} (s^{-1} K)	660[c]	650[c]	754[c]
C_{2m} (s^{-1} K)	660[d]	5000[d]	8000[d]
$E_{im} = E_{io}$ (kcal mol^{-1})	2.60 ± 0.14	2.61 ± 0.14	2.54 ± 0.15
$C_{1o} = C_{2o}$ (s^{-1} K)	$(1.32 \pm 0.44)\times10^{3}$	$(1.30 \pm 0.44)\times10^{3}$	$(1.51 \pm 0.51)\times10^{3}$
C_{ω} (s^{-1} K)	$(8.18 \pm 0.52)\times10^{6}$	$(7.55 \pm 0.85)\times10^{6}$	$(6.69 \pm 1.47)\times10^{6}$
$\lvert A/\hbar \rvert$ (s^{-1})[e]	1.16×10^{7}	1.07×10^{7}	9.46×10^{6}
T_e (s), 25 °C	$< 3.5\times10^{-12}$[f]	4.2×10^{-11}[g]	7.9×10^{-11}[g]

[a] The errors given are one standard deviation. [b] k is the first-order solvent exchange rate constant at 25 °C calculated from the $\Delta H^{\ddagger}$ and $\Delta S^{\ddagger}$ values listed above. [c] These values are fixed at half of those of C_{1o} during the least-squares fittings. [d] These values are not varied in least-squares fittings. [e] $\lvert A/\hbar \rvert$ is calculated from Eq 2.16 by using the $\lvert C_{\omega} \rvert$ value listed above. [f] The upper limit of T_e value is estimated from the Eq 2.35 by using the $\lvert A/\hbar \rvert$ and E_{im} listed above, and by assuming an upper limit of one standard deviation of C_{im} for $(C_{2m} - C_{1m})$. [g] T_e is calculated from Eq 2.35 by using the C_{1m}, C_{2m}, E_{im}, and $\lvert A/\hbar \rvert$ values listed above.

value of 5000 for C_{2m}. The observed and calculated relaxation rates are given in Table A-7 in Appendix.

In Table 2.8, E_{im}, C_{1o} (and C_{1m}) values were not sensitive to the change of C_{2m}values, and two sets of $\Delta H^{\ddagger}$, $\Delta S^{\ddagger}$, and C_{ω} values obtained at the two limiting C_{2m} values respectively are also close within their error limits. The calculated electron spin relaxation time T_e of 7.9×10^{-11} s by using C_{2m} = 8000 s^{-1} K seems to be more reasonable since it is comparable to that of 6.6×10^{-11} s in Table 2.3 for $Co(dmgH)_2$–CH_3OH. Thus, C_{2m} is more likely to be close to 8000 than to 660 s^{-1} K.

Discussions

There have been numerous studies of solvent exchange on octahedral solvated complexes of the divalent metal ions, such as Mn^{2+}, Co^{2+}, Fe^{2+} and Ni^{2+}. The mechanism of solvent exchange has been assigned by taking negative values of $\Delta V^{\ddagger}$ and $\Delta S^{\ddagger}$ to be indicative of an I_a mechanism, while positive values support an I_d mechanism.[23] In general, these studies have found that the mechanism of solvent exchange depends on the metal ion, but is independent of the nature of the solvent. A further relevant point from these studies is that acetonitrile and methanol solvent exchange have similar $\Delta H^{\ddagger}$ values (within 1-2 kcal mol^{-1}) for a particular metal ion.

The kinetic parameters from this study are collected in Table 2.9. With the exception of the $Co(dmgH)_2$–CH_3OH system, the $\Delta S^{\ddagger}$ values are negative and imply an I_a mechanism. This seems reasonable if these complexes have a five-coordinate ground state with one coordinated solvent ligand. Then a solvent molecule can approach from the side *trans* to the solvent ligand in an I_a mechanism.

As noted, $Co(dmgH)_2$–CH_3OH seems to be an exception to the above arguments because $\Delta S^{\ddagger}$ is positive. This would represent a rather unprecedented change of mechanism with change of solvent. This system also is unusual in that the $\Delta H^{\ddagger}$ for

Table 2.9. Kinetic Parameters for Solvent Exchange for Cobaloxime(II) Solutions

Complex	Solvent	$\Delta H^{\ddagger}$(kcal mol^{-1})	$\Delta S^{\ddagger}$(cal mol^{-1} K^{-1})	k_{obs} (s^{-1}, 25 °C)
$Co(dmgH)_2$	CH_3CN	7.24	-9.76	2.3×10^5
	CH_3OH	13.9	8.30	2.8×10^4
		9.7[a]	-6.0[a]	2.4×10^4 [a]
$Co(dmgBF_2)_2$	CH_3CN	4.33	-20.5	1.4×10^5
	Acetone	3.38	-21.8	3.5×10^5
$Co(dpgH)_2$	CH_3CN	—	—	$\geq 4\times10^5$ [b]
	CH_3OH	3.81	-18.0	1.2×10^6

[a] From the refit by fixing $\Delta S^{\ddagger}$ at -6 cal mol^{-1} K^{-1}, see the Results section and Table 2.4 for details. [b] Estimated from the low limit exchange rate constant of 3×10^3 s^{-1} at -45 °C (see text) with an assumed $\Delta H^{\ddagger}$ value of 5 kcal mol^{-1}.

methanol exchange is much higher than that for acetonitrile exchange. In order to determine if this unprecedented behavior was firmly supported by experimental data the system was reanalysed by fixing $\Delta S^{\ddagger}$ at -6 cal mol^{-1} K^{-1}, and the resulting fit of the data was only slightly worse than the best fit and gives a $\Delta H^{\ddagger} = 9.7$ kcal mol^{-1}. The latter is more consistent with the $\Delta H^{\ddagger}$ of 7.2 kcal mol^{-1} for acetonitrile exchange, and the analysis shows that a negative $\Delta S^{\ddagger}$ and I_a mechanism is possible for all the systems studied here.

Any differences between the $Co(dmgH)_2$ and $Co(dmgBF_2)_2$ systems are most likely to be due to the electron withdrawing effect of the $-BF_2$ substituents. This effect is shown by the reduction potentials (vs. NHE) in water of 0.69 V for $Co^{III/II}(dmgBF_2)_2$ and 0.36 V for $Co^{III/II}(dmgH)_2$. A similar effect was seen by Thompson and Stynes[24] for six coordinate iron(II) complexes where the reduction potential for $Fe^{III/II}(dmgBF_2)_2(MeIm)_2$ is 0.54 V more positive than that for $Fe^{III/II}(dmgH)_2(MeIm)_2$ in acetonitrile. The $-BF_2$ substituent also reduces the π-donation of these iron systems as seen by the CO stretching frequencies of 1985 and 2049 cm^{-1} for $Fe(dmgH)_2(Py)(CO)$ and $Fe(dmgBF_2)_2(Py)(CO)$, respectively. However, Thompson and Stynes found that the $-BF_2$ substituent has only a small effect on the rate of axial ligand substitutions. They suggest that the energy of the HOMO (d_{xz}, d_{yz}) is lowered by the $-BF_2$ and affects π bonding with dmgH, but has much less effect on axial ligand bonding in these six coordinate Fe(II) complexes.

For the Co(II) systems studied here, the $\Delta H^{\ddagger}$ for exchange of CH_3CN of the $-BF_2$ derivative is 2.9 kcal mol^{-1} smaller than for dmgH. This can be rationalized by an I_a mechanism, if $-BF_2$ makes the cobalt(II) center more positive and then it favors bonding of the solvent molecule entering the sixth coordination position. However, the lower $\Delta H^{\ddagger}$ is accompanied by an 11-12 cal mol^{-1} K^{-1} more negative $\Delta S^{\ddagger}$ for the $-BF_2$ system. This $\Delta S^{\ddagger}$ change compensates for the lower $\Delta H^{\ddagger}$, so that, the solvent exchange

rate constants at 25 °C for these two systems are of the same magnitude. This $\Delta S^{\ddagger}$ effect may be due to differences in solvation of the cobaloxime(II) complexes.

For the diphenylglyoxime systems, electronic differences are probably minimal relative to the methyl systems because these groups have rather smaller Taft substituent constants (0.00, $-CH_3$; 0.75, $-C_6H_5$).[25] Conjugation effects are expected to be small since the structure of $Co(dpgH)_2NO$[26] shows that the phenyl rings are twisted 30-80° out of the N_4 plane. The same structure also reveals that the phenyl groups are bent toward the NO ligand by 3-15°. This produces the possibility of steric interaction between an *ortho*– hydrogen of each phenyl ring and the axial ligand. A model of $Co(dpgH)_2(CH_3OH)$ indicates that such bending of the phenyls would produce steric crowding around the CH_3OH, while leaving the *trans* position quite open for coordination of an entering solvent molecule. Thus the greater lability of $Co(dpgH)_2$ compared to $Co(dmgH)_2$ in methanol could be attributed to steric weakening of the Co–CH_3OH bonding in the ground state.

The values of the electron spin relaxation time T_e, and temperature parameter E_i ($= E_{im} = E_{io}$) for inner-sphere and outer-sphere relaxation rates are summarized in Table 2.10. The estimated electron spin relaxation times at 25 °C for these cobaloxime(II) systems are much smaller than that of ~10^{-9} s found for Co(*trans*-[14]diene)$^{2+}$ in acetonitrile.[4] The short T_e for cobaloxime(II) systems are consistent with the fact that the scalar splitting structures of their EPR spectra are too broad to be seen in solution. It should be noted that these T_e values are of the same magnitude as the rotational correlation time τ_r for these complexes (~ 3-6$\times 10^{-11}$ s), so that both τ_r and T_e must contribute to the dipolar relaxation time τ_D according to Eq 2.31.

As noted in the Basic Equations section, if the temperature dependencies of both T_e and τ_r arise from the temperature-dependent tumbling of the complexes in solution, then the temperature parameter E_i should be similar to that of the solvent viscosities,

Table 2.10. Summary of Electron Spin Relaxation Times and Temperature Dependence of Relaxation Rates

Complex	Solvent	T_e (s)$\times 10^{11}$	E_i (kcal mol^{-1})
$Co(dmgH)_2$	CH_3CN	≤ 1.5	1.32
	CH_3OH	6.6	1.76
$Co(dmgBF_2)_2$	CH_3CN	≤ 4.8	2.12
	Acetone	6.4	1.82
$Co(dpgH)_2$	CH_3CN	—	1.48
	CH_3OH	7.9	2.54

which are 1.85, 2.5, and 1.7 kcal mol^{-1} for acetonitrile, methanol and acetone, respectively. Of the six systems studied here, $Co(dmgBF_2)_2$–Acetone and $Co(dpgH)_2$–CH_3OH show E_i values similar to those expected for tumbling. The differences for $Co(dmgBF_2)_2$–CH_3CN may be within the error limits. The other three systems, $Co(dmgH)_2$–CH_3CN, $Co(dmgH)_2$–CH_3OH and $Co(dpgH)_2$–CH_3CN, show E_i values lower than those expected for tumbling. Similar but larger differences were observed by Rusnak and Jordan[27] in their study of Ni(II)-Schiff base complexes in acetonitrile and methanol. They suggested that, following McLachlan,[28] the average electron spin relaxation time was related to a correlation time τ_v which describes the fluctuations in modulation of the zero-field splitting of the complex in solution. If the fluctuation is not governed by the tumbling of the complex in solution, i.e., $\tau_v \neq \tau_r$, then T_e may not have same temperature dependence as that for tumbling. The same argument could be used here to account for the discrepancy of the E_i values found for the three cobaloxime systems.

The scalar coupling constant $A/\hbar$ of five cobaloxime(II) systems are listed in Table 2.11 along with the $A/\hbar$ values for Co(*trans*-[14]diene)$^{2+}$ and Co^{2+} ions in acetonitrile and methanol.

Among the cobaloxime systems, the signs of the scalar coupling constants are only available for $Co(dmgH)_2$ in acetonitrile and methanol, where the directions of the proton contact shifts can be measured directly by NMR. This information can be used in determining the mechanism of delocalization of the unpaired electron spin density. The negative $A/\hbar$ for methyl protons of CH_3CN is consistent with the negative scalar coupling constants observed for Co(*trans*-[14]diene)$^{2+}$–CH_3CN[4] and $Co(CH_3CN)_6^{2+}$,[29] and indicates a spin polarization mechanism. The positive $A/\hbar$ values for CH_3 and OH protons indicates a direct transfer of unpaired spin from cobalt $3d_{z^2}$ orbital to the methanol oxygen orbital through the σ bond. From the oxygen, the spin density is then

Table 2.11. Summary of Proton Scalar Coupling Constants and Solvent Exchange Activation Enthalpies for Cobalt(II) Systems

Complex	Solvent	$A/\hbar$ (s^{-1})$\times 10^{-6}$ [a]	$\Delta H^{\ddagger}$ (kcal mol^{-1})
$Co(dmgH)_2$	CH_3CN	-4.88	7.24
	CH_3OH	+16 (CH_3), +15(OH)	9.7
$Co(dmgBF_2)_2$	CH_3CN	3.39	4.33
	Acetone	1.87	3.38
$Co(dpgH)_2$	CH_3OH	9.46	3.81
Co(*trans*-[14]diene])$^{2+}$ [b]	CH_3CN	-2.24	—
	CH_3OH	6.0 (OH)	—
Co^{2+}	CH_3CN[c]	-0.14	8.1
	CH_3OH[d]	+2.6 (CH_3), +5.0 (OH)	13.8

[a] $A/\hbar$ values with "+" or "-" signs are obtained from the shift measurements, whereas those without the signs are the absolute values obtained from the NMR relaxation rate analysis. [b] Reference 4. [c] Reference 29. [d] Reference 30.

transferred to the OH proton, and to the CH_3 protons *via* the carbon sp^3 orbitals.[30] The direct spin transfer mechanism would cause an increase in positive spin density for both the CH_3 and OH protons, as reflected by the similar positive $A/\hbar$ for OH and CH_3 protons. The larger $A/\hbar$ for OH relative to CH_3 for $Co(CH_3OH)^{2+}$ has been interpreted as the direct spin transfer to the OH proton by direct overlap of the cobalt t_{2g} orbital and the hydrogen 1*s* orbital.[30]

It is interesting to note that the $|A/\hbar|$ values for the low-spin cobaloxime(II) complexes are 5 to 20 times larger than those for the high-spin hexasolvated species. In principle, this should be of benefit to NMR solvent exchange studies such as this by amplifying the $\tau_m\Delta\omega_m^2$ contribution. Unfortunately this advantage is offset by the longer T_e values which make the R_{2m} and R_{2o} values larger compared to the high-spin cobalt(II) systems.

The $|A/\hbar|$ for $Co(dmgH)_2$–CH_3OH is more than three times larger than that for $Co(dmgH)_2$–CH_3CN, indicating that the direct spin transfer mechanism with CH_3OH as axial ligand is more effective than that of spin polarization with CH_3CN as axial ligand. On the other hand, larger $|A/\hbar|$ for $Co(dmgH)_2$–CH_3OH is associated with the large outer-sphere relaxation parameter C_{2o} as shown in Table 2.5. The fact that (C_{2o} -C_{1o}) is larger than (C_{2m} - C_{1m}) implies a greater outer-sphere scalar relaxation. It could be estimated, from the relative magnitude of the (C_{2o} -C_{1o}) and the (C_{2m} - C_{1m}), that the outer-sphere scalar relaxation contributes ~52% of the measured scalar coupling constants, if a similar electron spin relaxation time is assumed for both outer-sphere and inner-sphere scalar relaxations. The outer-sphere scalar interaction could be understood in terms of the spin delocalization in the $(dmgH)_2$ ligand, and the spin density may then be transferred to the outer-sphere methanol molecule through the hydrogen bonding between the CH_3OH and the H•••O—H group of the $(dmgH)_2$ ligand.

In the same solvent, the magnitude of the $|A/\hbar|$ might correlate with the lability

of the solvent exchange because $|A/\hbar|$ is related to the bonding between the metal and solvent ligand. For the two low-spin cobalt(II) systems in methanol and acetonitrile, a smaller $|A/\hbar|$ gives a smaller $\Delta H^{\ddagger}$. Clearly these conclusions are too limited to be definitive.

References

(1) Swift, T. J.; Connick, R. E. *J. Chem. Phys.* **1962**, *37*, 308.

(2) See, for example, (a) Schrauzer, G. N. *Acc. Chem. Res.* **1968**, *1*, 97. (b) Pratt, J. M. *Inorganic Chemistry of Vitamin B_{12}*; Academic: New York, NY, 1972.

(3) (a) Adin, A; Espenson, J. H. *Inorg Chem.* **1972**, *11*, 686. (b) Kita, E; Jordan, R. B. *Inorg. Chem.* **1989**, *27*, 1549. (c) Bakac, A; Brynildson, M. E.; Espenson, J. H. *Inorg. Chem.* **1986**, *25*, 4108.

(4) Rusnak, L. L.; Jordan, R. B. *Inorg. Chem.* **1976**, 15, 709.

(5) Luz, Z; Meiboom, S. *J. Chem. Phys.* **1964**, 40, 2686.

(6) Bloembergen, N.; Morgan, L. O. *J. Chem. Phys.* **1961**, *34*, 842.

(7) Litovit`z, T. A. *J. Chem. Phys.* **1952**, *20*, 1088.

(8) Krynicki, K. *Physica* **1966**, *32*, 167.

(9) Bloembergen, N. *J. Chem. Phys.* **1957**, *27*, 595.

(10) (a) Newman, K. E.; Meyer, F. K.; Merbach, A. E. *J. Am. Chem. Soc.* **1979**, *101*, 1470. (b) Granot, J.; Fiat, D. *J. Magn. Reson.* **1974**, *15*, 540.

(11) Solomon, I. *Phys. Rev.* **1955**, *99*, 559.

(12) Bloembergen, N. *J. Chem. Phys.* **1957**, *27*, 572.

(13) In our treatment, the longitudinal and transverse electron spin relaxation times T_{1e} and T_{2e} are assumed to be equal, i.e., $T_{1e} = T_{2e} = T_e$, so that, $\tau_{e1} = \tau_{e2} = \tau_e$.

(14) (a) Kitson, R. E. *Anal. Chem.* **1950**, *22*, 664. (b) Kupferschmidt W. C. H. *Ph.D. Thesis*, University of Alberta, **1982**, 37.

(15) Bakac, A.; Espenson, J. H. *J. Am. Chem. Soc.* **1984**, *106*, 5197.

(16) Grant, M.; Jordan, R. B. *Inorg. Chem.* **1981**, *20*, 55.

(17) Meiboom, S.; Gill, D. *Rev. Sci. Instrum.* **1958**, *29*, 688.

(18) Temperature dependence of relaxation rate R_i (i = 1 and 2) for pure CH_3CN and

CH_3OH are as follows: $R_i = (0.0057)\exp(1440/RT)$ for CH_3CN, and $R_i = (1.463/T)\exp(1801/RT)$ for CH_3OH, from Rusnak, L. L. *Ph.D. Thesis*, University of Alberta, **1971**.

(19) For a discussion on the solvation number of the $Co^{II}(dmgH)_2$, see Chapter 1 of this thesis.

(20) For acetone as σ type Lewis base, the C-O-M usually ranges from 120° to 150°, for example, see Cotton, F. A.; Matusz, M. *Inorg. Chem.* **1987**, *26*, 3468. Galeffi, B.; Simard, M.; Wuest, J. D. *Ibid.* **1990**, *29*, 951.

(21) Co-O bond length is taken as 2.3 Å from the Co-O bond length in $Co(dmgBF_2)_2(CH_3OH)_2$ from Reference 3b

(22) *Handbook of Chemistry and Physics*; 53rd ed, CRC Press, **1972**, F-37.

(23) Jordan, R. B. *Reaction Mechanisms of Inorganic and Organometallic Systems*; Oxford University Press: New York, 1991; Chapter 3.

(24) Thompson, D. W.; Stynes, D. V. *Inorg. Chem.* **1990**, *29*, 3815.

(25) Perrin, D. D.; Dempsey, B.; Sergeant, E. P. *pK_a Predictions for Organic Acids and Bases*; Chapman and Hall: London; 1981.

(26) Englert, U.; Stahle, J. *Gazzetta Chimica Italiana*, **1988**, *118*, 845.

(27) Rusnak, L. L.; Jordan, R. B. *Inorg. Chem.* **1975**, *14*, 988.

(28) McLachlan, A. D. *Proc. Roy. Soc., Ser. A* **1964**, *280*, 271.

(29) Matwiyoff, N. A.; Hooker, S. V. *Inorg. Chem.*, **1967**, *6*, 1127.

(30) Breivogel Jr., F. W. *J. Chem. Phys.* **1969**, 51, 445.

Chapter 3. NMR Shift and Relaxation of 1-Methylimidazole (MeIm) in MeIm-Co(dmgBF$_2$)$_2$ Complex in Acetonitrile

Introduction

NMR isotropic shifts of paramagnetic complexes have been studied extensively by many workers. Two mechanisms generally are thought to contribute to the observed chemical shift, the contact or scalar mechanism which results from electron spin delocalization onto the ligand L, and the pseudo contact or dipolar mechanism which results from magnetic anisotropy in the complex.

The most commonly used formulation of the contact term for an axially symmetric complex assumes that all thermally accessible states belong to a single spin state S, and then[1]

$$\frac{\Delta\nu_C}{\nu_0} = \frac{-A_s}{3(\gamma_1 / 2\pi)N\beta}\left(\frac{\chi_{xx}}{g_{xx}} + \frac{\chi_{yy}}{g_{yy}} + \frac{\chi_{zz}}{g_{zz}}\right) \tag{3.1}$$

where ν_0 is the measuring frequency, $\Delta\nu_C$ is the contact shift, A_s is the scalar coupling constant in Hz, N is the Avogadro's number, and χ_{jj} (j = x, y and z) is the principal component of magnetic susceptibility. Other parameters have their usual meanings as defined in the previous chapter. If there is no zero-field splitting, then the magnetic susceptibility terms are given by

$$\chi_{jj} = \frac{g_{jj}^{\,2} N\beta^2 (S)(S+1)}{3kT} \qquad (j = x, y, z) \tag{3.2}$$

Substitution of these into the previous equation gives

$$\frac{\Delta\nu_C}{\nu_0} = -\frac{A_s g_{ave}\beta(S)(S+1)}{3(\gamma_1/2\pi)kT} \tag{3.3}$$

where $g_{ave} = 1/3(g_{xx} + g_{yy} + g_{zz})$.

The dipolar contribution depends on the magnitude of the anisotropy as well as the distance and orientation of the ligand nucleus relative to the paramagnetic metal center. In its simplest form, the dipolar term for an axially symmetric complex is given by[1]

$$\frac{\Delta\nu_D}{\nu_0} = \frac{\beta^2(S)(S+1)}{9kT}\left(g_\perp{}^2 - g_\parallel{}^2\right)\left(\frac{3\cos^2\theta - 1}{r^3}\right) \tag{3.4a}$$

$$= \frac{1}{3N}\left(\chi_\perp - \chi_\parallel\right)\left(\frac{3\cos^2\theta - 1)}{r^3}\right) \tag{3.4b}$$

where $\Delta\nu_D$ is the dipolar shift, r is the distance from the paramagnetic metal center to the ligand nucleus, θ is the angle between the principal symmetry axis (usually the z axis) and the vector which joins the metal center and the ligand nuclei. The dipolar contribution can be calculated from the structure parameters and the magnetic susceptibility values, and the contact contribution may then be obtained by subtracting the dipolar contribution from the observed isotropic shift. According to Eq 3.4, isotropic shifts of nuclei with various orientations and distances should correlate with the geometric factor $(3\cos^2\theta - 1)/r^3$, if the shifts are indeed dipolar. Lack of a such correlation is taken to indicate a substantial contact contribution.

If the magnetic susceptibility follows the Curie law ($\chi = C/T$), then the contact and dipolar shifts show $1/T$ temperature dependence according to Eqs 3.3 and 3.4, and plots of the observed shift $\Delta\nu$ vs. $1/T$ should be linear with a zero intercept at $1/T = 0$.

However, it is not uncommon that a system may show temperature independent paramagnetism and the magnetic susceptibility is given by Eq. 3.5[2]

$$\chi = \frac{C}{T} + N\alpha \tag{3.5}$$

where C and $N\alpha$ are positive constants. Such a situation is sometimes referred to as non-Curie law behavior. The temperature independent paramagnetism ($N\alpha$) is attributed to orbital contribution to the ground state through spin-orbital coupling, so that $N\alpha$ is inversely proportional to the energy separations between the ground state and various excited states within the same spin state S.

If there is temperature independent paramagnetism, then plots of $\Delta\nu$ vs. $1/T$ should still be linear, but have a nonzero intercept at $1/T = 0$. Because both C and $N\alpha$ are positive, the slope and the intercept should have the same sign, being either positive or negative, depending on the sign of the other factors in the contact and dipolar shift equations (3.1 and 3.4). It should be noted that there are cases in the literature[3-6] where the plot of $\Delta\nu$ vs. $1/T$ is not linear, and where the slope and intercept do not have the same sign.

In order to anticipate what might be expected in the $Co(dmgBF_2)_2$-methylimidazole system, it is useful to review some previous observations on low-spin cobalt(II) systems. La Mar and Walker[3] studied several cobalt(II) porphyrin complexes and found reasonable Curie law dependence for $1/T < 3.5\times10^{-3}$, but at lower temperatures the porphyrin proton shifts drop off. La Mar and Walker suggested that this is due to the change in anisotropy with increasing solvation at low temperature. In any case, the shifts of the porphyrin protons are largely assigned to a dipolar mechanism because they correlate with the geometric factor.

Shirazi and Goff[7] studied the shifts in 4- and 5-coordinate cobalt(II) meso-tetraphenylporphyrins. Addition of pyridine or imidazole to make the 5-coordinate complex causes a substantial reduction in the dipolar shift of the porphyrin protons. The authors attribute this to a ≥ 20% reduction in ($\chi_\perp - \chi_\parallel$). The 5-coordinate species also gave greater linewidths. This was explained by a longer electron spin relaxation time T_{1e}, which could be due to a greater separation of ground and excited electronic states in the 5-coordinated species. The deuterium NMR of the pyridine-d_5 complex indicates a contact shift mechanism since the shifts at various position of pyridine decrease in the order $\alpha > \beta > \gamma$.

For non-porphyrin complexes the situation appears more complex. The systems studied are of the general type

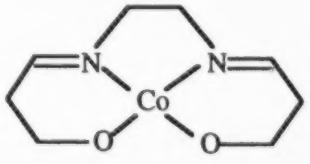

and are not axially symmetric. The ligands also have some flexibility and the cobalt may not be coplanar with the coordinating atoms. It is simplest to summarize these results by saying that the ligand shifts do not follow the Curie law. They sometimes fit to Eq 3.5 with a temperature independent paramagnetism, but the slope and intercept are not always of the same sign. Dramatic deviations of the latter type may reflect flexibility in the ligand conformation. The magnitude of the shifts generally indicate large contact and small dipolar contributions. The complexity is generally associated with the closeness in energy of states with the unpaired electron in the d_{yz} and d_{z^2} orbitals. The latter should not give ligand contact shifts unless the cobalt is above the ligand plane to remove the orthogonality of the metal and ligand *p* orbitals. Examples of these

problems can be seen in the studies by Migita et al.,[4] Srivanavit and Brown,[5] Richardson and Kreilick,[8] and Lutos-Grazynski.[9]

In this study, first, the formation constants of mono- and bis- MeIm adducts of $Co(dmgBF_2)_2$ in acetonitrile have been determined by spectrophotometry, and are compared to previous results on analogous systems. Second, the proton NMR shifts and the relaxation rates of the 1-methylimidazole have been measured, and analyzed to give the shift and relaxation parameters for protons in the mono- and bis- coordinated 1-methylimidazole.

Experimental Section

Materials and Sample Preparation. $Co^{II}(dmgBF_2)_2 \cdot 2H_2O$ was prepared by the method of Espenson et al.,[10] as described in the Experimental Section of Chapter 2. The 1-methylimidazole (MeIm) was reagent grade from Aldrich. Acetonitrile was Anachemia reagent containing 0.3% water, and was dried over 4-A molecular sieves (BDH) for at least 24 h before use.

The NMR samples containing $Co^{II}(dmgBF_2)_2$ and MeIm were prepared anaerobically. Care was taken to avoid direct mixing of $Co^{II}(dmgBF_2)_2$ and neat MeIm to prevent the possible displacement of the $dmgBF_2^-$ ligands by MeIm. This was done using a flask with an attached side tube. A known amount of MeIm was transferred with a microsyringe into the side tube, and a weighed amount of $Co^{II}(dmgBF_2)_2 \cdot 2H_2O$ was added into the flask. The whole flask was evacuated by one freeze-pump-thaw cycle to remove air in the MeIm and the water of crystallization from the cobalt complex. About 12 to 15 mL of acetonitrile, previously deoxygenated by at least two freeze-pump-thaw cycles on a vacuum line, was vacuum-distilled into the flask containing the cobalt complex. The solvent was thawed and the yellow-orange acetonitrile solution of $Co^{II}(dmgBF_2)_2$ was then mixed with the MeIm to give a yellow-

brown solution. The solution were weighed to determine the exact amount of solvent. Part of the solution was then transferred, under vacuum, to a 5-mm NMR tube (Wilmad Glass Co.) which contained a small amount of C_6D_6 (General Intermediate) for field locking during the NMR measurements, and the tube was flame sealed under vacuum. The molar concentrations of the cobalt and MeIm in each sample were calculated from the weights of cobalt complex and the solvent, the volume of MeIm, and the known densities of the solvent and MeIm.

The formation constants for mono- and bis- MeIm adducts were determined at three temperatures (35, 19, and 0 °C) by spectrophotometry. To 250 mL of a deoxygenated acetonitrile solution of $Co(dmgBF_2)_2$ (1.0×10^{-4} M), various amounts of MeIm were added with a microsyringe. After each addition, the solution was stirred for 5 min, then 5.0 mL of the solution was transferred with a syringe under argon to an argon filled 2-cm path length cylindrical cell that was sealed with a serum cap.

Instrumentation. Proton NMR spectra were recorded on a Bruker AM 400 MHz spectrometer. The temperature was controlled by a B-VP 1000 unit with an accuracy of ±0.5° measured by a copper-constantan thermal couple.

In order to measure the EPR spectrum, a sample containing 4.4×10^{-4} M $Co(dmgBF_2)_2$ and 0.34 M MeIm was frozen at liquid nitrogen temperature and transferred to the EPR spectrometer at 93 K. The instrument was a Bruker ER 200 D-SRC Electron Spin Resonance Spectrometer operating at the X-band frequency of 9.38 GHz, and the temperature was controlled by Bruker Variable Temperature Unit ER 4111VT.

The electronic spectra from 300 to 600 nm were recorded on a Hewlett Packard 8451 diode array spectrophotometer equipped with a standard temperature-controlled (± 0.2 °C) water flow system.

Results

Formation Constants of Mono- and Bis- 1-Methylimidazole Adducts. A solution of $Co^{II}(dmgBF_2)_2$ in acetonitrile shows a peak at 425 nm ($\varepsilon = 3.10\times10^3$ M^{-1} cm^{-1}) and a shoulder at 328 nm ($\varepsilon = 2.45\times10^3$ M^{-1} cm^{-1}). Addition of 1-methylimidazole (MeIm) to the above solution increases the absorbance in the 350 - 400 nm region until the MeIm reaches ~ 1×10^{-2} M. Further addition of MeIm increases the absorbance in the 500-550 nm region. The spectral changes correspond to the formation of mono- and bis- adduct, as shown by Eqs 3.6 and 3.7, respectively.

$$Co(dmgBF_2)_2 + MeIm \overset{K_1}{\rightleftharpoons} (MeIm)Co(dmgBF_2)_2 \qquad (3.6)$$

$$(MeIm)Co(dmgBF_2)_2 + MeIm \overset{K_2}{\rightleftharpoons} (MeIm)_2Co(dmgBF_2)_2 \qquad (3.7)$$

Since the spectral changes occur in two well separated MeIm concentration ranges, they can be used to obtain the values of K_1 and K_2 separately. The absorbance increase at 376 nm for 3.0×10^{-5}-6×10^{-3} M MeIm can be treated by the following equation:[11]

$$K_1 = \frac{[(MeIm)Co(dmgBF_2)_2]}{[Co(dmgBF_2)_2]}\times\frac{1}{[MeIm]} = \frac{(A-A_\infty)}{(A_0-A)}\times\frac{1}{[MeIm]} \qquad (3.8)$$

or

$$\log\frac{(A-A_\infty)}{(A_0-A)} = \log\,[MeIm] + \log K_1 \qquad (3.9)$$

where A_0, A, A_∞ are absorbances in the absence, presence, and large excess of MeIm, respectively. [MeIm] is the free MeIm concentration, and is given by

$$[\text{MeIm}] = [\text{MeIm}]_t - \frac{(A_0 - A)}{(A_0 - A_\infty)} \times [\text{Co}]_t \qquad (3.10)$$

where $[\text{MeIm}]_t$ and $[\text{Co}]_t$ are total concentrations of MeIm and cobalt complex, respectively. The A vs. [MeIm] data were fitted to Eq 3.8 by least-squares to obtain K_1. A plot of log $[(A-A_\infty)/(A_0-A)]$ vs. [MeIm], shown in Figure 3.1, is linear with a slope = 1 as expected from Eq 3.9. The absorbance changes (at 470 nm) at high MeIm concentrations (5.0×10^{-2} - ~1.5 M) were treated similarly to obtain K_2. A plot of log $[(A-A_\infty)/(A_0-A)]$ vs. log [MeIm] is shown in Figure 3.2. The results of the K_1 and K_2 measurements at three temperatures (35, 19 and 0 °C) are summarized in Table 3.1.

Both K_1 and K_2 increase as the temperature decreases. By substituting Eq 3.11, the temperature dependence for equilibrium constant, into Eq 3.8, the A vs. [MeIm] data at three temperatures were analyzed by least-squares to yield the corresponding $\Delta H°_i$ and $\Delta S°_i$ values (i = 1 and 2). The results are listed in Table 3.1, and the plots of ln K_i vs. $1/T$ are shown in Figure 3.3.

$$\ln K_i = \frac{-\Delta H°_i}{R} \times \frac{1}{T} + \frac{\Delta S°_i}{R} \qquad (3.11)$$

EPR of $Co(dmgBF_2)_2$-MeIm. The EPR spectrum of $Co(dmgBF_2)_2$-MeIm is typical of a low-spin d^7 systems,[12] and similar to those of other $(B)_2Co(dmgBF_2)_2$ complexes (B = CH_3CN[10] and py[13]). The EPR parallel components display eight lines that result from the hyperfine coupling of the unpaired electron in the d_{z^2} orbital to the nuclear spin of cobalt (I = 7/2). The axial N-donor ligands produce an additional fine structure due to the coupling of the nitrogen nuclear spin (I = 1). This superhyperfine (shf) coupling splits each of the eight cobalt hyperfine lines into three or five lines,

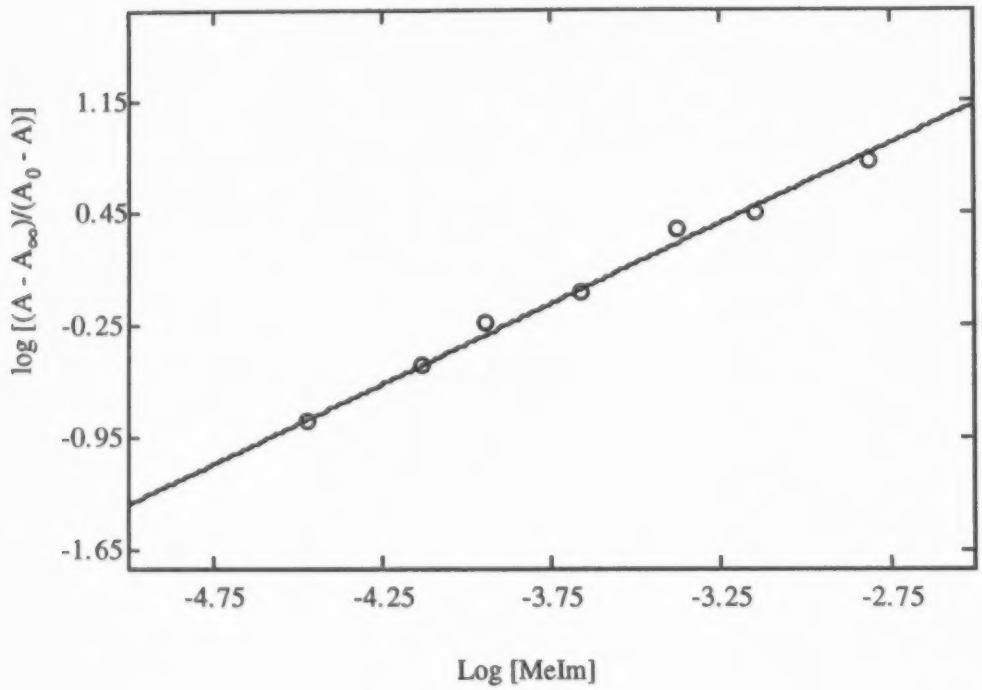

Figure 3.1. Determination of equilibrium constant K_1 for (MeIm)$Co^{II}(dmgBF_2)_2$ (Eq 3.6) at 19 °C. ($[Co]_t = 1.0\times10^{-5}$ M, 376 nm)

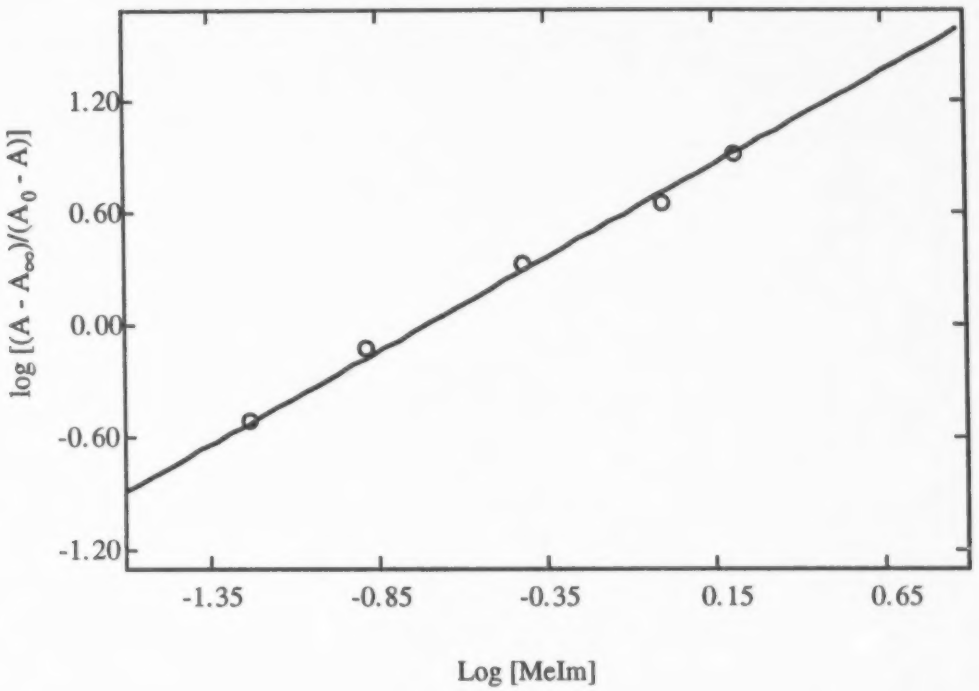

Figure 3.2. Determination of equilibrium constant K_2 for $(MeIm)_2Co^{II}(dmgBF_2)_2$ (Eq 3.7) at 19 °C. ($[Co]_t = 1.0\times10^{-5}$ M, 470 nm)

Table 3.1. Equilibrium Constants for Formation of Mono- and Bis- MeIm Adducts of $Co(dmgBF_2)_2$ in Acetonitrile[a]

		t (°C)		
		35	19	0
$K_1 \times 10^{-3}$[b] (M^{-1})		1.67 ± 0.30	4.42 ± 0.35	6.77 ± 0.56
K_2[b] (M^{-1})		2.26 ± 0.28	5.13 ± 0.24	9.26 ± 1.0
ΔH°_1(kcal mol^{-1})	-6.63 ± 0.74			
ΔS°_1(cal mol^{-1} K^{-1})	-6.59 ± 2.26			
ΔH°_2(kcal mol^{-1})	-6.65 ± 0.58			
ΔS°_2(cal mol^{-1} K^{-1})	-19.8 ± 2.0			

[a] K_1 and K_2 are defined in Eq 3.6 and 3.7, respectively. [b] Errors quoted are one standard deviation.

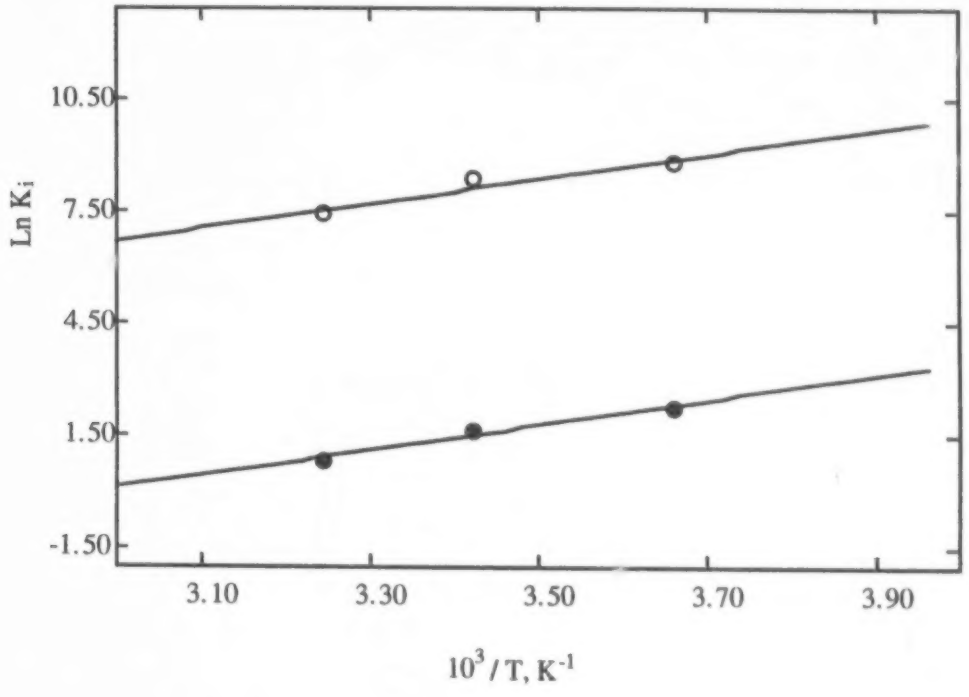

Figure 3.3. Temperature dependence of equilibrium constants K_1 (o) and K_2 (•).

depending on whether one or two axial ligands are present. The shf splitting indicates coordination of two MeIm ligands as expected from the spectrophotometric study for these conditions (0.34 M MeIm, $K_2 = 80$ at -40 °C). The EPR spectral parameters are $g_{\parallel} = 2.01$, $g_{\perp} = 2.27$, $A_{\parallel}^{Co} = 77.4\times10^{-4}$ cm^{-1} and $A_{\parallel}^{N} = 16.4\times10^{-4}$ cm^{-1}.

NMR Chemical Shifts and Relaxation Rates. The designation of the protons for peaks in the NMR spectrum of 1-methylimidazole is shown below

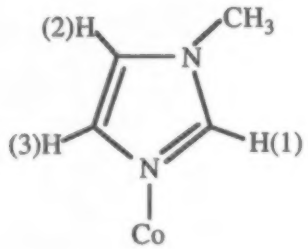

A typical spectrum is shown in Figure 3.4, where peaks numbered 1, 2, and 3 are assigned to the corresponding protons in the above structure according to the literature.[14]

The NMR lineshape of each peak can be described by the following Lorentizian function

$$I(\nu) = \frac{AT_2}{1+4\pi^2 T_2^{\,2}(\nu-\nu_0)^2} \tag{3.12}$$

where I (ν) is the intensity at frequency ν , A is an intensity scaling parameter, T_2 is the transverse relaxation time, and ν_0 is the resonance frequency. The spectral data were fitted graphically to Eq 3.12 to obtain the ν_0 and the relaxation rate R_2 (= T_2^{-1}, in s^{-1}). An observed and fitted spectra are shown in Figure 3.4. During the fitting of each spectrum, a linear base line correction of the type $I(\nu) = a + b\nu$, where a and b are

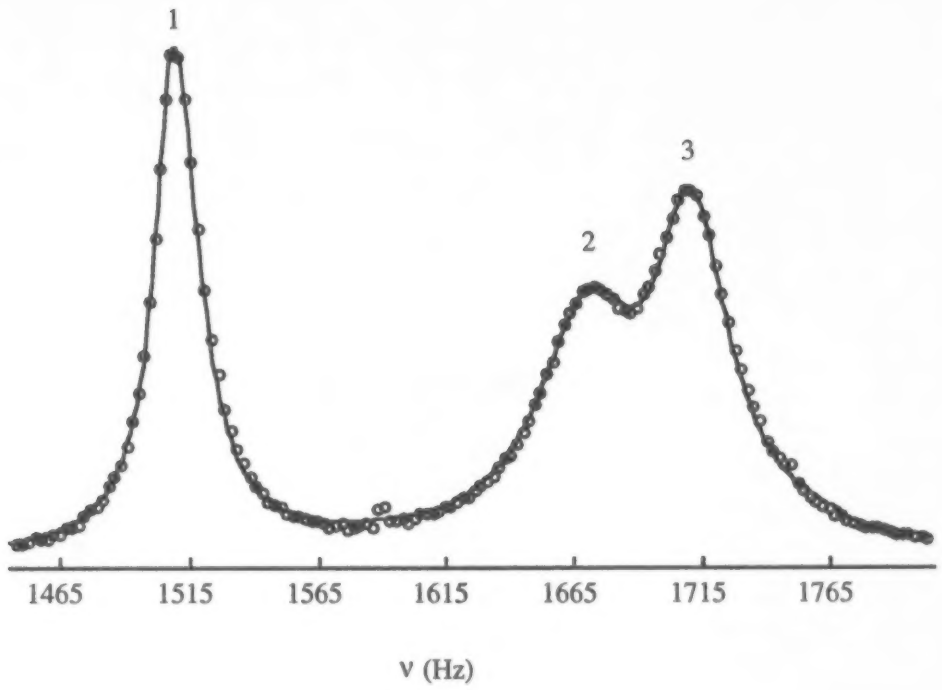

Figure 3.4. Proton NMR spectrum (400 MHz) of MeIm-Co($dmgBF_2$)$_2$ in acetonitrile at -35 °C ([Co($dmgBF_2$)$_2$]$_t$ = 4.4×10^{-4} M, [MeIm] = 0.34 M, the ν is relative to the proton resonance of CH_3CN at 788 Hz). The " o " and " — " represent the observed and fitted spectrum respectively.

constants for each spectrum, was used and the intensity parameters A for the three resonance peaks were assumed to be the same. The chemical shift $\Delta\nu_i$ (in Hz, i = 1, 2 and 3 for the MeIm protons designated above) was measured relative to that of solvent CH_3CN. Independently, the magnitude and temperature dependence of the chemical shift of the MeIm protons relative to solvent CH_3CN were determined in the absence of cobalt(II). Then these results were combined to obtain the shifts of the MeIm protons produced by the $Co(dmgBF_2)_2$.

The chemical shifts for all three peaks are downfield and their magnitudes increase as the temperature decreases. At a given set of conditions, the shifts are in the order peak 2 > peak 3 > peak 1.

The linewidths were corrected for the linewidths of the MeIm protons in the absence of $Co(dmgBF_2)_2$. All three peaks become broader with decreasing temperature, and peak 1 is always the narrowest, while peak 2 and 3 are similar at high temperature, but peak 2 becomes the broadest at low temperature.

Discussion

Formation Constants of Lewis Base Adducts of Cobaloximes(II). There have been several studies[11,15] on the equilibria for adduct formation of Lewis bases with cobaloximes(II). The previous and current results are summarized in Table 3.2.

The base adduct formation constant K_i, or in some cases, the cumulative formation constant β_2 ($\beta_2 = K_1 \times K_2$) generally correlates with the base strength as measured by pK_a of the conjugate acid of the base. For example, the order of log β_2 is Im > γ-Pic > Py which parallels order of pK_a's. The data for 2-EtIm and α-Pic are not in line with the pK_a correlation, and this can be attributed to a steric effect of the substituent adjacent to the donor N atom. The steric effect is best illustrated by the

Table 3.2. Formation Constants of $(Base)_nCo(dmgBF_2)_2$ and Other Complexes[a]

Cobaloxime	Base[b] (pK_a)	n	log K_n or Log β_2[c](*)	($\Delta H°$ and $\Delta S°$)[d]	Solvent	Method
$Co(dmgBF_2)_2$	Im (7.03)	1	4.04		DMF	VIS[e]
$Co(dmgBF_2)_2$	1-MeIm (6.97)	1	3.50	(-6.63, -6.59)	CH_3CN	VIS[f]
$Co(dmgBF_2)_2$	2-EtIm (7.99)	1	2.50		DMF	VIS[e]
$Co(dmgBF_2)_2$	Py (5.27)	1	2.25		DMF	VIS[e]
$Co(dmgBF_2)_2$	α-Pic (5.97)	1	0.16		DMF	VIS[e]
$Co(dmgBF_2)_2$	1-MeIm (6.97)	2	0.54	(-6.65, -19.8)	CH_3CN	VIS[f]
$Co(dpgBF_2)_2$	2-EtIm (7.99)	1	3.18		DMF	VIS[e]
$Co(dpgBF_2)_2$	Im (7.03)	2	7.19*		DMF	VIS[e]
$Co(dpgBF_2)_2$	γ-Pic (6.02)	2	4.46*		DMF	VIS[e]
$Co(dpgBF_2)_2$	Py (5.27)	2	4.20*		DMF	VIS[e]
$Co(dpgBF_2)_2$	α-Pic (5.97)	2	0.97*		DMF	VIS[e]
$Co(dpgH)_2$	Py (5.27)	1	2.94		DMF	VIS[e]
$Co(dmgH)_2$	Py (5.27)	1	2.24	(-3.9, -2.8)	CH_3OH	EPR[g]
$Co(dmgH)_2$	Py (5.27)	2	-0.08	(-3.9, -13.5)	CH_3OH	EPR[g]

[a] At 25 °C. [b] Im, imidazole; py, pyridine; 1-MeIm, 1-methylimidazole; 2-EtIm, 2-ethylimidazole, α-Pic, α-picoline; γ-Pic, γ-picoline. [c] $\beta_2 = K_1 \times K_2$. [d] $\Delta H°$ in kcal mol^{-1} and $\Delta S°$ in cal mol^{-1} K^{-1}. [e] Measured by visible spectrophotometry, from Reference 11. [f] This work. [g] Reference 15.

~$10^{3.5}$ difference in β_2 for α-Pic and γ-Pic (see illustration below) for adduct formation with $Co(dpgBF_2)_2$, since the two bases have very similar pK_a values.

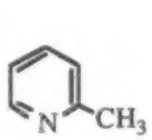

α-Picoline

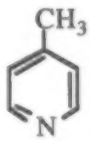

γ-Picoline

The temperature dependence of the formation constants is only available for two systems, $Co(dmgBF_2)_2$-MeIm and $Co(dmgH)_2$-Py. In both systems, the negative enthalpy values indicate that the formation constants increase as the temperature decreases. It is noteworthy that the ΔH°_1 and ΔH°_2 in these two systems are equal within the experimental errors. This could be simply rationalized by assuming that the solvated cobaloxime(II) complexes are 6-coordinate with two axial solvent ligands. Then formation of both mono- and bis- adducts would involve breaking the cobalt-solvent bond and making a cobalt-base bond. However this simple picture would lead one to expect that the K_1/K_2 ratio would just be controlled by probability, which predicts $K_1 \approx 4K_2$. This is certainly not true for the two systems where data are available. The value of K_2 is much smaller than predicted by probability, and has a less favorable ΔS° of 10-13 cal mol^{-1} K^{-1} compared to ~2.8 cal mol^{-1} K^{-1} predicted by probability.

NMR Shifts of MeIm. The spectrophotometric results show that at the concentrations of 0.1 to 0.34 M MeIm used in the NMR study, the only significant species are the mono- and bis- 1-methylimidazole complexes. Then there are three exchange reactions which should account for the effect of $Co(dmgBF_2)_2$ on the chemical shifts of uncoordinated MeIm as given in Scheme I

Scheme I

$$(L)Co(dmgBF_2)_2 + L \underset{}{\overset{k_{1ex}}{\rightleftharpoons}} (L)Co(dmgBF_2)_2 + L \qquad (3.13)$$

$$(L)_2Co(dmgBF_2)_2 + L \underset{}{\overset{k_{2ex}}{\rightleftharpoons}} (L)_2Co(dmgBF_2)_2 + L \qquad (3.14)$$

$$(L)Co(dmgBF_2)_2 + L \underset{k_{-2}}{\overset{k_2}{\rightleftharpoons}} (L)_2Co(dmgBF_2)_2 \qquad (3.15)$$

where L represents MeIm. If the system is in the fast exchange limit, and only the first two reactions are contributing, then simple extension of the Swift-Connick equations shows that the observed shift for a given proton of MeIm should be given by

$$\Delta\nu_{obs}{}^{i} = \frac{[(L)Co(dmgBF_2)_2]}{[L]} \times \nu_1{}^{i} + \frac{2[(L)_2Co(dmgBF_2)_2]}{[L]} \times \nu_2{}^{i} \qquad (3.16)$$

where $\nu_1{}^{i}$ and $\nu_2{}^{i}$ are the chemical shifts of the *i*th proton (i = 1, 2 and 3) in the mono- and bis- complexes respectively, following the number designation shown in the Results section.

The simplest assumption for the temperature dependence of $\nu_1{}^{i}$ and $\nu_2{}^{i}$ is that they follow the Curie law $\nu_j^{i} = C_j^{i}/T$, where C_j^{i} is a constant. With this assumption and standard equilibrium relationships, Eq 3.16 can be reformulated as

$$\Delta\nu_{obs}{}^{i} = \frac{[Co(dmgBF_2)_2]_t}{[L]} \times \left\{ \frac{C_1 + K_2[L]C_2}{1 + K_2[L]} \right\} \times \left(\frac{1}{T} \right) \qquad (3.17)$$

In order to determine if this Curie law model and the fast exchange assumption

are valid, it is useful to examine the results in the limit where > 85% of the cobalt(II) is present as the bis- MeIm complex. Under these conditions one would expect the C_2^i term to be dominant, and uncertainties in K_2 have a relatively small effect on the species distributions because $K_2[L] \gg 1$. The required conditions occur at high [L] and low temperature, and calculations show that they are true for 10 sets of conditions as shown in Table 3.3. These data can be used to estimate C_2^i from the following equation

$$C_2^{\,i} \approx \frac{\Delta\nu_{obs}^{\,i}[L](1+K_2[L])T}{[Co(dmgBF_2)_2]_t K_2[L]} \qquad (3.18)$$

If this Curie law model is justified, then the C_2^i should be constant, independent of T and [L]. If the C_2^i seems to vary with T, then the implication is that the Curie law assumption is not valid, and if they vary with [L], then the assumption of independent exchange processes might not be valid.

The calculated values of C_2^i are given in Table 3.3. The values are quite satisfactorily constant with maximum deviations from the average of ± 3%, ± 6% and ± 4 % for protons 1, 2 and 3 respectively. For protons 2 and 3, the variation of C_2^i for a particular sample (constant [L] and $[Co(dmgBF_2)_2]_t$) is even less and the variation between samples appears to result from small errors in the concentration. However the same effect is not observed for proton 1, and the variations must be due to experimental uncertainty in $\Delta\nu_{obs}^{\,2}$ and $\Delta\nu_{obs}^{\,3}$. The conclusion from this analysis is that the Curie law is satisfied for ν_2^i and good estimates of C_2^i have been obtained.

In order to analyze all the chemical shifts (and later the relaxation rates) the three-site exchange system as given in Scheme I has been used. The three sites are L (A), (L)Co(dmgBF$_2$)$_2$ (B) and (L)$_2$Co(dmgBF$_2$)$_2$ (C). The theory for such a system has been given by Led and Grant.[16] In the terminology of Led and Grant, the exchange

Table 3.3. Estimation of C_2^i Values From Chemical Shift $\Delta\nu_{obs}{}^i$

t (°C)	[L] (M)	% CoL_2	$\Delta\nu_{obs}{}^1$ (Hz)	C_2^1 ($\times10^{-6}$, s^{-1})	$\Delta\nu_{obs}{}^2$ (Hz)	C_2^2 ($\times10^{-6}$, s^{-1})	$\Delta\nu_{obs}{}^3$ (Hz)	C_2^3 ($\times10^{-6}$, s^{-1})
-20.0	0.34[a]	90.2	42.6	2.05	68.0	3.27	57.0	2.74
-24.6	0.34[a]	92.2	43.9	2.03	73.6	3.41	59.9	2.77
-29.3	0.34[a]	93.9	44.9	2.00	75.4	3.36	61.1	2.72
-35.0	0.34[a]	95.5	46.2	1.98	76.0	3.25	63.1	2.70
-35.0	0.34[b]	95.5	20.4	1.96	33.3	3.21	28.3	2.72
-24.6	0.18[c]	86.2	39.6	2.02	62.8	3.19	51.9	2.64
-29.3	0.18[c]	89.1	40.8	1.97	66.0	3.19	55.6	2.69
-35.2	0.18[c]	92.0	43.9	2.01	69.8	3.18	57.9	2.64
-36.0	0.10[d]	87.0	73.5	2.00	112	3.06	94.7	2.58
-41.0	0.10[d]	90.1	76.5	1.97	122	3.13	101	2.59
Average C_2^i				2.00		3.23		2.68

[a] $[Co(dmgBF_2)_2]_t = 9.9\times10^{-4}$ M. [b] $[Co(dmgBF_2)_2]_t = 4.4\times10^{-4}$ M. [c] $[Co(dmgBF_2)_2]_t = 5.1\times10^{-4}$ M. [d] $[Co(dmgBF_2)_2]_t = 5.0\times10^{-4}$ M.

lifetimes (τ) are defined by Scheme I as follows,

$$\frac{1}{\tau_{BA}} = k_{1ex}[L]; \qquad \frac{1}{\tau_{BC}} = k_2[L]$$

$$\frac{1}{\tau_{CB}} = \frac{k_2}{2K_2}; \qquad \frac{1}{\tau_{CA}} = \frac{k_{2ex}[L]}{2} + \frac{k_2}{2K_2}$$

where $K_2 = k_2/k_{-2}$ and K_2 is the previously determined equilibrium constant. Then the observed chemical shift can be calculated from Eq 21 of Led and Grant. These calculations have been done by assuming a Curie law temperature dependence for both ν_1^i and ν_2^i, an Eyring type temperature dependence for k_{1ex}, k_{2ex} and k_2, and the previously determined temperature dependence of K_2.

Initially the model was further simplified by assuming that all of the rate constants are large (1×10^9) so that the system is in the fast exchange limit. It is found that this adequately reproduces the observed shifts (±10% for most of the data) as shown in Table 3.4. Therefore, further refinements regarding the rate constants only provide lower limits on the values. For k_{2ex}, the value must be $\geq 6\times10^6$ at -35 °C, otherwise the calculated shifts level off and then decreases as the temperature decreases below -30 °C. Both k_{1ex} and k_2 provide an exchange pathway from (L)Co(dmgBF$_2$)$_2$, and if either of these rate constants is in the fast exchange limit, then the magnitude of the other does not significantly influence the calculations. It appears that either or both of k_{1ex} and k_2 must be $> 5\times10^5$ at -35 °C to maintain a reasonable fit.

NMR Relaxation Rates of MeIm. The lineshape analysis gives the transverse relaxation rates R_2^i for the 1-methylimidazole protons. The model used for the shifts should also reproduce the temperature and concentration dependence of the R_2^i values.

Table 3.4. Results of Calculated Chemical Shifts and Relaxation Rates (Proton 1)

t (°C)	$[Co]_t \times 10^4$ (M)	[MeIm] (M)	$\Delta\nu_{obs}^{-1}$ (Hz)	$\Delta\nu_{calcd}^{-1}$ (Hz) Curie law[a]	3-Site[b]	R_{2obs}^{-1} (s^{-1})	R_{2calcd}^{-1} (s^{-1}) Fast Exch[c]	O.S.[d]
35.0	5.0	0.10	43.9	42.0	43.3	35.0	36.7	35.1
10.0	5.0	0.10	47.8	50.4	51.7	59.8	58.4	56.9
-5.0	5.0	0.10	55.4	57.5	58.7	77.0	80.8	79.7
-20.0	5.0	0.10	61.2	65.4	66.7	119	115	115
-24.0	5.0	0.10	64.2	67.5	68.9	127	127	127
-30.0	5.0	0.10	69.9	70.7	72.1	142	146	147
-36.0	5.0	0.10	73.5	73.8	75.3	163	171	172
-41.0	5.0	0.10	76.5	76.3	77.8	195	194	196
35.0	5.1	0.18	26.9	25.2	25.9	22.6	21.7	21.8
10.0	5.1	0.18	30.7	30.6	31.3	38.5	34.9	35.7
-5.1	5.1	0.18	34.3	34.5	35.3	55.9	48.2	49.9
-20.0	5.1	0.18	39.9	38.6	39.4	70.1	67.3	67.3
-24.6	5.1	0.18	39.6	39.8	40.6	76.6	74.9	74.9
-29.3	5.1	0.18	40.8	41.0	41.9	88.4	83.7	88.3
-35.2	5.1	0.18	43.9	42.5	43.4	101	96.6	102
35.0	4.4	0.34	15.5	12.4	12.7	13.0	10.5	12.0
-5.1	4.4	0.34	17.1	16.5	16.9	28.2	22.9	27.3
-35.0	4.4	0.34	20.4	19.6	20.1	52.9	44.4	55.3
35.0	9.9	0.34	31.8	27.8	28.5	27.9	23.6	27.1
10.0	9.9	0.34	35.9	33.5	34.2	43.5	37.8	44.4
-5.0	9.9	0.34	38.3	37.2	38.0	64.1	51.4	61.4
-20.0	9.9	0.34	42.6	40.8	42.7	88.4	70.9	86.2
-24.6	9.9	0.34	43.9	41.8	42.7	103	78.5	96.1
-29.3	9.9	0.34	44.9	42.9	43.8	112	87.4	108
-35.0	9.9	0.34	46.2	44.2	45.2	123	99.9	124

[a] Calculated by Curie law model. [b] By 3-site exchange model. [c] Based on the fast exchange assumption. [d] By considering outer-sphere contribution.

The simple analysis of these results follows that described for $\Delta\nu_{obs}^{i}$ so that Eq 3.16 can be modified by replacing $\Delta\nu_{j}^{i}$ by R_{2m}^{i} and $\Delta\nu_{obs}^{i}$ by R_{2obs}^{i}. As described in Chapter 2, the temperature dependence of R_{2m}^{i} is expected to follow Eq 2.13, and a value of E_m = 2.12 kcal mol^{-1} has been assumed, based on that found in the Co(dmgBF$_2$)$_2$-CH$_3$CN solvent exchange study. Then $R_{2mj}^{i} = (C_{mj}^{i}/T)\exp(E_m/RT)$ (j = B or C) and the data should be fitted by varying C_{mB}^{i} and C_{mC}^{i} for the B and C sites respectively, along with the other parameters from fitting the shift data.

With the fast exchange assumption used for the shift data, the R_2 values can be calculated to agree well with the observed values at either 0.1 M MeIm or 0.34 M MeIm, but not at both. In either case, the agreement at 0.18 M MeIm is acceptable but shows persistent systematic deviation between observed and calculated values. This effect is observed for all three peaks. Qualitatively, the observations indicate that the R_2 values at the highest concentration are larger than predicted from the lowest concentration, or conversely that the values at low concentration are smaller than predicted for the highest concentration.

An explanation and resolution of this problem is made difficult because at low temperature the (L)$_2$Co(dmgBF$_2$)$_2$ species is dominant at either concentration being 90% at 0.1 M MeIm and -41 °C, and 95% at 0.34 M MeIm and -35 °C. As a result, any adjustment to the C_{mC}^{i} value has a very similar effect at the lower temperatures at both 0.10 and 0.34 M MeIm and cannot bring the data into better agreement. The same applies for adjustments in the rate constants. In addition, adjusting the rate constants to values where they affect the calculated R_{2m}, causes the $\Delta\nu_{obs}^{i}$ values to decrease at the lower temperatures so that they do not agree with the experimental $\Delta\nu_{obs}^{i}$ values.

The only explanation found that will explain the R_2 and $\Delta\nu$ observations is to propose formation of an outer-sphere complex which affects the linewidths but not the

shifts. If all of the cobalt(II) species are assumed to form an outer-sphere complex, with a formation constant K_{os}, then the concentration of this complex is given by

$$[(MeIm)_n\{Co(dmgBF_2)_2 \cdot MeIm\}] = \frac{K_{os}[L][Co]_t}{1+K_{os}[L]} \tag{3.19}$$

Then the observed relaxation rate for the *i*th proton (i = 1, 2 and 3) is given by

$$R_{2p}{}^{i} = R_2{}^{i}{}_{(3\text{-site})} + R_2{}^{i}{}_{(os)}$$

$$= R_2{}^{i}{}_{(3\text{-site})} + \frac{K_{os}[L][Co]_t C_{mo}{}^{i}}{1+K_{os}[L]}\exp(\frac{E_m}{RT}) \tag{3.20}$$

where $R_2{}^{i}{}_{(3\text{-site})}$ is calculated from the equations of Led and Grant[16] as described previously, and $C_{mo}{}^{i}$ is the outer-sphere pre-exponential factor analogous to the inner-sphere $C_m{}^{i}$. It is found that a satisfactory fit of the data can be obtained by setting the enthalpy change (ΔH°_{os}) for K_{os} at -1.0 kcal mol^{-1}, and by assuming that $K_{os}[L] \ll 1$. The value of ΔH°_{os} is not critical to the fit, but a value of the magnitude selected gives better agreement for the higher temperatures for 0.34 M MeIm. Then the $R_{2p}{}^{i}$ values are given by

$$R_{2p}{}^{i} = R_2{}^{i}{}_{(3\text{-site})} + \left\{(K_{os}' C_{mo}{}^{i})\exp(\frac{E_m - \Delta H^{\circ}{}_{os}}{RT})\right\} \times [L][Co]_t \tag{3.21}$$

where K_{os}' is the independent factor of the K_{os}. The calculated and observed values for proton 1 are compared in Table 3.4, and those for proton 2 and 3 are listed in Table A-8 and A-9 in the Appendix, respectively. The temperature independent constants $C_{mj}{}^{i}$ and

$K_{os}'C_{mo}^{i}$ are summarized in Table 3.5.

If the shift is due to a contact interaction, then C_j^i is proportional to the coupling constant $A/\hbar$ (Eq 2.16). If relaxation is due to a scalar mechanism, then C_{mj}^{i} is proportional to $(A/\hbar)^2$ (Eq 2.23). If these assumptions are true, then the ratio $(C_j^i)^2/(C_{mj}^{i})$ should be a constant. For $(L)_2Co(dmgBF_2)_2$, this ratio is 7.6×10^7, 8.09×10^7 and 7.8×10^7 for protons 1, 2 and 3 respectively. The reasonable constancy of the ratio is consistent with a contact shift and scalar relaxation for the MeIm protons in $(L)_2Co(dmgBF_2)_2$. This conclusion also is consistent with the fact that a pseudo contact shift and dipolar relaxation would predict that proton 2 should show the smallest shift and linewidth, while proton 2 actually has the largest shift and linewidth.

For $(L)Co(dmgBF_2)_2$, the ratio described above is 0.98×10^8, 1.05×10^8 and 1.02×10^8 for protons 1, 2 and 3 respectively. The constancy of this ratio leads to the same conclusion as above for the shift and relaxation mechanisms.

The outer-sphere parameter ($K_{os}'C_{mo}^{i}$) is expected to vary as the distance of the proton *i* from the paramagnetic center because dipolar relaxation normally is dominant for outer-sphere interactions (Eqs 2.23 and 2.37). The order of these values is proton 2 > proton 3 > proton 1, and the magnitudes relative to proton 2 are 1:0.79:0.34. The implication is that the outer-sphere methylimidazole is oriented with the protons assigned to peaks 2 and 3 closer to the cobalt(II) than proton 1. Since the outer-sphere contribution has been included as a somewhat arbitrary correction factor, it is probably not justified to speculate further on these values.

Table 3.5. Temperature Independent Shift and Relaxation Parameters

	Protons		
Parameters	i = 1	2	3
$10^{-6} \times C_1^i$ (Hz)	2.40	2.57	2.80
$10^{-6} \times C_2^i$ (Hz)	1.88	3.05	2.50
$10^{-4} \times C_{mB}^i$ (s^{-1} K)	6.00	6.30	7.70
$10^{-4} \times C_{mC}^i$ (s^{-1} K)	4.65	11.5	8.00
$10^{-4} \times K_{os}' C_{mo}^i$ (s^{-1} K)	2.5	7.3	5.8

References

(1) Jesson, J. P. In *NMR of Paramagnetic Molecules: Principles and Applications*; La Mar, G. N.; Horrocks, W. D. Jr.; Holms, R. H., Ed.; Academic Press: New York/London, 1973; Chapter 1.

(2) Mabbs, F. E.; Machin, D. J. *Magnetism and Transition Metal Complexes*; Chapman and Hall: London, 1973; Chapter 1.

(3) La Mar, G. N.; Walker, F. A. *J. Am. Chem. Soc.* **1973**, *95*, 1790.

(4) Migita, K.; Iwaizumi, M; Isobe, T. *J. Chem. Soc. Dalton Trans.* **1976**, 532; *J. Am. Chem. Soc.* **1975**, *97*, 4228.

(5) Srivanavit, C.; Brown, D. G. *Inorg. Chem.* **1975**, *12*, 2950; *J. Am. Chem. Soc.* **1976**, *98*, 4447.

(6) Botulinski, A. Buchler, J. W.; Tonn, B.; Wicholas, M. *Inorg. Chem.* **1985**, *24*, 3239.

(7) Shirazi, A.; Goff, H. M. *Inorg. Chem.* **1982**, *21*, 3420.

(8) Richardson, P. F.; Kreilick, R. W. *Inorg. Chem.* **1981**, *20*, 1978.

(9) Lutos-Grazynski, L. *Inorg. Chem.* **1985**, *24*, 1104.

(10) Bakac, A.; Brynildson, M. E.; Espenson, J. H. *Inorg. Chem.* **1986**, *25*, 4108.

(11) Nonaka, Y.; Hamada, K. *Bull. Chem. Soc. Jpn.* **1981**, *54*, 3185.

(12) See Chapter 1 and the references therein.

(13) Lance, K. A.; Goldshy, K. A.; Busch, D. H. *Inorg. Chem.* **1990**, *29*, 4537.

(14) Henderson, W. W.; Shepherd. R. E.; Abola, J. *Inorg. Chem.* **1986**, *25*, 3157.

(15) Rockenbauer, A.; Budo-Zahonyi, E.; Simandi, L. I. *J. Coord. Chem.* **1972**, *2*, 53.

(16) Led, J. J.; Grant, D. M. *J. Am. Chem. Soc.* **1977**, *99*, 5845.

Chapter 4. Kinetics of Water Proton Exchange of $(H_2O)_5CrCH_2CN^{2+}$ in Aqueous Acid*

Introduction

There have been many NMR studies of the rate of solvent exchange on paramagnetic metal ions because solvent exchange kinetics play a key role in the substitution reactivity of metal complexes. But there have been relatively few studies on the kinetics of proton transfer from such $M(OH_2)_n^{z+}$ systems, although such reactions generate $M(OH_2)_{n-1}(OH)^{(z-1)+}$ which is generally more substitutionally labile than the parent aqua species. The early work of Bloembergen and Morgan,[1] and Swift and Stephenson[2] demonstrated that water proton exchange may proceed by the reactions in Scheme I. These reactions can be distinguished by the hydrogen ion dependence of the proton exchange rate.

Scheme I

$$M(OH^*H)^{z+} + H_3O^+ \underset{k_{-1}}{\overset{k_1}{\rightleftharpoons}} M(OH_2)^{z+} + {}^*HH_2O^+$$

$$M(OH^*H)^{z+} + H_2O \underset{k_{-2}}{\overset{k_2}{\rightleftharpoons}} M(OH)^{(z-1)+} + {}^*HH_2O^+$$

$$M(OH)(OH^*H)^{(z-1)+} + H_2O \underset{k_{-3}}{\overset{k_3}{\rightleftharpoons}} M(OH)_2^{(z-2)+} + {}^*HH_2O^+$$

Eyring and coworkers[3] used electric field dissociation relaxation to show that k_{-2} is near the diffusion control limit and is relatively independent of the type of metal ion. Therefore, determination of k_2 allows one to estimate the hydrolysis constant (K_m =

---

* A version of this chapter has been published. Kefei Wang and R. B. Jordan *Inorg. Chem.* 1993, *32*: 895-897.

k_2/k_{-2}). In addition, the work of Morgan and Bloembergen showed that the relaxation effect of the paramagnetic ion provides characteristic information on its electron spin correlation time which in turn depends on the electronic structure of the species.

The present study explores the NMR relaxation effect on the solvent water protons of an organo-chromium(III) species, $(H_2O)_5Cr(CH_2CN)^{2+}$.This complex is a representative of a series of organo-chromium(III) species which have unusual electronic spectra[4] and substitution lability[5] for the water ligand *trans* to the organo-ligand. The results will be compared to previous work on $Cr(OH_2)_6^{3+}$ [2] and $(H_2O)_5Cr(N_3)^{2+}$ [6] to determine if the organo-chromium species causes unusual relaxation effects which might be indicative of unusual electronic properties. The acid dependence of the solvent proton relaxation rate will be used to determine the rate constants in Scheme I, and to estimate the hydrolysis constant for $(H_2O)_5Cr(CH_2CN)^{2+}$. The latter cannot be measured directly because of the hydrolytic instability of these species at pH ≥ 3.

Experimental Section

Solutions of $(H_2O)_5CrCH_2CN^{2+}$ in aqueous perchloric acid were prepared and purified by ion exchange chromatography as described previously.[5] A stock solution of 7.51×10^{-3} M $(H_2O)_5CrCH_2CN^{2+}$ in 0.051 M $HClO_4$ was adjusted to higher acidity by addition of 1.067 M $HClO_4$ and to lower acidity by addition of weighed amounts of Na_2CO_3. The solutions for NMR measurements were kept under an argon atmosphere in 10 mm tubes sealed with a serum cap.

The NMR relaxation rates were determined by standard 180-τ-90 (R_1) and Carr-Purcell-Meiboom-Gill methods (R_2) on a Bruker SXP 4-100 pulsed spectrometer at 89.5 MHz. The instrumentation is fully described elsewhere.[7,8] The temperature was

measured in a blank sample tube with a copper-constantan thermocouple before and after each set of measurements. The reported relaxation rates are the average of at least 5 replicate determinations, with a typical precision of ± 2% for R_1 and ± 5% for R_2.

Results

The measured water proton relaxation rates (R_{iobs}, i = 1 or 2) for solutions of $(H_2O)_5Cr(CH_2CN)^{2+}$ in aqueous perchloric acid have been corrected for pure solvent relaxation (R_{isolv}) and normalized for the [Cr(III)] according to Eq 4.1

$$R_{ip} = \frac{1}{P_m}(R_{iobs} - R_{isolv}) \tag{4.1}$$

where P_m = $[(H_2O)_5CrCH_2CN^{2+}]/[H_2O]$ is the molar ratio of chromium(III) to solvent water. The number of exchanging sites is introduced below.

Representative results of the temperature dependence of the solvent proton longitudinal (R_{1p}) and transverse (R_{2p}) relaxation rates are shown in Figure 4.1. The temperature dependence of the $R_{1,2p}$ curves is consistent with the predictions of the theory developed by Swift and Connick[9] which predicts that R_{2p} is given by Eq 4.2

$$R_{2p} = n \times r_m \left(\frac{R_{2m}(R_{2m} + r_m) + \Delta\omega_m^{\,2}}{(R_{2m} + r_m) + \Delta\omega_m^{\,2}} \right) + R_{2o} \tag{4.2}$$

where r_m is the chemical exchange rate, R_{2m} is the nuclear relaxation rate of the coordinated protons, $\Delta\omega_m$ is the chemical shift difference between coordinated and bulk solvent protons, and R_{2o} is the outer-sphere relaxation rate and n is the number of water ligands with exchanging hydrogens. For present purposes, it has been assumed that n = 5 (i.e. all the water protons are involved in the exchange process), to be consistent

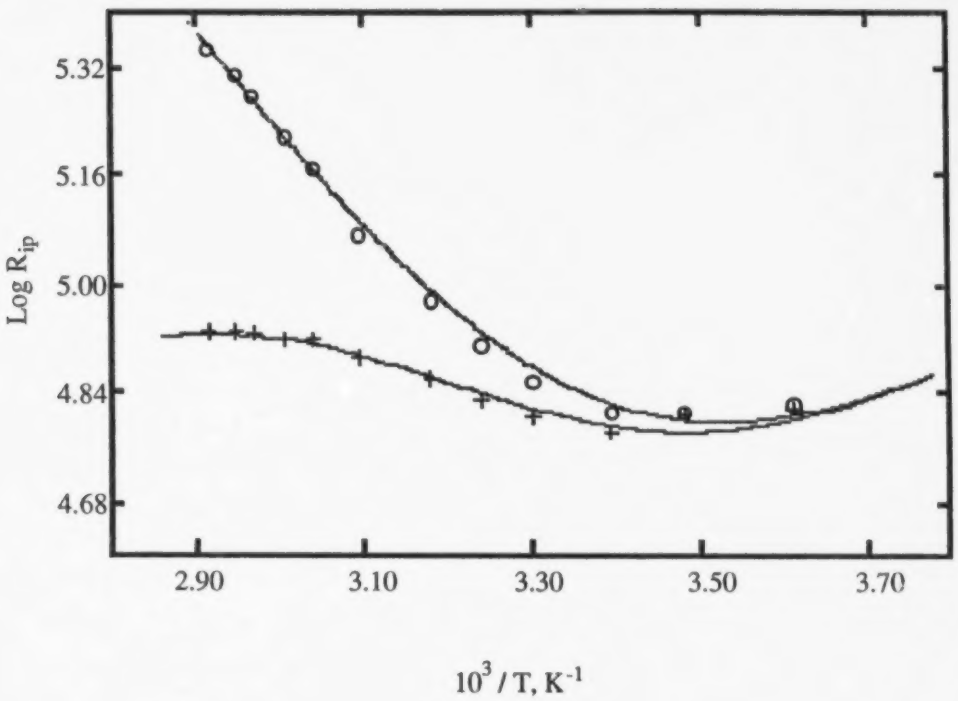

Figure 4.1. Solvent water proton transverse (R_2 o) and longitudinal (R_1 +) relaxation rates for a solution of $(H_2O)_5CrCH_2CN^{2+}$ in 0.051 M $HClO_4$.

with the earlier studies on aquachromium(III) species. A similar expression[9] applies for R_{1p} except that the $\Delta\omega_m$ term is omitted and R_{2m} and R_{2o} are replaced by R_{1m} and R_{1o}. The temperature dependence of these factors is given by the following standard equations.[10]

$$R_{im} = \frac{C_{im}}{T}\exp\left(\frac{E_{im}}{RT}\right) \tag{4.3}$$

$$R_{io} = \frac{C_{io}}{T}\exp\left(\frac{E_{io}}{RT}\right) \tag{4.4}$$

$$r_m = 2.083\times10^{10}\,T\exp\left(\frac{-\Delta H^{\ddagger} + T\Delta S^{\ddagger}}{RT}\right) \tag{4.5}$$

$$\Delta\omega_m = \frac{C_\omega}{T} \tag{4.6}$$

where the C's are temperature independent constants.

At low temperature, the relaxation rates show the onset of a flat temperature dependence which is typical of outer-sphere relaxation (R_{1o}). As the temperature increases, there is a long region in which R_{2p} increases with increasing temperature as expected for chemical exchange rate (r_m) control of the relaxation. For R_{1p}, this region is shorter and less pronounced because of the onset of control of the relaxation by the inner-sphere relaxation rate (R_{1m}). This does not appear with R_{2p}, either because R_{2m} is much larger, or because the chemical shift difference of the free and coordinated protons ($\Delta\omega_m$) is large enough to provide effective R_2 relaxation through dephasing. There is an added complication in the system because the chemical exchange process has a dependence on the hydrogen ion concentration as shown in Figure 4.2.

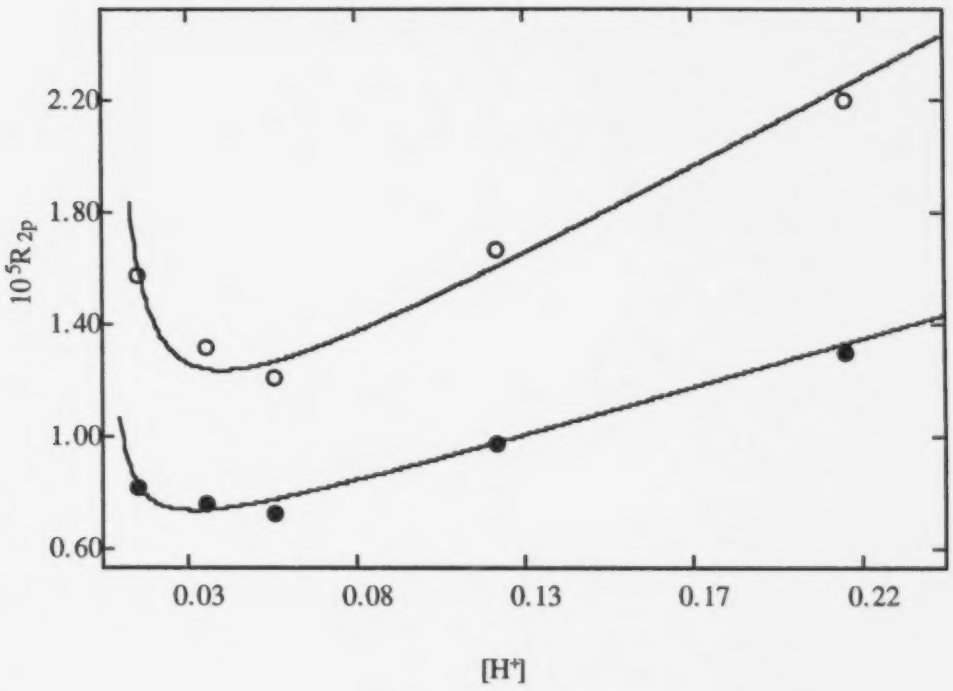

Figure 4.2. Hydrogen ion dependence of the transverse relaxation rate of the water protons in solutions of $(H_2O)_5CrCH_2CN^{2+}$ at 50 ± 1 °C (o) and 30 ±1 °C (●).

This is consistent with the expectation from the reactions in Scheme I which predict that r_m is described by the rate law given by Eq 4.7.

$$r_m = k_1[H^+] + k_2 + k_3[H^+]^{-1} \quad (4.7)$$

Therefore the temperature dependence of r_m will be more complex than described by Eq 4.5, and will depend on the $\Delta H^{\ddagger}$ and $\Delta S^{\ddagger}$ values for each of k_1, k_2 and k_3.

The analysis of the temperature dependence of $R_{1,2}$ relies first of all on the fact that R_2 has a well defined region where chemical exchange is rate controlling so that the activation parameters $\Delta H^{\ddagger}$ and $\Delta S^{\ddagger}$ can be defined using estimated values for the activation energy for the outer-sphere process (E_o). Then these activation parameters can be used in the analysis of the R_1 values to obtain E_o which is assumed to be equal to the activation energy for the R_{1m} process (E_m). Then the R_2 values can be refitted and the process repeated to obtain self-consistency between the parameters. In the final analysis, the R_{1p} and R_{2p} data were combined to determine the most self-consistent parameters. This procedure takes advantage of the fact that the R_{2p} data primarily determine the $\Delta H^{\ddagger}$ and $\Delta S^{\ddagger}$ values, while the R_{1p} data are most sensitive to E_o and E_m. As expected, the combined fit did not change the parameters much, but it did reveal that the best overall fit is obtained with $E_m > E_o$. The final best-fit parameter values are listed in Table 4.1 and shown by the calculated curves in Figure 4.3. The observed and calculated values are given as supplementary material in Tables A-10 and A-11 in the Appendix.

Discussion

One purpose of this study is to compare the proton exchange rate from $(H_2O)_5CrCH_2CN^{2+}$, $(H_2O)_5Cr(N_3)^{2+}$ [6] and $Cr(OH_2)_6^{3+}$ [2,3] in order to assess whether the

Table 4.1. Least-squares Best-fit Parameters for the Temperature Dependence of the Solvent Water Proton Relaxation Rates in Acidic Solutions of $(H_2O)_5CrCH_2CN^{2+}$

Parameter[a]	Value[b]
$\Delta H_1^{\ddagger}$	3.65 ± 0.29
$\Delta S_1^{\ddagger}$	-24.4 ± 0.90
k_1 (M^{-1} s^{-1}), 25 °C	6.4×10^4
$\Delta H_2^{\ddagger}$	7.97 ± 0.28
$\Delta S_2^{\ddagger}$	-14.9 ± 0.86
k_2 (s^{-1}), 25 °C	4.9×10^3
$\Delta H_3^{\ddagger}$	9.66 ± 0.77
$\Delta S_3^{\ddagger}$	-19.38 ± 2.45
k_3 (M s^{-1}), 25 °C	30
C_{im} (s^{-1} K)	$(3.0 \pm 1.4)\times10^5$
E_{im} (kcal mol^{-1})	2.17 ± 0.32
C_o (s^{-1} K)	$(5.47 \pm 0.19)\times10^4$
E_{im} (kcal mol^{-1})	3.0 ± 0.3

[a] The $\Delta H^{\ddagger}$ and $\Delta S^{\ddagger}$ values are in kcal mol^{-1} and cal mol^{-1} K^{-1}, respectively. [b] Errors given are one standard deviation.

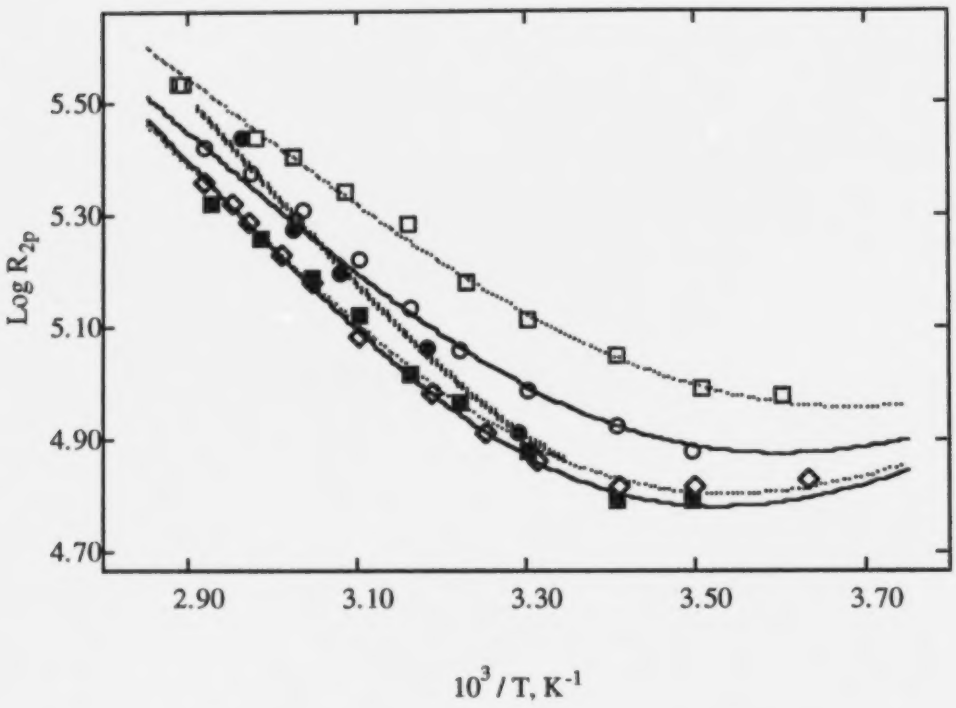

Figure 4.3. Temperature and [H^+] dependence of R_{2p} for solvent water protons in solutions of $(H_2O)_5CrCH_2CN^{2+}$. The H^+ concentrations (M) are 0.220 (···□···), 0.117 (—o—), 0.051 (···◇···), 0.0306 (—■—), 0.0105 (Ⅲ●Ⅲ).

organo-chromium(III) species can be viewed as a normal dicationic chromium(III) complex. The kinetic results for these complexes, which are summarized in Table 4.2, reveal that there is nothing particularly unusual about the organo-chromium(III) complex. The exchange rates and activation parameters are of similar magnitude to those of the other chromium(III) complexes.

The activation parameters for k_1 are strikingly similar for $(H_2O)_5CrCH_2CN^{2+}$ and $(H_2O)_5Cr(N_3)^{2+}$. The published value[2] of $\Delta H_1^{\ddagger}$ for $Cr(OH_2)_6^{3+}$ is surprisingly smaller, since one might expect that the higher positive charge would make protonation more difficult. A reanalysis reveals that the data of Swift and Stephenson[2] are not inconsistent with $\Delta H_1^{\ddagger}$ = 3.6 kcal mol^{-1} and $\Delta S_1^{\ddagger}$ = -24.1, giving $k_1 = 8\times10^4$ M^{-1} s^{-1} at 25 °C. This observation indicates that the k_1 process is kinetically relatively independent of the charge on the metal complex. This is consistent with the published results of Swift and Stephenson which imply that this path is similar for $Ni(OH_2)_6^{2+}$ and $Cr(OH_2)_6^{3+}$.

The values of the rate constant for the k_2 path differ by a factor of two between the NMR and electric field dissociation methods. This difference is probably due, at least in part, to the ionic strength, which was near zero for the electric field dissociation study, but in the range of 1 M for the NMR work. For the acid dissociation of $Cr(OH_2)_6^{3+}$, the ΔH_2° and ΔS_2° are 9.30 kcal mol^{-1} and 12.3 cal mol^{-1} K^{-1} (pK = 4.13 (25 °C), μ = 0.5 M).[11] Therefore, if k_{-2} is a diffusion controlled process with $\Delta H^{\ddagger} \approx 2$ kcal mol^{-1}, then k_2 is predicted to have $\Delta H^{\ddagger} \approx 7.3$ kcal mol^{-1} in good agreement with the NMR results. The experimental values of k_2 can be combined with the appropriate equilibrium constant (pK = 4.29 at μ = 1.0 [12], pK = 3.95 at $\mu \approx 0$ [13]) to give k_{-2} values (M^{-1} s^{-1}, 25 °C) of 9.8×10^8 and 1.3×10^9 from the NMR and electric field dissociation studies respectively.

From the above analysis, it seems reasonable to assume that $k_{-2} \approx 1\times10^9$ M^{-1} s^{-1}.

Table 4.2. Comparison of Exchange Rate Parameters for Coordinated Water Protons on Several Chromium(III) Complexes

Parameter[a]	$(H_2O)_5CrCH_2CN^{2+}$	$(H_2O)_5Cr(N_3)^{2+}$	$Cr(OH_2)_6^{3+}$
$10^{-4} \times k_1$	6.4	16[c]	5[b] (8)[c]
$\Delta H_1^{\ddagger}$	3.7	3.2[c]	0.5[b] (3.6)[c]
$\Delta S_1^{\ddagger}$	-24.4	-24[c]	-36[b] (-24.1)[c]
$10^{-4} \times k_2$	0.49	1.3[c]	7.0[c] (14)[d]
$\Delta H_2^{\ddagger}$	8.0	9.3[c]	7.5[c]
$\Delta S_2^{\ddagger}$	-15	-8.5[c]	-11.3[c]
k_3	30	–	42[c,e] (10^2)[f]

[a] Units as in Table 4.1. [b] Values from Reference 2. [c] Values from reanalysis of the data in References 2 and 6 using the temperature dependence of R_{2m} and R_{2o} found in this work. [d] Value from Reference 3. [e] At 283 K. [f] Estimated at 25 °C using the $\Delta H_3^{\ddagger}$ in Table 4.1.

This value can be combined with the measured k_2 to estimated the pK of the chromium(III) complexes. The resulting pK values are 4.8 and 4.3 for $(H_2O)_5Cr(N_3)^{2+}$ and $(H_2O)_5CrCH_2CN^{2+}$, respectively. These values assume that all coordinated water hydrogens are exchanging and would increase by log(5/4) = 0.1 if the hydrogens of four waters dominate the exchange process, and log(5) = 0.7 if one set is exchanging must faster than the others. The latter would seem to be a possibility, since the protons *trans* to Cl^- exchange more rapidly in $(H_3N)_5CoCl^{2+}$ [14], although the chemical analogy of the chromium(III) and cobalt(III) systems is certainly questionable.

The k_3 path is apparent in the data of Swift and Stephenson[2] but was ignored in their analysis. Our analysis of their data gives $k_3 = 42 \pm 4$ M s^{-1} at 283 K for $Cr(OH_2)_6^{3+}$ and an estimate of $k_3 \approx 10^2$ M s^{-1} at 25 °C if $\Delta H_3^{\ddagger}$ is the same as for $(H_2O)_5CrCH_2CN^{2+}$. The k_3 values can be used analogously to the k_2 values to estimate the second ionization constant of these aquachromium(III) species. The estimated pK_2's are 7.5 and 7.0 for $(H_2O)_5CrCH_2CN^{2+}$ and $Cr(OH_2)_6^{3+}$, respectively. The latter value is somewhat larger than that of 6.1 obtained by Stünzi and Marty[12] from potentiometric titrations, but is in marked disagreement with the value of 9.7 suggested by Schwarzenbach.[15] The NMR estimate may be slightly low because of uncertainty about the number of exchanging sites, as discussed above, while the potentiometric value could be low because of difficulties in correcting for oligomerization reactions.

Finally, we just comment on the general relaxation effects of these chromium(III) complexes. The values of R_{2p} are of the order of 10^5 for both $(H_2O)_5Cr(N_3)^{2+}$ and $(H_2O)_5CrCH_2CN^{2+}$, and about 10 times larger for $Cr(OH_2)_6^{3+}$. This is consistent with the relaxation being controlled by the electron spin relaxation time of chromium(III). The lower symmetry of the former two complexes should make this time shorter and thereby reduce the solvent proton R_{2p} values. The similarity of

$(H_2O)_5Cr(N_3)^{2+}$ and $(H_2O)_5CrCH_2CN^{2+}$ indicates that there is nothing remarkably special about the electron spin properties and therefore the electronic state of the organo-chromium species.

References

(1) Bloembergen, N.; Morgan, L. O. *J. Chem. Phys.* **1961**, *34*, 842.

(2) Swift, T. J., Stephenson, T. A. *Inorg. Chem.* **1966**, *5*, 1100.

(3) Rich, L. D.; Cole, D. L.; Eyring, E. M. *J. Phys. Chem.* **1969**, *73*, 713.

(4) Espenson, J. H. *Adv. Inorg. Bioinorg. Mech.* **1982**, *1*, 1

(5) Sisley, M. J.; Jordan, R. B. *Inorg. Chem.* **1991**, *30*, 1279; *ibid.* **1988**, *27*, 4483; *ibid.* **1987**, *26*, 2833.

(6) Balahura, R. J.; Jordan, R. B. *Inorg. Chem.* **1970**, *9*, 2639.

(7) Chopra, S.; McClung, R. E. D.; Jordan, R. B. *J. Magn. Reson.* **1984**, *59*, 361.

(8) Grant, M.; Jordan, R. B. *Inorg. Chem.* **1981**, *20*, 55.

(9) Swift, T. J., Connick, R. E. *J. Chem. Phys.* **1962**, *37*, 307.

(10) Rusnak, L. L.; Jordan, R. B. *Inorg. Chem.* **1976**, *15*, 709.

(11) Xu, F.-C.; Krouse, H. R.; Swaddle, T. W. *Inorg. Chem.* **1985**, *24*, 267.

(12) Stünzi, H.; Marty, W. *Inorg. Chem.* **1983**, *22*, 2145.

(13) Tsuchiya, R.; Umayahara, A. *Bull. Chem. Soc. Japan* **1963**, *36*, 554.

(14) Buckingham, D. A.; Marzilli, P. A.; Sargeson, A. M. *Inorg. Chem.* **1969**, *8*, 1595; Buckingham, D. A.; Cresswell, P. J.; Sargeson, A. M. *Inorg. Chem.* **1975**, *7*, 1485.

(15) Schwarzenbach, G. *Pure Appl. Chem.* **1962**, *5*, 377.

Chapter 5

Electron-Transfer Kinetics of Cobaloximes

Introduction

As discussed in Chapter 1, bis(dimethylglyoximato)cobalt(II) complexes are mild reducing agents, and the electron-transfer can be either by an inner-sphere or an outer-sphere mechanism, depending on the nature of the oxidant. The oxidation of $(H_2O)_2Co^{II}(dmgH)_2$ by $XCo^{III}(NH_3)_5^{2+}$ (X = halides and pseudohalides) has been studied by Adin and Espenson.[1] They suggested the X-bridged inner-sphere pathway shown in Scheme I (charges are omitted), based on the identification of the bridge-transferred product $X(H_2O)Co^{III}(dmgH)_2$, and the observed rate order of $Br^- > Cl^- » F^-$.

Scheme I

$$(H_3N)_5Co^{III}X + (H_2O)_2Co^{II}L \overset{fast}{\rightleftharpoons} (H_3N)_5Co^{III}\text{-}X\text{-}Co^{II}(OH_2)L + H_2O$$

$$(H_3N)_5Co^{III}\text{-}X\text{-}Co^{II}(OH_2)L \xrightarrow{k_{et}} (H_3N)_5Co^{II}\text{-}X\text{-}Co^{III}(OH_2)L$$

$$(H_3N)_5Co^{II}\text{-}X\text{-}Co^{III}(OH_2)L \xrightarrow{fast} Co^{II} + 5NH_3 + XCo^{III}(OH_2)L$$

$L = (dmgH)_2$

The studies on the reduction of various $L_2Co^{III}(dmgH)_2^+$ and $XLCo^{III}(dmgH)_2$ (X = halide or pseudo-halide, L = amine or pyridine) complexes by aqueous V^{2+}, Fe^{2+}, and Cr^{2+} have suggested that another possible bridging site in an inner-sphere pathway could be the oxygen atom(s) of the oxime ligand. These studies were out carried in acidic media (pH < 4), and the $[H^+]$ dependence of the reaction rate was used as an important criterion to assign the mechanism. The $[H^+]$ dependence is believed to result

from the protonation equilibrium of the dmgH ligand in Eq 5.1:

$$XLCo^{III}(dmgH)(dmgH_2)^+ \overset{K_a}{\rightleftharpoons} XLCo^{III}(dmgH)_2 + H^+ \qquad (5.1)$$

An inverse [H⁺] dependence of the rate indicates that the protonated form is less reactive than the normal form, and this has been taken to suggest an inner-sphere mechanism.

Prince and Segal[2] studied the reduction of $L_2Co^{III}(dmgH)_2^+$ (L = NH_3 and $EtNH_2$) by V^{2+}, and suggested the mechanism in Scheme II.

Scheme II

$$(H_3N)_2Co^{III}(dmgH)_2 + V^{II} \xrightarrow{slow} \{(H_3N)_2Co^{III}(dmgH)_2\text{–}V^{II}\}$$

$$\{(H_3N)_2Co^{III}(dmgH)_2\text{–}V^{II}\} \xrightarrow{fast} \{(H_3N)_2Co^{II}(dmgH)_2\text{–}V^{III}\}$$

$$\{(H_3N)_2Co^{II}(dmgH)_2\text{–}V^{III}\} + 2H^+ \xrightarrow{fast} Co^{II} + 2NH_3 + 2dmgH_2 + V^{III}$$

The rate is independent of [H⁺] in the range of 0.012 to 0.092 M [H⁺], but shows an inverse dependence at 0.992 M [H⁺]. This is consistent with an inner-sphere mechanism if $K_a \gg 0.10$ M for these cations. Prince and Segal also suggested that the $\Delta S^{\ddagger}$ of -11 cal mol^{-1} K^{-1} is indicative of an inner-sphere mechanism compared to ca. -30 cal mol^{-1} K^{-1} expected for an outer-sphere mechanism.[3] Prince and Segal proposed that bridging of V^{2+} occurs at the oxygen atom(s) of the $(dmgH)_2$ ligand because the axial NH_3 cannot be a bridging ligand.

However, the V^{2+} reduction of the seemingly analogous $(PhNH_2)_2Co^{III}(dmgH)_2^+$ has a positive [H⁺] dependence and the $(py)_2Co^{III}(dmgH)_2^+$

complex has no $[H^+]$ dependence, from 9.45×10^{-3} to 0.976 M $[H^+]$, in both cases.[2] Since $PhNH_3^+$ (pK_a 4.7) and pyH^+ (pK_a 5.2) are much stronger acids than NH_4^+ (pK_a 9.25) or $EtNH_3^+$ (pK_a 10.7), it could be argued that $PhNH_2$ and py are poorer electron donors to Co^{III}. This would make the oxime oxygens less basic so that K_a would be larger, and formation of a bridged complex at the oxime oxygen(s) would also be less favorable than with NH_3 and $EtNH_2$. Prince and Segal used the $\Delta S^{\ddagger}$ values of -31.6 cal mol^{-1} K^{-1} ($PhNH_2$) and -30.6 cal mol^{-1} K^{-1} (py) to assign an outer-sphere mechanism for these reductions.

The Fe^{2+} reduction of $X(py)Co^{III}(dmgH)_2$ (X = halides) studied by Dayalan and Vijayaraghavan[4] shows an inverse $[H^+]$ dependence, and therefore was assigned an inner-sphere mechanism. The rate order of $I^- > Br^- > Cl^-$ found for these reactions is not consistent with that of $F^- > Cl^- > Br^- > I^-$ found for the X-bridged inner-sphere reduction of $Co(NH_3)_5X^{2+}$ by Fe^{2+}.[5] Therefore, Dayalan and Vijayaraghavan suggested that the bridging site is the oxime rather the X atom. It should be noted that the acid dissociation constant K_a values are ca. $(1.7–5.0)\times10^{-3}$, depending upon the axial X ligands.

There is a problem with the $(X)(H_3N)Co^{III}(dmgH)_2$ reductions by Fe^{2+} and V^{2+} when they are compared to the $L_2Co^{III}(dmgH)_2^+$ systems (L = NH_3 and $EtNH_2$). As noted above, the Fe^{2+} reaction ($X = Br^-$)[6] has an inverse $[H^+]$ dependence but the V^{2+} reactions have a positive $[H^+]$ dependence ($X = Cl^-$ or Br^-).[7] If Eq 5.1 is taken into account, then the apparent second-order rate constants for these reactions should be given by Eq 5.2

$$k_2 = \frac{k_0 K_a + k_H[H^+]}{K_a + [H^+]} \tag{5.2}$$

where k_0 and k_H are specific rate constants for reduction of the normal and protonated

complexes, respectively. If the K_a is ca. $(2\text{-}5)\times10^{-3}$ M as suggested by Dayalan and Vijayaraghavan,[2] then the complexes should be fully protonated for $[H^+] = 0.194 - 0.984$ M in the V^{2+} study of Prince and Segal.[7] Then $[H^+] \gg K_a$ and the above equation cannot reduce to a form with a positive $[H^+]$ dependence. One possible, but unproven way out of this anomaly is to suggest that the complexes can undergo a second protonation, with $K_{a2} > 2$. If this is the case, then the values assigned to k_0 and k_H by Prince and Segal are really rate constants for reduction of the protonated and diprotonated complexes respectively.

A further complexity of these systems is illustrated by the study of the V^{2+} reductions of $(Y)(L)Co^{III}(dmgH)_2$ complexes ($Y = N_3^-$, NCS^-, NO_2^-; L = py, NH_3, $PhNH_2$).[8,9] All of these show rates which are essentially independent of $[H^+]$ (0.003 to 0.10 M). However the Fe^{2+} reductions of some of the same systems ($Y = N_3^-$, L = py or NH_3)[10] have an inverse $[H^+]$ dependence indicative of an inner-sphere mechanism and with $K_a = 7.3\times10^{-4}$ (L = py) and 1.9×10^{-3} (L = NH_3). The $[H^+]$ independence of the V^{2+} reductions can only be rationalized by Eq 5.2 if k_0 is essentially equal to k_H. Balasubramanian and Vijayaraghavan[8] suggested that this is the case because the rate is controlled by the rate of substitution on $V(OH_2)_6^{2+}$ to form the bridged complex (first step in Scheme II). This process might not be very sensitive to protonation of the oxime if the substitution is at the Y ligand. The upper limit of the rate constant for the substitution can be estimated as < 30 M^{-1} s^{-1}, based on the water exchange rate on $V(OH_2)_6^{2+}$ ($k_{exch} = 89$ s^{-1}; $\Delta H^{\ddagger} = 14.8$ kcal mol^{-1} and $\Delta S^{\ddagger} \approx 0$).[11] For two systems, $(N_3)(py)Co^{III}(dmgH)_2$ and (NCS-)$(py)Co^{III}(dmgH)_2$,[8] the reduction rate constants of 71 and 284 M^{-1} s^{-1} exceed the estimated limit. Balasubramanian and Vijayaraghavan assigned outer-sphere mechanisms to these reactions, but it is not clear why these complexes should have a different mechanism, or why they do not show the positive $[H^+]$ dependence if they are outer-sphere.

The best criterion for establishing an inner-sphere mechanism is to identify the bridging ligand transferred product.[11] This is best done with Cr^{2+} as the reducing agent because the Cr^{III} product is substitution inert and can be separated and identified by standard methods. Unfortunately, only rather limited studies of this type have been done. Segal and Prince[12] studied the Cr^{2+} + $(H_3N)_2Co^{III}(dmgH)_2^+$ reaction (k_2 = 40 + 780×[H^+] M^{-1} s^{-1}, 25 °C) and initially reported no bridge-transferred product, but later separated, by ion–exchange chromatography, a fraction containing dmgH and Cr^{3+}. Balasubramanian and Vijayaraghavan[9] did a product study for Cr^{2+} + $(N_3)(H_3N)Co^{III}(dmgH)_2$ and reported $Cr(dmgH)^+/CrN_3^{2+}$ = 2:1 and also reported a ratio of 1:2 for Cr^{2+} + $(N_3)_2Co^{III}(dmgH)_2^-$. These results indicate competitive bridging of azide and the oxime, with the latter being more important for the neutral complex. However, it remains possible that the $Cr(dmgH)^+$ was formed by oxidation of a Cr^{2+}–dmgH complex during product analysis.

There are no reports of definite outer-sphere reductions of the cobaloxime(III). However, outer-sphere reductions of structurally similar Co(III) tetraaza macrocyclic complexes have been studied extensively by Endicott et al.[13-17] In these complexes, the tetraaza ligands form a square planar chelating ring binding to the Co cation, with the two axial positions of Co occupied by water ligands. The cross reactions between these $(H_2O)_2Co^{III}(N_4)^{3+}$ and $(H_2O)_2Co^{II}(N'_4)^{2+}$ (N_4 and N'_4 stand for different tetraaza macrocyclic ligands) are supposed to be outer-sphere, and the cross reaction rates have been determined and used with Marcus theory (see Results section), to calculate the rates for the electron self-exchange reactions defined as follows:

$$Co^{III}(N_4)^* + Co^{II}(N_4) \longrightarrow Co^{III}(N_4) + Co^{II}(N_4)^* \qquad (5.3)$$

where N_4 are identical, and the label * is used to differentiate the electron acceptor and

the donor. The self-exchange rates were discussed in terms of the Franck-Condon barrier, which is the inner-sphere reorganization energy resulting from the bond length changes accompanying the electron-transfer process, and the nonadiabaticity factor resulting from the poor overlap of the Co(II) and Co(III) orbitals. In the case of electron transfer from high-spin Co(II) to low-spin Co(III), a spin state rearrangement before the electron-transfer will impose an extra energy barrier which would contribute to the nonadiabaticity.

In this study, the electron-transfer kinetics of the diaqua-cobaloxime complexes have been examined. The work is divided into two parts. In the first part, the rates of oxidation of $(H_2O)_2Co^{II}(dmgBF_2)_2$ by $XCo^{III}(NH_3)_5^{2+}$ (X = Br^-, Cl^- and N_3^-) have been measured to provide a comparison with the results of Adin and Espenson[1] on $(H_2O)_2Co^{II}(dmgH)_2$. In the second part, the reduction reactions of $Co^{III}(dmgH)_2^+$ and $Co^{III}(dmgBF_2)_2^+$ by the cobalt(II) sepulchrate ion ($Co(sep)^{2+}$) have been studied. The structure of $Co(sep)^{2+}$, illustrated below, has the cobalt(II) ion encapsulated within a macrocyclic ligand cage.

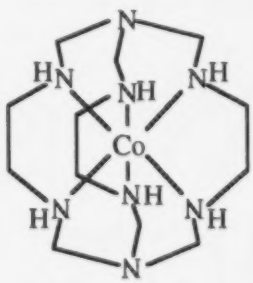

The cage ligand prevents substitution on the cobalt(II) ion, so that the electron-transfer from $Co(sep)^{2+}$ to the cobaloximes(III) must be *via* an outer-sphere mechanism. The observed reaction rates are used to estimate the cobaloxime(III)/(II) electron self-exchange rates by the Marcus cross relationship (see Results section). The self-

exchange rates are then compared with those of various $(H_2O)_2Co(N_4)^{3+/2+}$ complexes, and discussed in terms of the Franck-Condon barrier and the nonadiabatic factors in both self-exchange and cross reactions. The self-exchange rates calculated from the Marcus theory are much smaller than predicted by the Franck-Condon factor. Based on the average nonadiabaticity for the reduction of $(H_2O)_2Co^{III}(N_4)^{3+}$ and other cobalt(II) complexes by $Co(sep)^{2+}$,[15,17] the self-exchange rates obtained for cobaloxime(III)/(II) should be multiplied by a correction factor of ~ $10^{2.6}$.

Experimental Section

Materials. $Co(dmgBF_2)_2 \cdot 2H_2O$ was prepared according to Espenson et al.,[18] and has been described in the Experimental Section of Chapter 2. $[(H_2O)_2Co^{III}(dmgH)_2]ClO_4$, was prepared by the method of Ablov et al.[19,21,22] through a series of cobaloxime(III) intermediates as described below.

$[Cl_2Co^{III}(dmgH_2)(dmgH)] \cdot 2H_2O$, *trans*-dichlorobis(dimethylglyoximato)cobalt-(III).[19] To a finely ground mixture of 2.38 g (0.01 mol) of $CoCl_2 \cdot 6H_2O$ (Fisher) and 2.32 g (0.01 mol) of dimethylglyoxime ($dmgH_2$, Fisher), ca. 15 mL of water was added. The slurry was stirred on a hot plate at 70 - 80 °C for 15 min. Three to four milliliters of H_2O_2 (30%, Fisher) were added gradually with stirring after the heating was turned off. After the excess amount of H_2O_2 was removed by boiling the solution for about 10 min, ca. 30 mL of concentrated HCl (36%, BDH) was added to yield a dark-green precipitate. The mixture was cooled to room temperature, and then in an ice bath. The solid product was collected on a sintered glass filter and washed twice with dilute HCl (5% v/v), ethanol and diethyl ether. Yield: ca. 80%. The product was formulated as $[Cl_2Co^{III}(dmg_2H_3] \cdot 2H_2O$ according to the elemental analysis. Anal Calcd for $[Co(C_4H_6O_2N_2)_2H_3Cl_2] \cdot 2H_2O$: C 24.2; H 4.78; N 14.1; Cl 17.9. Found: C 24.4; H 4.88; N 13.9; Cl 18.2. NMR measurement of this complex in d_6-DMSO (General)

shows a single peak at 2.35 ppm for methyl protons and a broad peak at 7.5 ppm for water. The methyl proton resonance in $dmgH_2$ under the same condition is at 1.91 ppm. The 0.44 ppm downfield shift upon coordination of $dmgH^-$ to cobalt(III) is consistent with the reported value of ~ 0.4 ppm for cobaloxime(III) complexes.[20]

$[Cl(H_2O)Co^{III}(dmgH)_2]$, *trans*-chloroaquabis(dimethylglyoximato)cobalt(III), was prepared by aquation of $[Cl_2Co^{III}(dmg_2H_3]\cdot 2H_2O$:[19] 1.8 g of the dichloro salt was covered with 6-8 mL of boiling water. The mixture was stirred for 20 min on a steam bath, and then cooled in ice. The greenish yellow solid obtained by filtration was washed twice with the ice-cold water, ethanol and diethyl ether. Yield: 75-85%.

$[(HO)(H_2O)Co^{III}(dmgH)_2]$, *trans*-hydroxoaquabis(dimethylglyoximato)cobalt-(III).[21] 1.4 g of $[Cl(H_2O)Co^{III}(dmgH)_2]$ was covered with ca. 4 mL of a cold solution of concentrated Na_2CO_3, and the mixture was stirred until the color changed from a yellowish green to gray-yellow. The precipitate was filtered, washed twice with small amounts of cold water and cold ethanol, and finally with diethyl ether. Yield: 55%.

$[(H_2O)_2Co^{III}(dmgH)_2]ClO_4\cdot H_2O$, *trans*-diaquo-bis(dimethylglyoximato)cobalt-(III) perchlorate.[22] 0.7 g of $[(HO)(H_2O)Co(dmgH)_2]$ was dissolved in 4 mL of 2 M $HClO_4$, yellowish brown solid precipitated, and more was formed as a few drops of concentrated $HClO_4$ were added. The product was filtered, and washed twice with small amounts of ice-cold water and methanol, and finally with diethyl ether. Yield: ca. 35%. The product was formulated based on the elemental analysis. Calcd for $[(H_2O)_2Co(C_4H_7O_2N_2)_2]ClO_4\cdot H_2O$: C 21.7; H 4.55; N 12.7. Found: C 21.6; H 4.62; N 12.4. NMR spectrum in d_6-DMSO shows the methyl protons at 2.54 ppm (s), and the water protons at 7.4 ppm (s, broad). The electronic spectrum has a maximum at 240 nm with a molar absorptivity coefficient of 2.2×10^4 M^{-1} cm^{-1}, consistent with the values of 2.1×10^4 M^{-1} cm^{-1} (240 nm) and 1.95×10^4 M^{-1} cm^{-1} (238 nm) reported by Heckman and Espenson,[23] and Kita and Jordan,[24] respectively. Reduction of this

complex in aqueous solution with amalgamated zinc under an argon atmosphere produces a bright yellow solution of $(H_2O)_2Co^{II}(dmgH)_2$, which has a distinctive absorption maximum at 462 nm, with a molar absorptivity coefficient of 3.42×10^3 M^{-1} cm^{-1}, in agreement with a reported values of 3.40×10^3 M^{-1} cm^{-1}.[23]

Solutions of $(H_2O)_2Co^{III}(dmgBF_2)_2^+$ were prepared by electrolysis of $(H_2O)_2Co^{II}(dmgBF_2)_2$ immediately before use. The electrolysis was done in an H-shaped electrolysis cell, with a sintered glass filter (10-20 μ) separating the anode and cathode compartments. $Cu^{2+}(aq)/Cu$ was used as cathode, and Pt as anode in the $Co^{II}(dmgBF_2)_2$ solution. $LiClO_4$ (Amend) was added as the supporting electrolyte at a concentration of 0.09 M in both compartments. To avoid the diffusion of Cu^{2+} ion into the anode compartment, the small amount of $Cu(NO_3)_2$ solution was carefully placed with a dropper at the bottom of the cathode compartment, and only the anode tube was stirred during the electrolysis. The electrolysis was carried at ~1 volt and 0.4-0.6 mA for 0.5-1h, during which time most of the yellow color of the $Co^{II}(dmgBF_2)_2$ solution faded. If acetate buffer was required for the kinetic studies, the buffer was added to the solution of $Co^{II}(dmgBF_2)_2$ at pH ~ 4.7. The pH was adjusted with NaOH to the desired values for kinetic studies after the electrolysis.

The two halopentaamminecobalt(III) complexes, $[(H_3N)_5CoCl](ClO_4)_2$[25] and $[(H_3N)_5CoBr](ClO_4)_2$,[25] and the azidopentaamminecobalt(III) complex $[(H_3N)_5CoN_3]Cl_2$[26] were prepared according to the published methods.

1,3,6,8,10,13,16,19-Octaazabicyclo[6.6.6]eicosanecobalt(III) trichloride (cobalt(III) sepulchrate trichloride, or $Co(sep)Cl_3$) was obtained from Aldrich, and the solution of $Co(sep)^{2+}$ was prepared by reduction of the cobalt(III) sepulchrate solution over amalgamated zinc under argon.

Redistilled water was used in all preparations and kinetic studies. Other chemicals used in the preparations are of reagent or analytical grade. For buffer

preparations, sodium acetate was from Fisher, chloroacetic acid from BDH, and MES hydrate and PIPES from Aldrich.

Kinetic Measurements. All kinetic runs were carried out at 25 ± 0.2 °C. The ionic strength was maintained at 0.100 M with $LiClO_4$, and the total buffer concentration is 0.01 M. Acetate buffer was used in the studies of $Co^{II}(dmgBF_2)_2$ with $(H_3N)_5CoX^{2+}$, and the pH was kept at 4.72 ± 0.02 for all runs. Other buffers, MES, PIPES and chloroacetic acid, were used in appropriate pH ranges in the studies of the cobaloxime(III)–$Co(sep)^{2+}$ system. The pH of each solution was measured with a Corning 125 pH meter.

The absorbance decrease due to the oxidation of $Co^{II}(dmgBF_2)_2$ by $(H_3N)_5CoCl^{2+}$ and $(H_3N)_5CoN_3^{2+}$ was followed on a Hewlett Packard 8451 diode array spectrophotometer at 454 nm, with the oxidant in excess. A 5-cm cylindrical spectrophotometer cell was used, and the reactant solutions were degassed with argon before measurement. The absorbance-time data (80 points over 3 to 4 half-lives) were analyzed by least-squares to obtain the first-order rate constants. The reported second-order rate constants are the average of three measurements at different $(H_3N)_5CoX^{2+}$ concentrations.

The reaction between $(H_3N)_5CoBr^{2+}$ and $Co^{II}(dmgBF_2)_2$ was so rapid that its rate was measured on a stopped-flow spectrophotometer (Cantech Scientific Ltd) at 454 nm. The data (256 points/trace) were collected to an MS-DOS 486 PC computer and at least 150 points for each trace were analyzed by least-squares to give the first-order rate constants. The reported rate constants are the averages of at least 6 runs at each of three oxidant concentrations.

The kinetics of reduction of $Co^{III}(dmgH)_2^+$ and $Co^{III}(dmgBF_2)_2^+$ by $Co(sep)^{2+}$ were followed by stopped-flow spectrophotometry at 460 nm and 452 nm, respectively, with the $Co(sep)^{2+}$ in excess. The kinetic measurements were performed

under anaerobic conditions, since the $Co(sep)^{2+}$ can reduce O_2 in the acidic media to produce H_2O_2 and $Co^{II}(dmgH)_2$ is extremely sensitive to O_2 and H_2O_2. The $Co(sep)^{2+}$ solution was transferred to the stopped-flow storage syringe through a serum cap under argon and the cobaloxime(III) solution in the other syringe was capped with a serum cap and degassed with argon for at least 20 min. The reduction of $Co^{III}(dmgH)_2^+$ shows biphasic behavior due to the formation and then decomposition of $Co^{II}(dmgH)_2$. The absorbance-time profiles were fitted to a biphasic model to obtain the first-order rate constants for the reduction and decomposition.

Results

$(H_3N)_5CoX^{2+}$ Oxidation of $(H_2O)_2Co^{II}(dmgBF_2)_2$. The values of the second-order rate constant k_2 are collected in Table 5.1. For the purpose of comparison, Table 5.1 also includes kinetic data previously reported by Adin and Espenson[1] on the oxidation of $(H_2O)_2Co^{II}(dmgH)_2$.

Reduction of Cobaloximes(III) by $Co(sep)^{2+}$. The second-order rate constants for reduction of $(H_2O)_2Co^{III}(dmgH)_2^+$ and $(H_2O)_2Co^{III}(dmgBF_2)_2^+$ by cobalt(II) sepulchrate decrease with the acidity, as shown in Figures 5.1 and 5.2, respectively. This kind of dependence suggests an equilibrium involving the dissociation of the proton from the axial coordinated water, as shown in Scheme III, with the diaqua form more reactive than the hydroxoaqua form.

The observed second-order rate constant k_{obs} is given by Eq 5.4

$$k_{obs} = \frac{k_a[H^+] + k_b K_a}{K_a + [H^+]} \tag{5.4}$$

where K_a, k_a and k_b are defined in Scheme III.

Table 5.1. Kinetic Data for Reactions Between $(H_3N)_5Co^{III}X^{2+}$ and Diaquacobaloximes(II)[a]

	k_2 (M^{-1} s^{-1})[b]	
X	$(H_2O)_2Co^{II}(dmgH)_2$[c]	$(H_2O)_2Co^{II}(dmgBF_2)_2$[d]
Br	$(3.2 \pm 0.3)\times10^5$	50 ± 9
Cl	$(1.4 \pm 0.08)\times10^4$	2.6 ± 0.2
N_3	$(6.4 \pm 0.3)\times10^3$	5.9 ± 1.0
NCS	$(1.4 \pm 0.08)\times10^2$	
OH	$(7.7 \pm 1.5)\times10^2$	
F	10.5 ± 0.9	

[a] At 25 °C in acetate buffer (0.01 M) with $\mu = 0.10$ M by $LiClO_4$; Detailed results are listed in Table A-12 in the Appendix. [b] Errors quoted are one standard deviations. [c] At 25 °C in acetate buffer, from Reference 1. [d] pH = 4.74.

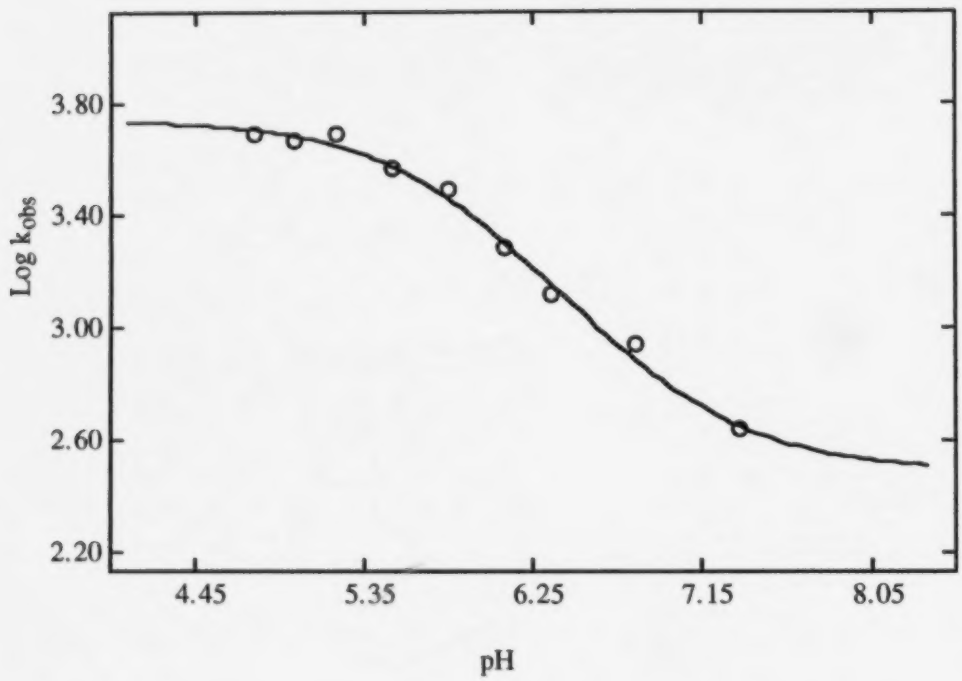

Figure 5.1. pH dependence of the second-order rate constants for reduction of $Co^{III}(dmgH)_2$ by $Co(sep)^{2+}$ (25 °C, μ = 0.10 M, the calculated curve is generated by using parameters in Table 5.2)

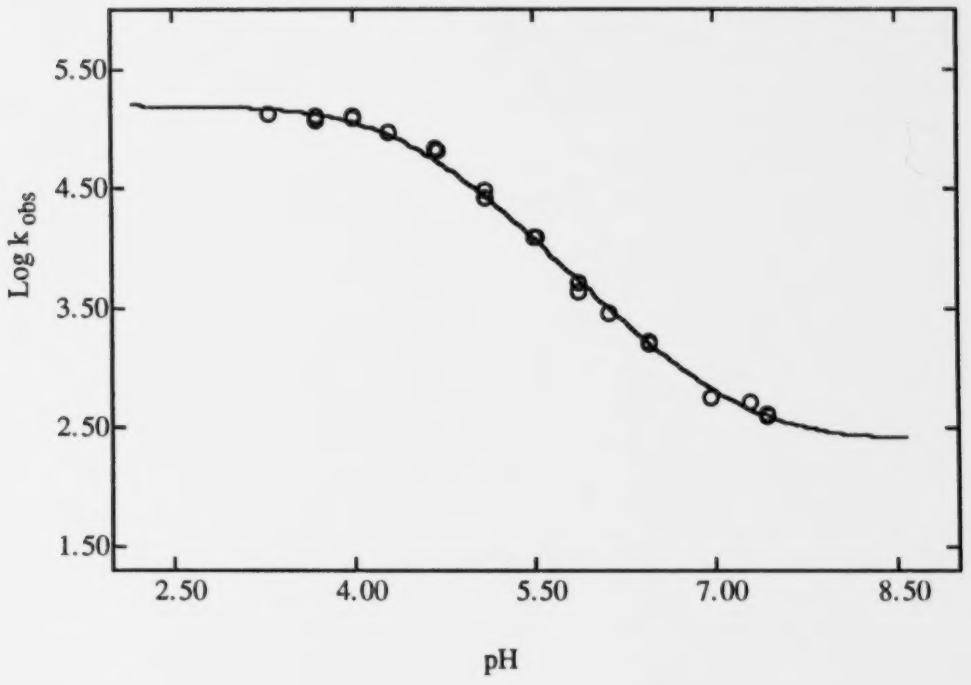

Figure 5.2. pH dependence of the second-order rate constants for reduction of $Co^{III}(dmgBF_2)_2$ by $Co(sep)^{2+}$ (25 °C, μ = 0.10 M, the calculated curve is generated by using parameters in Table 5.2)

Scheme III

$$(H_2O)_2Co^{III}L^+ \rightleftharpoons (HO)(H_2O)Co^{III}L + H^+ \quad (K_a)$$

$$(H_2O)_2Co^{III}L + Co(sep)^{2+} \xrightarrow{k_a} (H_2O)_2Co^{II}L + Co(sep)^{3+}$$

$$(HO)(H_2O)Co^{III}L + Co(sep)^{2+} \xrightarrow{k_b} (HO)(H_2O)Co^{II}L^- + Co(sep)^{3+}$$

L = $(dmgH)_2$ or $(dmgBF_2)_2$

The values of pK_a, k_a and k_b, obtained by least-squares analysis of the observed k_{obs} vs. $[H^+]$ data, are given in Table 5.2, and used to obtain the calculated curves shown in Figures 5.1 and 5.2. The detailed fitting results are listed in Table A-13 and Table A-14 in the Appendix.

The pK_a of 5.78 for $(H_2O)_2Co(dmgH)_2^+$ is in reasonable agreement with the value of 5.14 ± 0.02 (at 25 °C, in 0.1 M $NaClO_4$) obtained from potentiometric titration by Ablov et al.[27] The lower pK_a for $(H_2O)_2Co(dmgBF_2)_2^+$ by 1.4 units is reasonable if one considers the strong electron-withdrawing effect of the $-BF_2$ substituents in the modified macrocycle. In the pH ranges of our kinetic studies (4.8–7.4 for $Co^{III}(dmgH)_2^+$ and 3.3–7.4 for $Co^{III}(dmgBF_2)_2^+$), neither the ionization of the second proton (pK_{a2} = 8.38 ± 0.03 for $(H_2O)_2Co^{III}(dmgH)_2^+$ [27]) nor the protonation of dmgH ligand (eq 5.1, pK_a ~ 2.5)[2] seems to have an influence on the k_{obs} measurement.

The values of equilibrium constant K_{12} of the reactions in Table 5.2 were estimated from the electrode potentials of $Co(sep)^{3+/2+}$ and cobaloximes(III)/(II) by the following equation

$$\log K_{12} = 16.913\Delta E^\circ \qquad (5.5)$$

Table 5.2. Kinetic Results of Reactions of Cobaloxime(III) with $Co(sep)^{2+}$ [a]

Cobaloxime(III)	k_{12} (M^{-1} s^{-1}) [b] (k_a or k_b)	pK_a [b]
$(H_2O)_2Co(dmgBF_2)_2^+$	$(1.55 \pm 0.09) \times 10^5$	4.40 ± 0.03
$(H_2O)_2Co(dmgH)_2^+$	$(5.53 \pm 0.33) \times 10^3$	5.78 ± 0.07
$(HO)(H_2O)Co(dmgH)_2$	$(3.11 \pm 0.45) \times 10^2$	
$(HO)(H_2O)Co(dmgBF_2)_2$	$(2.46 \pm 0.30) \times 10^2$	

[a] At 25 °C with $\mu = 0.10$ M. [b] Errors quoted are one standard deviation.

where K_{12} is the equilibrium constant, and ΔE° is the difference between the electrode potentials of oxidant and reductant. The E° value for $Co(sep)^{3+/2+}$ is taken from results of Sargeson et al.,[28] and E° for the two diaquo cobaloximes are available from Espenson and co-workers.[18,23] However, E° values for the hydroxoaqua forms of the cobaloximes are not known. These values are estimated from the reaction cycle in Scheme IV, and are listed in Table 5.3.

Scheme IV

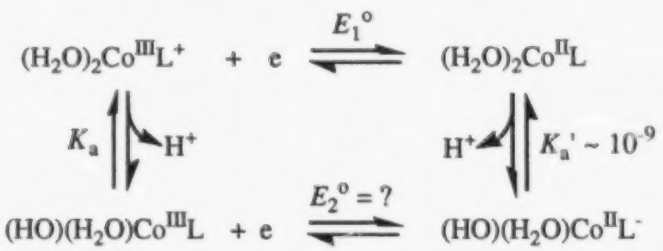

L = $(dmgH)_2$ or $(dmgBF_2)_2$

The pK_a values in Scheme IV are determined from the kinetic results in Table 5.2. The pK_a' is the acid dissociation constant for diaqua cobaloximes(II), and is assumed to be 9, a value which is typical for bivalent first-row transition metal ions. As noted above, pK_a' for the $-BF_2$ substituted complex may be lower than that for dmgH complex. However, this has a minor effect on the estimated values of E_2°, since lowering pK_a' to 8 only reduces E_2° by 0.06 V for $(HO)(H_2O)Co^{III}(dmgBF_2)_2$ reduction.

The main purpose of this study is to estimate the self-exchange rate constants for the cobaloxime(III)/(II) couples. Since $Co(sep)^{2+}$ is an outer-sphere reducing agent, the reactions between the cobaloximes(III) and $Co(sep)^{2+}$ can be analyzed by the following equations derived from Marcus theory[29]

$$k_{12} = (k_{11}k_{22}K_{12}f_{12})^{1/2} W_{12} \quad (5.6)$$

where k_{12} is the cross reaction rate (= k_{obs}), k_{11} and k_{22} are the self-exchange rates for oxidant and reductant, K_{12} is the equilibrium constant of the cross reaction. The f_{12} and work term corrections (W_{12} and w_{ij}) have been calculated from the following equations[30]

$$\ln f_{12} = \frac{[\ln K_{12} + (w_{12} - w_{21})/RT]^2}{4\ln(k_{11}k_{22}/Z^2) + (w_{11} + w_{22})/RT} \quad (5.7)$$

$$W_{12} = \exp[-(w_{12} + w_{21} - w_{11} - w_{22})/2RT] \quad (5.8)$$

$$w_{ij} = \frac{(4.225\times10^3)z_i z_j}{r(1+0.3285r\sqrt{\mu})} \quad (5.9)$$

where Z is the collision frequency, taken to be 1×10^{11} M^{-1} s^{-1}, r is the sum of the radii of the reactants in Å, μ is the ionic strength, z_i is the charge on the ion, the numerical constants are for water at 25 °C and w_{ij} values are in cal mol^{-1}. The self-exchange rates (k_{11}) can be calculated from eq 5.6 using the measured rate constants (k_{12}) and the known self-exchange rate constant for $Co(sep)^{3+/2+}$ (k_{22}). The calculated values of k_{11} are given in Table 5.3. The k_{22} value of 3.5 M^{-1} s^{-1} is taken from the results of Doine and Swaddle.[31]

Decomposition of $(H_2O)_2Co^{II}(dmgH)_2$. $(H_2O)_2Co^{II}(dmgH)_2$ decomposes in the acidic solution as shown by Eq 5.10

$$Co^{II}(dmgH)_2 + 2H^+ \rightleftharpoons Co^{2+} + 2\,dmgH_2 \quad (5.10)$$

The role of H^+ in this process is the protonation of the oxygens of the $dmgH^-$ ligand thereby destroying the O•••H—O hydrogen bond which links two $dmgH^-$ ligands to form a chelate ring. Adin and Espenson[1] found that the first order decomposition rate constant k_d in acetate buffer (pH 4.7 to 6.1) is given by $k_d = 2.84\times10^5[H^+]^{1.24}$.

Our rate constants (k_d') for decomposition of $(H_2O)_2Co^{II}(dmgH)_2$ values in the pH range of 4.7 to 6.8 are in poor agreement with those of Adin and Espenson (Table 5.4), especially at high pH's. Further experiments have shown that our k_d' values are a mixture of decomposition and oxidation by O_2 because the mixing syringes of the stopped-flow system are not completely air-proof. If $Co^{II}(dmgH)_2$ at pH=7.2 is mixed with an air saturated solution of PIPES buffer, the first-order oxidation rate constant is ~ 0.1 s^{-1}. ($[O_2] \sim 1\times10^{-4}$ M)

Discussions

$(H_3N)_5CoX^{2+}$ Oxidation of $(H_2O)_2Co^{II}(dmgBF_2)_2$. A bridged inner-sphere mechanism was established by Adin and Espenson[1] to explain their kinetic results for oxidation of $(H_2O)_2Co^{II}(dmgH)_2$ by $(NH_3)_5CoX^{2+}$ ($Br^- > Cl^- \gg F^-$), based on the identification of $X(H_2O)Co^{III}(dmgH)_2$ as the exclusive product. They interpreted the variation of k_2 with bridging ligands as the order of stability of the X-bridged precursor complexes following the analysis suggested by Haim.[32] The order of k_2 values suggests soft acid character for the $(H_2O)_2Co^{II}(dmgH)_2$ complex.

It would be expected that $(H_2O)_2Co^{II}(dmgBF_2)_2$ is also a soft acid and this is consistent with the observed order of k_2 ($Br^- > Cl^-$) if the X-bridged inner-sphere mechanism, suggested by Adin and Espenson, is operative. A common mechanism is consistent with the rate constant ratio $k_{2Br}/k_{2Cl} \approx 20$ for both cobaloxime(II) complexes. For $X = Cl^-$ and N_3^-, the reactivity difference is smaller for both $(H_2O)_2Co^{II}(dmgBF_2)_2$ and $(H_2O)_2Co^{II}(dmgH)_2$, with k_{2Cl}/k_{2N_3} ratio of ~0.4 in the former and ~ 2 for the latter.

Table 5.3. Results of Self-Exchange Rates Calculated by Marcus Relationship[a]

Cobaloxime(III)	E^{o} (V)[b]	logk_{12}	Log K_{12}	W_{12}	f_{12}	k_{11}[e]
$(H_2O)_2Co(dmgH)_2^+$	0.36[c]	3.7	10.5	2.5	2.9×10^{-3}	7.7×10^{-4}
$(H_2O)_2Co(dmgBF_2)_2^+$	0.65[c]	5.2	15.4	2.5	5.8×10^{-2}	1.5×10^{-4}
$(HO)(H_2O)Co(dmgH)_2$	0.17[d]	2.5	7.3	5.7	7.0×10^{-2}	1.9×10^{-4}
$(HO)(H_2O)Co(dmgBF_2)_2$	0.38[d]	2.4	10.8	5.7	2.4×10^{-1}	1.2×10^{-7}

[a] At 25 °C with μ = 0.10 M. [b] vs. NHE. [c] Reference 18. [d] Estimated by assuming a pK_a' = 9 for $(H_2O)_2Co^{II}L$ (L = $(dmgH)_2$ and $(dmgBF_2)_2$); see text. [e] In calculating the k_{11}, E^{o} = - 0.26 V (vs. NHE, Reference 28) and k_{22} = 3.49 M^{-1} s^{-1} (in 0.1M NaCl; Reference 31) are used for $Co(sep)^{3+/2}$.

Table 5.4. Observed First-Order Decomposition Rate of $Co^{II}(dmgH)_2$ at 25 °C

pH	k_d' (s^{-1})[a]	k_d (s^{-1}, Adin & Espenson)[b]
4.76	0.76 ± 0.04	0.36
4.97	0.74 ± 0.04	0.20
5.20	0.64 ± 0.03	0.10
5.50	0.58 ± 0.02	4.3×10^{-2}
5.80	0.43 ± 0.04	1.8×10^{-2}
6.10	0.30 ± 0.03	7.7×10^{-3}
6.35	0.14 ± 0.01	3.8×10^{-3}
6.80	0.12 ± 0.02	1.1×10^{-3}

[a] Errors quoted are one standard deviations. [b] k_d values are based on interpolation and extrapolation of the linear pH dependence (in Reference 1) which gives $k_d = 2.84\times10^{5}[H^+]^{1.24}$.

The different order may be due to some differences in affinity of Cl^- and N_3^- toward the two cobaloxime(II) complexes.

As noted by Taube,[33] for outer-sphere reduction of $(H_3N)_5CoX^{2+}$ (X = halide) by cations, the rate constant increases as the size of halide increases, and therefore follows the same trend of $Br^- > Cl^- > F^-$. In an effort to distinguish between the two mechanisms, Marcus[34] suggested that, for an outer-sphere mechanism, the reactivity pattern (relative ratio of the rate constants) for a series of $(H_3N)_5CoX^{2+}$ will be the same for different outer-sphere reductants. The ratios of rate constants k_{2Br}/k_{2Cl} and k_{2Cl}/k_{2N_3} are ~20 and 0.4-2, respectively, for the two cobaloxime(II) complexes and are different from those of 6 and ~140 respectively for reduction of $(H_3N)_5CoX^{2+}$ by the outer-sphere reductant $Ru(NH_3)_6^{2+}$.[5] From Marcus's suggestion, this difference is consistent with inner-sphere rather than outer-sphere oxidation of cobaloxime(II) by $(H_3N)_5CoX^{2+}$.

The values of k_2 for $(H_2O)_2Co^{II}(dmgBF_2)_2$ oxidations are about $5\text{-}6\times10^3$ times smaller than those of the corresponding $(H_2O)_2Co^{II}(dmgH)_2$ complexes. Since the substitution liability for these two cobaloxime(II) complexes is not expected to differ substantially based on our observed comparable solvent exchange rates for the two complexes in acetonitrile at 25 °C,[35] the marked differences in their k_2 may indicate that the bridge-mediated electron-transfer process is the rate-controlling step in the inner-sphere mechanism. The slower oxidation of the former complex may be due to its higher standard electrode potential (Co(III)/Co(II)) of 0.65 V (NHE) against that of 0.36 V (NHE) for the latter. If the Marcus theory[34] prediction of a square root dependence on the equilibrium constant (see Eq 5.6) is also applicable to these inner-sphere electron transfers, then $(H_2O)_2Co^{II}(dmgH)_2$ is predicted to be ca. 2.8×10^2 more reactive. This factor seems to account for most, but not all, of the reactivity difference of the cobaloximes.

Self-Exchange Rates of Cobaloximes(III)/(II). The free energy dependencies of the rates of $Co(sep)^{2+}$ reduction of cobalt(III) complexes from the literature and our studies are shown in Fig 5.3 as a plot of log k_{12} vs. Log K_{12}. There is a reasonable linear relationship with a slope of 0.5. Such a correlation is predicted by the Marcus relationship (Eq 5.6) if f_{12} and $W_{12} \approx 1$ and k_{11} is the same for all the systems.

It has been noted by Endicott et al.[15] that, for cobalt macrocyclic complexes, the main energy barrier for the self-exchange is the Franck-Condon barrier (inner-sphere reorganization energy). The Franck-Condon barrier, according to either the classical (harmonic oscillator) or quantum mechanical models, is associated with changes in metal ligand bond length accompanying the electron transfer. The classical model is shown by the following equations

$$k_{11}(\mathrm{FC}) = 10^{11} \times \exp(-\frac{\Delta G^{\ddagger}_{\mathrm{FC}}}{RT}) \tag{5.11}$$

$$\Delta G^{\ddagger}_{\mathrm{FC}} = \frac{n}{2} \frac{f_{\mathrm{II}} f_{\mathrm{III}}}{f_{\mathrm{II}} + f_{\mathrm{III}}} (\Delta d)^2 \tag{5.12}$$

where $\Delta G^{\ddagger}_{\mathrm{FC}}$ and k_{11} (FC) are the calculated Franck-Condon activation energy and the corresponding self-exchange rate, n is the number of bonds, and f_{II} and f_{III} are the corresponding force constants for stretching the metal-ligand bonds for the Co(II) and Co(III) complexes.

Endicott et al.[15] have studied the variation of self-exchange rates with structure changes for a series of homologous *trans*-$(H_2O)_2Co(N_4)^{3+/2+}$ couples (Table 5.5; N_4 stands for 14-member macrocyclic ligands). The self-exchange rates were evaluated from the cross reaction rates among these complexes by the Marcus square

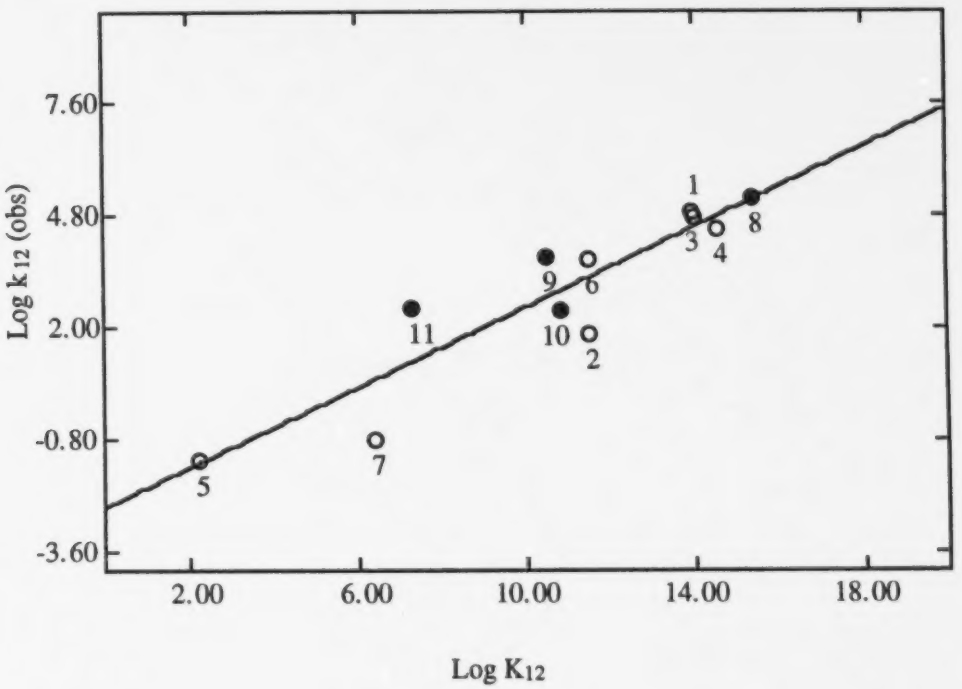

Figure 5.3. Correlation between the observed electron transfer rates and the driving forces for reduction of cobalt(III) complexes by $Co^{II}(sep)^{2+}$ (1, $(H_2O)_2Co(Me_4[14]tetraeneN_4)^{3+}$; 2, $(H_2O)_2Co([14]aneN_4)^{3+}$; 3, $(H_2O)_2Co(Me_4pyo[14]trieneN_4)^{3+}$; 4, $(H_2O)_2Co(Me_2[14]trieneN_4\text{-}13\text{-}one)^{3+}$; 5, $Co(en)_3^{3+}$; 6, $Co(phen)_3^{3+}$; 7,$Co(NH_3)_3^{3+}$; 8, $(H_2O)_2Co(dmgBF_2)_2^{+}$; 9, $(HO)(H_2O)Co(dmgBF_2)_2$; 10, $(H_2O)_2Co(dmgH)_2^{+}$; 11, $(HO)(H_2O)Co(dmgH)_2$); All data at 25 °C).

root equation (the simplified form of Eq 5.6 with f_{12} and W_{12} being assumed to be 1). The X-ray studies have shown that the structural parameters change little from cobalt(III) to cobalt(II) for these $(H_2O)_2Co(N_4)$ complexes, except that the axial Co–OH_2 bond lengths are 0.38–0.57 Å longer for Co(II) because the unpaired electron occupies the antibonding d_{z^2} orbital. Thus, Endicott et al. attributed the observed variation of the self-exchange electron-transfer rates to the reorganization energies which result from changes in Co-OH_2 bond length Δd. However, the calculated Franck-Condon barriers $\Delta G^{\ddagger}_{FC}$ were always found to be insufficient to account for the observed activation barriers. Endicott et al. further suggested that self-exchange reactions for $(H_2O)_2Co(N_4)^{3+/2+}$ are "nonadiabatic", i.e.

$$k_{11}\,(\text{obs}) = k_{11}\,(\text{FC}) \times \kappa_{11} \tag{5.13}$$

where k_{11} (obs) is the observed self-exchange rate constant, and κ_{11}, the electron transmission coefficient, is a measure of the nonadiabaticity for the self-exchange. For adiabatic self-exchange electron-transfer, $\kappa_{11} = 1$, and is less than 1 for nonadiabatic exchange. Based on a consistent discrepancy of ~ 2.5 kcal/mol between the observed and calculated activation barriers, Endicott et al. estimated the nonadiabatic factor $\kappa_{11} \approx 10^{-3\pm1}$ for self-exchange reactions for $(H_2O)_2Co(N_4)^{3+/2+}$ couples.

The cobaloxime systems are structurally similar to the CoN_4 complexes in that the equatorial Co–N bond lengths are 1.87–1.89 Å, and are very similar for cobalt(III) and cobalt(II) forms.[36] Only the axial Co–OH_2 bonds lengthen from cobalt(III) to cobalt(II). This lengthening (Δd) is estimated as 0.31 Å for the $(dmgH)_2$ complex, from the Co–N(py) bond lengths in the $(py)_2Co^{II}(dmgH)_2$[37] and $(py)_2Co^{III}(dmgH)_2^+$.[38] For the $(dmgBF_2)_2$ complex, Co(II)–OH_2 and Co(III)–OH_2 bond lengths can be estimated as 2.28 Å and 1.97 Å from the Co–O bond lengths in

$(CH_3OH)_2Co^{II}(dmgBF_2)_2$[18] and $X(H_2O)Co^{III}(dmgH)_2$ (X = halide ions).[36] Therefore, Δd for both diaqua cobaloxime(II) complexes is estimated to be ~ 0.31 Å.

If the nonadiabaticity factor (κ_{11}) is about the same for various Co(III)/Co(II) systems, then the Franck-Condon model (Eqs 5.11 and 5.12) predicts that k_{11} should vary inversely with $(\Delta d)^2$ and systems with the same Δd should have the same k_{11}. The results in Table 5.5 show that the cobaloximes(III)/(II) do not fit this expectation. The cobaloximes have the smallest Δd values, but their k_{11} values are smaller than those of the three other systems. Thus, other electronic (non-structural) factor(s) may contribute to the retardation of cobaloxime(III)/(II) exchange rates calculated by the Marcus cross relationship.

Self-exchange for $Co(sep)^{3+/2+}$ involves the electron-transfer from the high-spin $Co(sep)^{2+}$ to the low-spin $Co(sep)^{3+}$. Such a spin state change is believed to impose an energy barrier which will contribute to the nonadiabaticity for the $Co(sep)^{3+/2+}$ exchange. However, Doine and Swaddle[30] concluded, from the activation volume, that the electron self-exchange for $Co(sep)^{3+/2+}$ is adiabatic. It is interesting to note that the $Co(NH_3)_6^{3+/2+}$ exchange is distinctly nonadiabatic[11], although the spin state and structural changes are similar to those of $Co(sep)^{3+/2+}$. Sargeson et al.[39] have attributed the larger exchange rate with sepulchrate to the strain in the cage ligand because the Co(III) ion is a bit too small to fit into the cage and Co(II) is a bit too large. As a result, bond length distortion toward the transition state is favorable for $Co(sep)^{3+/2+}$ exchange.

If the self-exchange for $Co(sep)^{3+/2+}$ is indeed adiabatic, then the much smaller self-exchange rates for cobaloximes(III)/(II) may result from the nonadiabaticity of the cross reactions. The nonadiabatic factor κ_{12} for a cross reaction can be defined analogously to κ_{11} as follows

$$k_{12}(\text{obs}) = k_{12}(\text{calcd}) \times \kappa_{12} \qquad (5.14)$$

Table 5.5. Summary of Self-Exchange Rates (25 °C) of $(H_2O)_2CoL(III)/(II)$

L	k_{11}	Δd (Å)
$(dmgH)_2^{2-}$	7.7×10^{-4} [a]	~ 0.31[c]
$(dmgBF_2)_2^{2-}$	1.5×10^{-4} [a]	~ 0.31[d]
Me_4[14]tetraeneN_4	5.0×10^{-2} [b]	0.38[e]
Me_2[14]1,11-dieneN_4-13-one	4.4×10^{-3} [b]	0.43[e]
Me_6[14]4,11-dieneN_4	4.5×10^{-5} [b]	0.57[e]
[14]aneN_4	8×10^{-4} [b]	
Me_2pyo[14]trieneN_4	9.3×10^{-2}	

[a] Calculated with the Marcus theory, see Table 5.3. [b] CoN_4 data are from Reference 15. [c] Estimated from Δd for Co-N (py) bonds from References 37 (standard deviation: ±0.02 Å) and 38. [d] Estimated from Co(II)-O bond in $(CH_3OH)_2Co^{II}(dmgBF_2)_2$ (Reference 18, standard deviation: ±0.004 Å) and Co(III)–OH_2 in $X(H_2O)Co^{III}(dmgH)_2$ (Reference 36, standard deviation: ±(0.004-0.01) Å). [e] Reference 15 (standard deviation: ±0.005 Å).

where k_{12}(calcd) is the calculated adiabatic cross reaction rate, and κ_{12} is the electron transmission coefficient for the cross reaction. As noted by Endicott et al.[15-17], nonadiabaticity is common for cross reactions between cobalt(III) and cobalt(II) complexes because of the poor donor-acceptor overlap and the change of spin state, and tends to become more severe as the electronic structures of the reactants and products become more dissimilar.

Examination of the kinetic data[15-17] for reduction of cobalt macrocyclic complexes by $Co(sep)^{3+/2+}$ (Table 5.6) reveals that the cross reactions involving the $Co(sep)^{2+}$ are nonadiabatic. In all cases, the k_{12}(obs) values are about 10^{-1}-10^{-3} times smaller than those of k_{12}(calcd) by the Marcus relationship based on the observed self-exchange rates in Table 5.5. Figure 5.4 illustrates the correlation between the log k_{12}(obs) and log k_{12}(calcd). The plotted line with unit slope yields an intercept of ~ -1.3, and from this, an average nonadiabatic factor κ_{12} value of $10^{-1.3}$ is obtained for these reactions. If reactions between the cobaloximes(III) and $Co(sep)^{2+}$ are retarded by a similar nonadiabatic factor κ_{12}, then the smaller self-exchange rates obtained may be explained. A κ_{12} value of $10^{-1.3}$ will result in an factor of $10^{-2.6}$ for the calculated self-exchange rates by Eq 5.6 for the cobaloximes(III)/(II), and k_{11} becomes 0.31 M^{-1} s^{-1} and 0.06 M^{-1} s^{-1} for the two diaqua dmgH and $-BF_2$ systems, respectively. These values are more consistent with values expected from the Δd correlation.

Table 5.6. Comparison of the Calculated and Observed Cross Reaction Rates for Reduction of Some Cobalt(III) Complexes by $Co(sep)^{2+}$ at 25 °C

Cobalt(III)	k_{12} (obs)[a]	k_{12} (calcd)[b]
$(H_2O)_2Co(Me_2pyo[14]triene)^{3+}$	5.4×10^{4}	7.7×10^{5}
$(H_2O)_2Co(Me_4[14]tetraeneN_4)^{3+}$	6.8×10^{4}	5.6×10^{5}
$(H_2O)_2Co(Me_2[14]1,11\text{-}dieneN_4\text{-}13\text{-}one)^{3+}$	3.0×10^{4}	3.0×10^{5}
$(H_2O)_2Co([14]ane)^{3+}$	6.5×10^{1}	1.1×10^{4}
$Co(en)_3^{3+}$	5.0×10^{-2}	1.3×10^{-1}
$Co(phen)_3^{3+}$	4.8×10^{3}	4.8×10^{5}
$Co(NH_3)_6^{3+}$	1.5×10^{-1}	5.5

[a] From References 15 and 17. [b] Calculated with the Marcus theory (Eqs 5.6 and 5.7) by assuming $W_{12} = 1$ and ignoring w_{ij}.

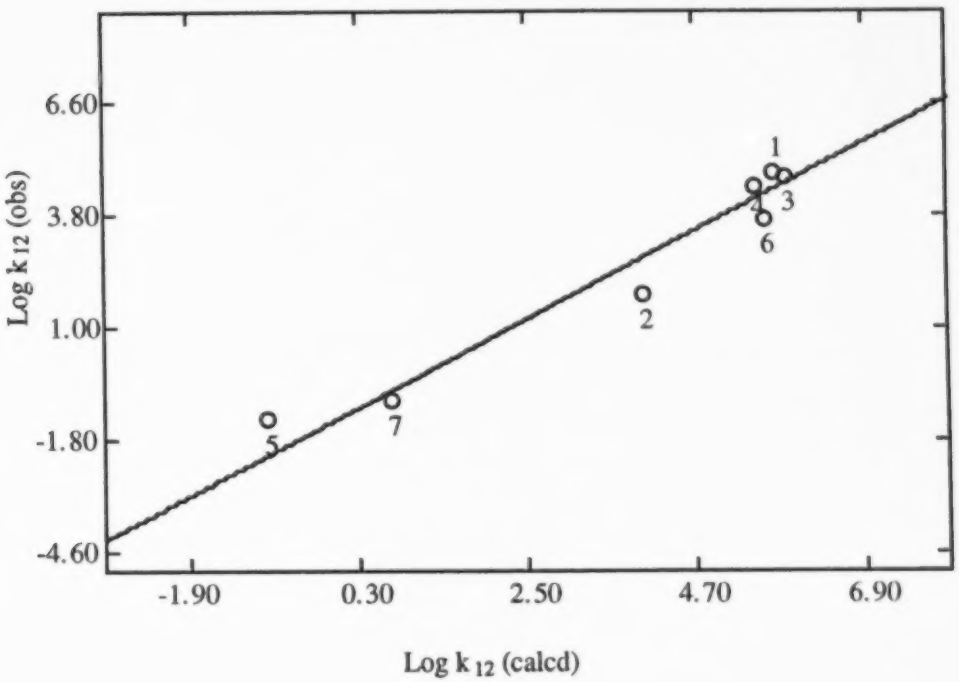

Figure 5.4. Correlation between the observed and calculated cross reaction rates for reduction of some cobalt(III) complexes by $Co^{II}(sep)^{2+}$ (For notations of data, see Figure 5.3).

References

(1) Adin, A.; Espenson, J. H. *Inorg. Chem.* **1972**, *11*, 686.

(2) Prince, R. H.; Segal, M. G. *J. Chem. Soc. Dalton Trans.* **1975**, 1245.

(3) Wilkins, R. G. *Kinetics and Mechanism of Reactions of Transition Metal Complexes*, 2nd Edition; VCH: New York,1991.

(4) Dayalan, A.; Vijayaraghavan, V. R. *J. Chem. Soc. Dalton Trans.* **1992**, 2491.

(5) Diebler, H.; Taube, H. *Inorg. Chem.* **1965**, *4*, 1029.

(6) Balasubramanian, G.; Thothadri, T.; Vijayaraghavan, V. R. *Indian J. Chem.* **1988**, *27A*, 997.

(7) Prince, R. H.; Segal, M. G. *J. Chem. Soc. Dalton Trans.* **1975**, 330.

(8) Balasubramanian, G.; Vijayaraghavan, V. R. *Indian J. Chem.* **1981**, *20A*, 892.

(9) Balasubramanian, G.; Vijayaraghavan, V. R. *Inorg. Chem. Acta.* **1981**, *53*, L209.

(10) Balasubramanian, G.; Vijayaraghavan, V. R. *Inorg. Chem. Acta.* **1980**, *38*, 49.

(11) Jordan, R. B. *Reaction Mechanisms of Inorganic and Organometallic Systems*; Oxford University Press: New York, 1991.

(12) Prince, R. H.; Segal, M. G. *Nature*. **1974**, *249*, 246.

(13) Rellema, D. P.; Endicott, J. F.; Patel, R. *J. Am. Chem. Soc*. **1972**, *94*, 394.

(14) Glick, M. D.; Kuszaj, J. M.; Endicott, J. F. *J. Am. Chem. Soc*. **1973**, *95*, 5097.

(15) Endicott, J. F.; Durham; B., Glick, M. D.; Anderson, T. J.; Kuszaj, J. M.; Schmonsees, W. G.; Balakrishnan, K. P. *J. Am. Chem. Soc*. **1981**, *103*, 1431.

(16) Endicott, J. F.; Durham, B.; Kumar, K. *Inorg. Chem.* **1982**, *21*, 2437.

(17) Ramasami, T; Endicott, J. F. *J. Am. Chem. Soc*. **1985**, *107*, 389.

(18) Bakac, A.; Brynildson, M. E.; Espenson, J. H. *Inorg. Chem.* **1986**, *25*, 4108.

(19) Ablov, A. V.; Samus, N. M. *Russ. J. Inorg. Chem.* **1960**, *5*, 410.

(20) Dash, K. *Proc. Indian Natl. Sci. Acad.* **1989**, *55A*, 212.

(21) Ablov A. V.; Samus, N. M. *Dokl. Akad. Nauk SSSR* **1957**, *113*, 1265.

(22) Ablov, A. V.; Filippov, M. P.; Samus, N. M. *Dokl. Akad. Nauk SSSR* **1960**, *133*, 575.

(23) Heckman, R. G.; Espenson, J. H. *Inorg. Chem.* **1979**, *18*, 38.

(24) Kita, E.; Jordan, R. B. *Inorg. Chem.* **1989**, *28*, 1549.

(25) Zhang, Z.; Jordan, R. B. *Inorg. Chem.* **1994**, *33*, 680.

(26) Schlessinger, G. G. *Inorganic Laboratory Preparations*; Chemical Publishing Co. Inc.: New York, 1962.

(27) Ablov, A. V.; Bovykin, B. A.; Samus, N. M. *Russ. J. Inorg. Chem.* **1966**, *11*, 978.

(28) Creaser, I. I.; Sargeson, A. M.; Zanella, A. W. *Inorg. Chem.* **1983**, *22*, 4022.

(29) Marcus, R. A.; Sutin, N. *Biochem. Biophys. Acta* **1985**, *811*, 265.

(30) Zahir, K.; Espenson, J. H.; Bakac, A. *J. Am. Chem. Soc.* **1988**, *110*, 5059.

(31) Doine, H.; Swaddle, T. W. *Inorg. Chem.* **1991**, *30*, 1858.

(32) Haim, A. *Prog. Inorg. Chem.* **1983**, *30*, 273.

(33) Taube, H. *Electron Transfer Reactions of Complex Ions in Solution*, Academic Press: New York, 1970.

(34) Marcus, R. A. *J. Phys. Chem. 1963*, **67**, 853.

(35) See Chapter 2 of this thesis.

(36) Bresciani-Pahor, N.; Forcolin, M.; Marzilli, L. G.; Randaccio, L; Summers, M. F.; Toscano, P, J. *Coord. Chem. Rev.* **1985**, *63*, 1.

(37) Fallon, G. D.; Gatehouse, B. M. *Cryst. Struct. Comm.* **1978**, *7*, 263.

(38) Ablov, A. V.; Dvorkin, A. A.; Simonov, Y. A.; Bologa, O. A.; Malinovskii, T. I. *Dokl. Akad. Nauk SSSR* **1974**, *217*, 89.

(39) Creaser, I. I.; Geue, R, J.; Harrowfield, J. M.; Herlt, A. J.; Sargeson, A. M.; Snow, M. R.; Springborg, J. *J. Am. Chem. Soc.* **1982**, *104*, 6016.

Chapter 6. Conclusions

A large part of this work has centered on the solvent exchange kinetics studied by the temperature dependence of the proton NMR transverse relaxation rate R_2. Such studies on three complexes, $Co(dmgH)_2$, $Co(dmgBF_2)_2$ and $Co(dpgH)_2$ are reported in Chapter 2. The results may be summarized by noting that a well defined solvent exchange controlled region was found for $Co(dmgH)_2$ in acetonitrile and methanol, while the other systems were generally in the fast exchange region with some exchange control evident near the low temperature limit for the particular solvent. An I_a exchange mechanism was suggested, based on the negative $\Delta S^{\ddagger}$ values found for these systems. However, this assignment for the $Co(dmgH)_2$-CH_3OH system is equivocal because the initial analysis of the relaxation data indicated a positive $\Delta S^{\ddagger}$, although further analysis demonstrated that the data also can be fitted with a negative $\Delta S^{\ddagger}$.

As noted earlier, another indicator of mechanism is the activation volume $\Delta V^{\ddagger}$, from the analysis of the pressure dependence of the exchange rate.[1] Normally, a positive $\Delta V^{\ddagger}$ indicates an I_d mechanism, while a negative $\Delta V^{\ddagger}$ indicates an I_a mechanism. However, this general rule may not be applicable to the cobaloxime(II) systems if they are 5-coordinate. The shape of such a 5-coordinate cobaloxime molecule could be visualized as a half-ellipsoid, while the 6-coordinate species would be like an ellipsoid, and the solvent shape would be a smaller ellipsoid. Then, in an associative exchange process, a 6-coordinate transition state may have a larger volume than the sum of those of 5-coordinate reactant and the solvent. Thus, the $\Delta V^{\ddagger}$ might not be negative for an I_a exchange process. Nevertheless, it still would be tempting to measure the $\Delta V^{\ddagger}$ for the $Co(dmgH)_2$-CH_3CN and $Co(dmgH)_2$-CH_3OH systems which have well defined solvent exchange regions, to see if the $\Delta V^{\ddagger}$ values for the two systems have the same sign, which would be consistent with the suggestion above that

the $\Delta S^{\ddagger}$ values have the same sign.

For systems in the fast exchange region with a less definitive exchange region, the R_{2m} term is too large and the $\Delta\omega_m$ is too small to give a well defined contribution of the $\Delta\omega_m^2/r_m$ term which could be analyzed to give r_m. For example, for the $Co(dmgBF_2)_2$-CH_3CN system at 25 °C, the ratio of $(\Delta\omega_m^2/r_m)/(R_{2m})$ is only ~0.65 estimated from the parameters in Table 2.5. In principle, by raising $\Delta\omega_m$ and lowering R_{2m}, it is possible to move the kinetic region into the "window" of NMR observation. One approach to achieve this is to use high field NMR. By taking the measurement at 400 MHz instead of 89.5 MHz, the $\Delta\omega_m$ will increase by a factor of ~4.5 (400/89.5). The R_{2m}, which is almost exclusively dipolar in $Co(dmgBF_2)_2$-CH_3CN, will decrease by ~10% as a result of a reduction of the spectral density $f_{D2}(\tau_D)$. Thus, the $(\Delta\omega_m^2/r_m)/(R_{2m})$ ratio will increase by a factor of ~20 (4.5^2) as a result of changing to 400 MHz. For the present example, the ratio will become ~13 at 25 °C, indicating that R_2 is now dominated by $\Delta\omega_m^2/r_m$, and the ratio will be even more favorable at lower temperature. Applying such an analysis to the $Co(dmgBF_2)_2$-acetone system and using parameters in Table 2.6, also shows an increase of the $(\Delta\omega_m^2/r_m)/(R_{2m})$ ratio by the same factor (~4.5^2) from ~0.2 to ~2.5 at 25 °C. Thus, for these two systems, more definitive kinetic information would be obtained by undertaking the measurement at 400 MHz NMR.

Another potentially useful approach to raise the $(\Delta\omega_m^2/r_m)/(R_{2m})$ ratio is to measure the relaxation rate of solvent nuclei other than ^1H, such as ^{17}O, ^{14}N, ^{13}C in solvents such as $^{13}CH_3OH$, $CH_3{}^{17}OH$, $CH_3C^{14}N$, $CH_3{}^{13}CN$ and $^{13}CH_3CN$.[2,3] These nuclei are generally closer to the paramagnetic center than ^1H, thus giving rise to a larger scalar coupling constant $A/\hbar$, hence increasing $\Delta\omega_m$. But a larger $A/\hbar$ would also increase the scalar contribution R_{2SC} to R_{2m}, and if $R_{2m} \approx R_{2SC}$, then the $(\Delta\omega_m^2/r_m)/(R_{2m})$ ratio would be the same as that of ^1H. On the other hand, changing nuclei will affect the

dipolar term R_{2DD} because it depends on the magnetogyric ratio (γ_I) and the distance (r) between the nuclei and the metal center (R_{2DD} is proportional to γ_I^2/r^6). Therefore, by changing nuclei, the optimized condition would be to have a greater $\Delta\omega_m$ and a R_{2m} term dominated by R_{2DD} with a smaller γ_I^2/r^6 ratio. For the $Co(dmgBF_2)_2$ in acetonitrile and acetone, without a knowledge of $A/\hbar$ for nuclei other than ^1H, the change of $\Delta\omega_m$ and the contribution of R_{2SC} to the R_{2m} are difficult to estimate. However, for ^{13}C in $^{13}CH_3CN$ and $^{13}CH_3CO^{13}CH_3$, R_{2m} may still be dominated by R_{2DD} based on the dominant R_{2DD} for the neighboring ^1H relaxation found in the present study. Hence the R_{2m} for ^{13}C in the two solvents would reduce to only ~10% of that for ^1H as a result of a decrease of the γ_I^2/r^6 ratio. Therefore, by using ^{13}C NMR, the $(\Delta\omega_m^2/r_m)/(R_{2m})$ ratio would be expected to improve by a factor of 10 (at 25 °C) for the two systems discussed.

As noted in Chapter 1, the solvation number of the cobaloximes(II) in solution is still unclear, and in the current study, a solvation number $n = 1$ was assumed. A method based on the dependence of the rotating frame relaxation rate $R_{1\rho}$ on the spin-locking field ω_1 has been developed recently in this laboratory to determine the number of exchanging solvent molecules on a labile paramagnetic ion.[4] The $R_{1\rho}$ vs. ω_1 data at a particular temperature can be analyzed to give $\Delta\omega_m$ without a knowledge of the solvation number. Then the $\Delta\omega_m$ value can be compared to $n\Delta\omega_m$, from the Swift-Connick analysis of the temperature dependence of R_2 or from chemical shift measurement, to give a solvation number n. One limitation of such an experiment is the requirement that r_m, $\Delta\omega_m \gg R_{2m}$. Two of the present systems, $Co(dmgH)_2$-CH_3CN and $Co(dmgH)_2$-CH_3OH, meet this requirement, and thus could be used to determine the solvation number.

The stepwise formation constants K_1 and K_2, and their temperature dependence

ΔH° and ΔS° for mono- and bis- 1-methylimidazole complexes with $Co(dmgBF_2)_2$ have been measured in acetonitrile by spectrophotometry. As shown in Table 3.2, for many cobaloxime(II) complexes, only K_1 or cumulative formation constant $K_1 \times K_2$ have been reported, and the ΔH° and ΔS° are available for only one other system. Therefore, more work is needed before any detailed general picture of these complexation reactions can be proposed.

Proton NMR shift and relaxation studies of free 1-MeIm in the presence of $Co(dmgBF_2)_2$ have been studied in acetonitrile. The results are consistent with a 3-site fast exchange model involving the free, mono- and bis- coordinated MeIm. In the present study, the shift and relaxation parameters for bis- coordinated MeIm are better defined than those in the mono- complex, because the bis- complex is the dominant species, under most of the experimental conditions ([MeIm] and temperatures). A better defined mono- complex system could be obtained by selecting an imidazole derivative with a smaller K_2 value. As noted in Chapter 3, 2- substituted imidazole has a smaller formation constant due to the steric effect of the substituent adjacent to the donor N atom. Therefore, NMR study of systems such as 2-MeIm may provide a better chance to characterize the shift and relaxation of the mono- imidazole complex, and complement the results of the present study.

Variation of the proton exchange rates with $[H^+]$ for the $(H_2O)_5CrCH_2CN^{2+}$ system indicates pathways which are first-order, zero-order and inverse first-order in $[H^+]$. The rate constants of the latter two pathways were used to estimate the first and second deprotonation constant of the complex respectively. The kinetic parameters and general relaxation effects for the complex are similar to those for $Cr(OH_2)_6^{3+}$ and $(H_2O)_5Cr(N_3)^{2+}$. The $(H_2O)_5CrCH_2CN^{2+}$ complex is only one of a series of organochromium(III) complexes of the type $(H_2O)_5CrR^{2+}$ (R = alkyl groups).[5] It would be of interest to apply the same study to some other organochromium(III) complexes to

study the effect of the R group on the ionization constants, and to test whether the kinetic and relaxation information from the present study is general for these complexes. The species chosen would need to be stable for at least several hours in order to measure the NMR relaxation rates. Only a few complexes, such as those with the R = $-CH_2OCH_3$, $-CH_2X$ and CHX_2 (X = halogens), and $-CF_3$, meet this criterion.

Electron self-exchange rate constants (k_{11}) for cobaloxime(III)/(II) couples were found to be much smaller than predicted by the Franck-Condon factor because of the nonadiabacity of the cross reactions. After correction for the nonadiabacity, the k_{11} are 0.31 and 0.06 M^{-1} s^{-1} for $Co(dmgH)_2^{+/0}$ and $Co(dmgBF_2)_2^{+/0}$ respectively. It would be interesting to compare these k_{11} to measured values. One method to measure k_{11} for such a system is to study the effect of added paramagnetic species on the NMR linewidth or the relaxation rate R_2 of nuclei in the diamagnetic species.[6] However for our systems, the change of linewidth of the methyl protons of the cobaloxime(III) (= $k_{11}\times$[Co(II)]/π) due to the added cobaloxime(II) would be too small to measure if our calculated k_{11} values are true. For the accessible concentration range of $< 10^{-2}$ M of $Co(dmgH)_2$ added, a k_{11} value of 0.31 would predict a linewidth change of only ~ 1×10^{-3} Hz.

Another way to measure k_{11} is to study the rate of isotope exchange between the species. The limitation of this method applied to current cobaloxime systems will be the solubility of cobaloximes in solution. The best choice would be $Co(dmgH)_2$ in acetonitrile because $Co(dmgH)_2$ can be dissolved up to ~2×10^{-2} M in this solvent. If normal $Co(dmgH)_2^+$ were mixed with the $-CD_3$ substituted $Co(dmgH)_2$ in acetonitrile, the attenuation of the $-CH_3$ peak with time due to the electron "self-exchange" between the two species could be monitored by NMR. The deuterated d_8-$dmgD_2$ could be prepared by isotopic exchange reaction of the $dmgH_2$ with DCl.[7]

References

(1) Jordan, R. B. *Reaction Mechanisms of Inorganic and Organometallic Systems*; Oxford University Press: New York, 1991; Chapter 3 and references therein.

(2) Monnerat, A.; Moore, P.; Newman, K. E.; Merbach, *Inorg. Chim. Acta.* **1981**, *47*, 139.

(3) Yano, Y.; Fairhurst, M. T.; Swaddle, T. W. *Inorg. Chem.* **1980**, *19*, 3267.

(4) Chopra, S.; McClung, R. E. D.; Jordan, R. B. *J. Magn. Reson.* **1984**, *59*, 361.

(5) Espenson, J. H. *Adv. Inorg. Bioinorg. Mech.* **1982**, *1*, 1.

(6) Donlevy,T. M.; Gahan, L. R.; Hambley, T. W. *Inorg. Chem.* **1994**, *33*, 2668

(7) (a) Golding, B. T.; Kemp, T. J.; Sellers, P. J.; Nocchi, E. *J. Chem. Soc. Dalton Trans.* **1977**, 1266. (b) Maillard P.; Giannotti, C. *Can. J. Chem.* **1982**, *60*, 1402.

Appendix: Tables of Experimental Data

Table A-1. Solvent Proton Relaxation Rates of Acetonitrile Solution of $Co(dmgH)_2$ ($P_m = 2.73 \times 10^{-4}$; solvation number $n = 1$)

Temp (°C)	R_1 (s^{-1}) Obsd	R_1 (s^{-1}) Calcd	R_2 (s^{-1}) Obsd	R_2 (s^{-1}) Calcd
34.5	0.20	0.21	0.29	0.30
25.6	0.24	0.23	0.34	0.37
15.7	0.26	0.25	0.49	0.50
6.4	0.27	0.28	0.66	0.68
1.6	0.31	0.29	0.86	0.82
-7.4	0.31	0.32	1.11	1.18
-13.8	0.35	0.35	1.55	1.52
-17.8	0.37	0.37	1.95	1.75
-23.0	0.41	0.39	2.09	1.98
-27.6	0.44	0.41	2.10	2.07
-28.2	0.45	0.42	2.18	2.07
-34.6	0.44	0.48	1.88	1.90
-39.1	0.45	0.47	1.61	1.64
-42.6	0.46	0.48	1.37	1.42
-44.5	0.50	0.49	1.31	1.30
-46.1	0.48	0.49	1.17	1.20

Table A-2. Solvent Proton Relaxation Rates of Methanol Solution of $Co(dmgH)_2$ (P_m = 1.21×10^{-4}; solvation number n = 1)

Temp (°C)	R_1 (s^{-1}) Obsd	Calcd	Calcd*	R_2 (s^{-1}) Obsd	Calcd	Calcd*
61.5	0.26	0.26	0.26	1.28	1.31	1.36
51.6	0.29	0.29	0.29	1.78	1.75	1.87
39.1	0.33	0.34	0.33	2.80	2.64	2.65
32.8	0.37	0.37	0.36	2.98	3.06	2.89
27.1	0.38	0.39	0.39	3.07	3.14	2.88
26.7	0.39	0.39	0.39	3.01	3.13	2.87
17.5	0.42	0.43	0.44	2.66	2.53	2.48
12.4	0.45	0.47	0.47	2.23	2.15	2.22
5.4	0.50	0.51	0.51	1.71	1.80	1.93
-2.5	0.57	0.53	0.57	1.58	1.65	1.76
-13.5	0.69	0.61	0.64	1.82	1.73	1.75
-25.0	0.77	0.69	0.73	2.35	2.03	1.98
-50.8	1.12	1.13	1.15	3.64	3.39	3.24
-60.0	1.41	1.41	1.43	3.65	4.20	4.04

* These calculated values are obtained from the least-squares fittings by assuming $\Delta S^{\ddagger}$ = -6 cal mol^{-1} K^{-1}.

Table A-3. Solvent Proton Relaxation Rates of Acetonitrile Solution of $Co(dmgBF_2)_2$ ($P_m = 2.42 \times 10^{-4}$; solvation number $n = 1$)

Temp (°C)	R_1 (s^{-1})		R_2 (s^{-1})	
	Obsd	Calcd	Obsd	Calcd
26.2	0.28	0.27	0.39	0.38
18.4	0.31	0.30	0.44	0.44
10.8	0.33	0.33	0.52	0.52
2.6	0.37	0.38	0.61	0.63
-1.7	0.42	0.40	0.70	0.69
-7.7	0.42	0.43	0.79	0.81
-11.3	0.44	0.47	0.84	0.88
-14.0	0.48	0.49	0.92	0.95
-18.1	0.52	0.53	1.10	1.05
-21.2	0.56	0.56	1.21	1.13
-24.2	0.58	0.59	1.25	1.21
-27.0	0.61	0.61	1.29	1.29
-31.2	0.68	0.66	1.40	1.40
-36.2	0.74	0.72	1.46	1.51
-40.2	0.79	0.76	1.57	1.58

Table A-4. Solvent Proton Relaxation Rate (R_{1obs}) of Acetone Solvent

Temp (°C)	R_1 (s^{-1}) Obsd	Calcd
24.9	0.0583	0.0558
-28.8	0.110	0.113
-57.5	0.178	0.187
-89.7	0.405	0.386

Table A-5. Solvent Proton Relaxation Rates of Acetone Solution of $Co(dmgBF_2)_2$ ($P_m = 5.22 \times 10^{-4}$; solvation number $n = 1$)

Temp (°C)	R_1 (s^{-1})		R_2 (s^{-1})	
	Obsd	Calcd	Obsd	Calcd
25.7	0.38	0.36	0.43	0.42
-17.9	0.71	0.70	0.83	0.88
-39.0	1.03	1.04	1.41	1.40
-56.7	1.38	1.53	2.22	2.20
-64.0	1.87	1.81	2.82	2.67
-74.5	2.38	2.34	3.34	3.45
-85.5	3.22	3.09	4.02	4.16
-91.8	3.58	3.60	4.60	4.45

Table A-6. Solvent Proton Relaxation Rates of Acetonitrile Solution of $Co(dpgH)_2$ ($P_m = 3.88 \times 10^{-4}$; solvation number $n = 1$)

Temp (°C)	R_1 (s^{-1}) Obsd	R_1 (s^{-1}) Calcd	R_2 (s^{-1}) Obsd	R_2 (s^{-1}) Calcd
26.5	0.24	0.24	0.50	0.51
2.6	0.31	0.32	0.68	0.68
-13.5	0.38	0.39	0.88	0.84
-20.3	0.42	0.43	0.92	0.93
-34.6	0.54	0.54	1.10	1.17
-40.8	0.60	0.60	1.36	1.30

Table A-7. Solvent Proton Relaxation Rates of Methanol Solution of $Co(dpgH)_2$ (P_m = 1.82×10^{-4}; solvation number $n = 1$)

Temp (°C)	R_1 (s^{-1}) Obsd	R_1 (s^{-1}) Calcd*	R_2 (s^{-1}) Obsd	R_2 (s^{-1}) Calcd*
25.9	0.21	0.20	0.64	0.56
15.9	0.23	0.23	0.63	0.69
6.4	0.26	0.27	0.79	0.86
-9.8	0.37	0.37	1.39	1.28
-21.7	0.43	0.47	1.73	1.75
-40.2	0.67	0.73	3.08	2.94
-45.2	0.81	0.83	3.65	3.36
-62.0	1.64	1.34	4.22	4.65
-71.5	2.09	1.80	4.60	4.89
-73.7	2.11	1.93	5.14	4.83
-86.1	2.54	2.19	5.42	4.72
-90.5	2.54	2.96	4.60	4.78

* Calculated from the following set of parameters: $\Delta H^{\ddagger}$ = 3.35 kcal mol^{-1}, $\Delta S^{\ddagger}$ = -20.5 cal mol^{-1} K^{-1}, $E_{im} = E_{io}$ = 2.61 kcal mol^{-1}, C_{1m} (=0.5 C_{1o}) = 650 s^{-1} K^{-1}, C_{2m} = 5000 s^{-1} K^{-1}, $C_{1o} = C_{2o} = 1.30\times10^{3}$ s^{-1} K^{-1}, $C_{\infty} = 7.54\times10^{6}$ s^{-1} K^{-1}.

Table A-8. Results of Calculated Chemical Shifts and Relaxation Rates (Proton 2)

t (°C)	$[Co]_t$ ($\times 10^4$, M)	[MeIm] (M)	$\Delta\nu_{obs}^2$ (Hz)	$\Delta\nu_{calcd}^2$ (Hz) Curie law[a]	3-Site[b]	R_{2obs}^2 (s^{-1})	R_{2calcd}^2 (s^{-1}) Fast Exch[c]	O.S.[d]
35.0	5.0	0.10	56.6	51.0	52.9	47.6	51.8	51.6
10.0	5.0	0.10	64.2	67.6	69.6	94.6	100	101
-5.0	5.0	0.10	74.9	82.2	84.2	159	157	160
-20.0	5.0	0.10	87.6	98.6	101	261	247	253
-24.0	5.0	0.10	95.1	103	105	295	278	285
-30.0	5.0	0.10	106	109	112	322	332	340
-36.0	5.0	0.10	112	115	118	382	394	405
-41.0	5.0	0.10	122	120	123	470	455	467
35.0	5.1	0.18	36.8	32.5	36.7	37.8	34.5	37.0
10.0	5.1	0.18	43.1	43.4	44.6	77.8	67.0	72.1
-5.1	5.1	0.18	51.1	51.6	52.9	115	102	110
-20.0	5.1	0.18	65.2	59.7	61.4	165	153	165
-24.6	5.1	0.18	62.8	62.1	63.7	185	172	187
-29.3	5.1	0.18	66.0	64.5	66.1	250	195	212
-35.2	5.1	0.18	69.8	67.3	69.0	261	228	248
35.0	4.4	0.34	21.3	17.0	17.5	20.6	19.0	24.4
-5.1	4.4	0.34	26.5	25.5	26.2	67.2	51.4	65.4
-35.0	4.4	0.34	33.3	31.4	32.2	141	107	140
35.0	9.9	0.34	46.3	38.8	39.4	49.9	42.7	54.9
10.0	9.9	0.34	53.2	50.0	51.3	93.6	80.0	101
-5.0	9.9	0.34	59.3	57.4	58.8	141	115	147
-20.0	9.9	0.34	68.0	64.3	66.0	231	166	214
-24.6	9.9	0.34	68.0	66.3	73.6	254	186	240
-29.3	9.9	0.34	75.4	68.3	70.1	277	208	271
-35.0	9.9	0.34	76.0	70.6	72.5	327	240	315

[a] Calculated by Curie law model. [b] By 3-site exchange model. [c] Based on the fast exchange assumption. [d] By considering outer-sphere contribution.

Table A-9. Results of Calculated Chemical Shifts and Relaxation Rates (Proton 3)

t (°C)	$[Co]_t$ ($\times 10^4$, M)	[MeIm] (M)	$\Delta\nu_{obs}{}^3$ (Hz)	$\Delta\nu_{calcd}{}^3$ (Hz) Curie law[a]	3-Site[b]	$R_{2obs}{}^3$ (s^{-1})	$R_{2calcd}{}^3$ (s^{-1}) Fast Exch[c]	O.S.[d]
35.0	5.0	0.10	57.8	53.7	52.4	50.5	52.5	49.9
10.0	5.0	0.10	61.3	65.2	64.6	88.4	89.8	86.3
-5.0	5.0	0.10	69.7	74.8	74.8	130	131	126
-20.0	5.0	0.10	82.4	85.6	89.8	195	194	189
-24.0	5.0	0.10	82.4	88.6	89.8	217	216	210
-30.0	5.0	0.10	91.1	92.9	94.4	243	253	247
-36.0	5.0	0.10	94.7	97.1	99.0	295	297	291
-41.0	5.0	0.10	101	100	103	340	340	334
35.0	5.1	0.18	35.5	32.4	31.9	36.1	32.4	32.9
10.0	5.1	0.18	39.9	39.8	39.8	67.3	56.1	57.4
-5.1	5.1	0.18	45.0	45.2	45.6	91.6	80.6	83.0
-20.0	5.1	0.18	55.0	50.7	51.6	123	116.2	121
-24.6	5.1	0.18	51.9	52.3	53.4	134	130	136
-29.3	5.1	0.18	55.6	54.0	55.1	170	146	153
-35.2	5.1	0.18	57.9	56.0	57.3	192	170	178
35.0	4.4	0.34	16.0	16.0	20.5	18.0	16.4	20.0
-5.1	4.4	0.34	21.3	21.7	22.1	50.6	39.3	48.6
-35.0	4.4	0.34	28.3	26.0	26.6	97.6	79.0	102
35.0	9.9	0.34	43.4	36.0	35.9	42.5	37.0	44.9
10.0	9.9	0.34	46.6	43.8	44.3	80.6	63.1	77.2
-5.0	9.9	0.34	51.1	48.8	49.7	112	88.3	109
-20.0	9.9	0.34	57.0	53.7	54.9	159	124	156
-24.6	9.9	0.34	59.9	55.2	56.4	179	138	175
-29.3	9.9	0.34	61.0	56.6	58.0	197	154	197
-35.0	9.9	0.34	63.1	58.3	59.8	231	178	228

[a] Calculated by Curie law model. [b] By 3-site exchange model. [c] Based on the fast exchange assumption. [d] By considering outer-sphere contribution.

Table A-10. Transverse Nuclear Relaxation Rates for Solvent Protons in Solutions of $(H_2O)_5CrCH_2CN^{2+}$ in Aqueous Acid

Temp °C	$10\times[H^+]$ M	$10^4\times P_m$	R_2, s^{-1} Obsd	Calcd
4.4	2.20	5.63	11.23	11.14
11.8	2.20	5.63	11.48	11.71
20.1	2.20	5.63	12.96	12.98
29.5	2.20	5.63	14.88	15.26
29.7	2.20	5.63	14.84	15.32
36.3	2.20	5.63	17.21	17.52
43.2	2.20	5.63	21.70	20.40
50.9	2.20	5.63	24.98	24.39
57.5	2.20	5.63	28.61	28.51
62.3	2.20	5.63	31.09	31.92
72.3	2.20	5.63	38.47	40.11
73.0	2.20	5.63	38.65	40.73
12.8	1.17	6.32	9.94	10.28
20.2	1.17	6.32	10.95	11.02
29.5	1.17	6.32	12.58	12.73
37.2	1.17	6.32	14.72	14.89
42.9	1.17	6.32	17.42	16.99
49.2	1.17	6.32	21.23	19.88
56.2	1.17	6.32	25.82	23.86
57.1	1.17	6.32	24.94	24.43
63.0	1.17	6.32	30.06	28.58
69.2	1.17	6.32	33.56	33.66
2.0	0.510	6.76	9.62	9.30
12.5	0.510	6.76	9.22	9.01
20.0	0.510	6.76	9.18	9.43
28.5	0.510	6.76	10.06	10.60

34.2	0.510	6.76	11.31	11.86
40.3	0.510	6.76	13.17	13.68
49.2	0.510	6.76	16.47	17.380
54.9	0.510	6.76	20.62	20.51
58.8	0.510	6.76	23.07	23.03
63.2	0.510	6.76	26.39	26.29
65.5	0.510	6.76	28.48	28.17
69.2	0.510	6.76	31.04	31.46
12.8	0.306	4.06	5.42	5.26
20.2	0.306	4.06	5.34	5.46
29.5	0.306	4.06	6.38	6.21
37.2	0.306	4.06	7.73	7.33
42.9	0.306	4.06	8.64	8.50
49.2	0.306	4.06	10.84	10.20
55.1	0.306	4.06	12.64	12.22
61.7	0.306	4.06	14.88	15.06
68.5	0.306	4.06	17.12	18.68
30.5	0.105	6.76	11.34	11.11
41.0	0.105	6.76	15.82	15.09
51.3	0.105	6.76	21.40	21.47
57.3	0.105	6.76	25.60	26.58
64.2	0.105	6.76	37.18	33.94

Table A-11. Longitudinal Nuclear Relaxation Rates for Solvent Protons in Solutions of $(H_2O)_5CrCH_2CN^{2+}$ in Aqueous Acid

Temp °C	$10\times[H^+]$ M	$10^4\times P_m$	R_1, s^{-1} Obsd	Calcd
4.4	2.20	5.63	10.39	10.33
11.8	2.20	5.63	10.45	10.32
20.1	2.20	5.63	10.65	10.54
29.5	2.20	5.63	10.95	10.89
36.3	2.20	5.63	11.37	11.13
43.2	2.20	5.63	11.44	11.28
50.9	2.20	5.63	11.11	11.31
57.5	2.20	5.63	10.41	11.20
73.0	2.20	5.63	9.85	10.56
12.8	1.17	6.32	9.66	9.55
20.2	1.17	6.32	9.81	9.72
29.5	1.17	6.32	10.26	10.18
37.2	1.17	6.32	10.89	10.66
42.9	1.17	6.32	11.41	10.99
49.2	1.17	6.32	11.76	11.28
56.2	1.17	6.32	12.04	11.47
57.1	1.17	6.32	11.78	11.48
63.0	1.17	6.32	11.92	11.50
69.2	1.17	6.32	11.79	11.40
2.0	0.510	6.76	9.52	9.18
12.5	0.510	6.76	9.15	8.67
20.0	0.510	6.76	8.56	8.77
28.5	0.510	6.76	8.94	9.22
34.2	0.510	6.76	9.44	9.66
40.3	0.510	6.76	10.13	10.20
49.2	0.510	6.76	10.87	10.94

54.9	0.510	6.76	11.50	11.32
58.8	0.510	6.76	11.49	11.51
63.0	0.510	6.76	11.74	11.65
65.5	0.510	6.76	11.86	11.70
69.2	0.510	6.76	11.78	11.71
12.8	0.306	4.06	5.04	5.11
20.2	0.306	4.06	5.01	5.14
29.5	0.306	4.06	5.20	5.45
37.2	0.306	4.06	5.78	5.85
42.9	0.306	4.06	6.14	6.19
49.2	0.306	4.06	6.69	6.54
55.1	0.306	4.06	6.93	6.81
61.7	0.306	4.06	7.12	7.01
68.5	0.306	4.06	7.23	7.10
30.5	0.105	6.76	8.97	9.43
41.0	0.105	6.76	10.16	10.76
51.3	0.105	6.76	11.4	11.90
57.3	0.105	6.76	12.13	12.33
64.2	0.105	6.76	12.66	12.56

Table A-12. Rates of $(NH_3)_5Co^{III}X^{2+}$ Oxidation of $(H_2O)_2Co^{II}(dmgBF_2)_2$ at 25 °C (in 0.01 M acetate buffer with $\mu = 0.1M$ by $LiClO_4$)[a]

X	$[(NH_3)_5Co^{III}X^{2+}]$ (M)	$k_1(s^{-1})$[b]	k_2 (M^{-1} s^{-1})[c]
Br	4.88×10^{-3}	0.23 ± 0.01	47± 2
	1.01×10^{-2}	0.51 ± 0.01	50 ± 1
	1.53×10^{-2}	0.82 ± 0.03	54 ± 2
Cl	5.55×10^{-4}	$(1.39 \pm 0.07)\times10^{-3}$	2.5 ± 0.1
	1.08×10^{-3}	$(2.78 \pm 0.22)\times10^{-3}$	2.6 ± 0.2
	1.72×10^{-3}	$(4.43 \pm 0.32)\times10^{-3}$	2.6 ± 0.2
N_3	6.96×10^{-4}	$(3.82 \pm 0.12)\times10^{-3}$	5.5 ± 0.2
	1.48×10^{-3}	$(8.60 \pm 0.81)\times10^{-3}$	5.8 ± 0.6
	2.31×10^{-3}	$(1.45 \pm 0.05)\times10^{-2}$	6.3 ± 0.2

[a] $Co^{II}(dmgBF_2)_2$ concentrations of 1.02×10^{-4}, 5.29×10^{-5}, and 6.24×10^{-5} M are used in reactions with X = Br, Cl, and N_3, respectively. [b] First-order rate constants. [c] Second-order rate constants.

Table A-13. Rates of Reduction of $Co^{III}(dmgH)_2^+$ by $Co(sep)^{2+}$ at 25 °C (μ = 0.10 M by $LiClO_4$)

pH	Buffer	$[Co(sep)^{2+}]$ (10^3M)	k_{12obs} (s^{-1})	$k_{12calcd}$ (s^{-1})
4.76	Acetate	0.824	4.06	4.18
4.97	Acetate	1.20	5.56	5.80
5.20	Acetate	1.25	6.15	5.56
5.50	Acetate	1.13	4.18	4.22
5.80	MES	1.75	5.39	5.01
6.10	MES	1.40	2.69	2.81
6.35	MES	1.57	2.05	2.23
6.80	PIPES	1.44	1.26	1.11
7.35	PIPES	1.32	5.73	5.92

Table A-14. Rates of Reduction of $Co^{III}(dmgBF_2)_2^+$ by $Co(sep)^{2+}$ at 25 °C (μ = 0.10 M by $LiClO_4$)

pH	Buffer	$[Co(sep)^{2+}]$ (10^3M)	k_{12obs} (s^{-1})	$k_{12calcd}$ (s^{-1})
3.30	Chloroacetate	0.150	19.4	21.5
3.30	Chloroacetate	0.300	40.0	43.0
3.70	Acetate	0.161	18.8	20.7
3.70	Acetate	0.304	37.0	38.9
4.00	Acetate	0.642	80.9	71.0
4.00	Acetate	1.17	137	129
4.30	Acetate	0.300	27.7	25.9
4.68	Acetate	0.629	41.3	33.5
4.69	Acetate	0.553	34.6	29.0
4.70	Acetate	0.691	43.3	35.7
5.10	Acetate	0.201	51.6	52.0
5.10	Acetate	0.402	11.8	10.4
5.50	Acetate	0.732	88.1	84.8
5.52	Acetate	0.589	7.05	6.55
5.86	MES	0.545	2.37	2.95
6.12	MES	0.790	2.23	2.47
6.45	MES	0.652	1.05	1.05
6.45	MES	1.21	2.02	1.94
6.95	PIPES	0.660	0.377	0.488
7.29	PIPES	0.847	0.433	0.376
7.42	PIPES	0.980	0.400	0.385
7.42	PIPES	1.66	0.663	0.652